https://ntrs.nasa.gov/search.jsp?R=19720014350 2020-03-23T10:59:23+00:00Z

TECH LIBRARY KAFB, NM
0061339
NASA CR-2
e.1

NASA CONTRACTOR REPORT

LOAN COPY: RETURN TO
AFWL (DOUL)
KIRTLAND AFB, N. M.

NASA CR-2021

A STABILITY ANALYSIS OF CABLE-BODY SYSTEMS TOTALLY IMMERSED IN A FLUID STREAM

by James D. DeLaurier

Prepared by
STANFORD UNIVERSITY
Stanford, Calif.
for Langley Research Center

NATIONAL AERONAUTICS AND SPACE ADMINISTRATION • WASHINGTON, D. C. • APRIL 1972

TECH LIBRARY KAFB, NM
0061339

1. Report No.	2. Government Accession No.	3. Recipient's Catalog No.
NASA CR-2021		

4. Title and Subtitle	5. Report Date
A STABILITY ANALYSIS OF CABLE-BODY SYSTEMS TOTALLY IMMERSED IN A FLUID STREAM	April 1972
	6. Performing Organization Code
7. Author(s)	8. Performing Organization Report No.
James D. DeLaurier	SUDAAR-411
	10. Work Unit No.
9. Performing Organization Name and Address	11. Contract or Grant No.
Department of Aeronautics and Astronautics Stanford University Stanford, Calif. 94025	NGL 05-020-243
	13. Type of Report and Period Covered
12. Sponsoring Agency Name and Address	Contractor Report
National Aeronautics and Space Administration Washington, D.C. 20546	14. Sponsoring Agency Code

15. Supplementary Notes

16. Abstract

A general stability analysis of a cable-body system immersed in a fluid stream is presented. The analytical portion of this analysis treats the system as being essentially a cable problem, with the body dynamics giving the end conditions. The mathematical form of the analysis consists of partial differential wave equations, with the end and auxiliary conditions being determined from the body equations of motion. The equations uncouple to give a "lateral" problem and a "longitudinal" problem as in first order airplane dynamics. A series of tests on a tethered wind tunnel model provide a comparison of the theory with experiment.

17. Key Words (Suggested by Author(s))	18. Distribution Statement
Stability of tethered bodies Cable-body math model Cable-body tether tests Tethered bodies	Unclassified - Unlimited

19. Security Classif. (of this report)	20. Security Classif. (of this page)	21. No. of Pages	22. Price*
Unclassified	Unclassified	93	$3.00

*For sale by the National Technical Information Service, Springfield, Virginia 22151

1. Equations of motion
2. Towing cables - analysis

ABSTRACT

There are numerous examples of research dealing with towed and tethered bodies. Besides the classical problem of kites and towed gliders, recent work has been done on towed decelerators for reentry bodies and towed underwater devices.

Previous analytical treatment of the body-cable system has assumed a rigid body problem, where the cable effect is accounted for by some force condition at the attachment point. The present approach treats the system as being essentially a cable problem, with the body dynamics giving end conditions.

The mathematical form of the first order problem is a nonhomogeneous initial-boundary value problem in the partial differential wave equation. All equations, including end and auxiliary conditions, are linear with constant coefficients. Further, these equations uncouple to give a "lateral" problem and a "longitudinal" problem —— as in first order airplane dynamics. The solution of either problem takes the form of a transcendental characteristic equation for the stability roots. These roots are extracted by using an electronic computer and a roots locus plot.

A series of tests on a tethered wind tunnel model provided a comparison of the theory with experiment. The equilibrium properties of the system were found by force measurements and photographs for various wind speeds, but the stability derivatives were found entirely from theory. This, along with the fact that the model was flying near stall, gave rise to a certain amount of difference between the theoretical and experimental results. Nevertheless, within the estimated error limits, the comparison is good and provides a convincing argument for the theory.

TABLE OF CONTENTS

FIGURES

LIST OF FIGURES

Figure

Figure

LIST OF SYMBOLS

$\vec{a}_{c_r}$ ≡ Acceleration of the body mass center with respect to $\mathcal{R}'$.

a_1, a_2, a_3 ≡ Acceleration components in the $\vec{e}_1$, $\vec{e}_2$ and $\vec{e}_3$ directions respectively.

$\hat{a}_1, \hat{a}_2, \hat{a}_3$ ≡ Nondimensional acceleration components defined by equations (2.61)→(2.63).

$A_1 \rightarrow A_{24}$ ≡ Functions of λ defined in equations (3.26) and (3.27).

b ≡ Body characteristic length.

$\vec{b}_1, \vec{b}_3$ ≡ Unit vectors defined in Figure 1.

$\mathfrak{b}$ ≡ Cable buoyancy force per unit length.

B ≡ Body buoyancy force.

$\hat{B}$ ≡ Nondimensional body buoyance force defined by (2.44).

c ≡ Chord of lifting surface.

$\hat{C}$ ≡ Nondimensional cable equation coefficient defined by (1.25).

$C(\ )$ ≡ Abbreviation for cosine ( ).

C_a ≡ Cable force coefficient defined by (1.7).

C_{a_o} ≡ Cable force coefficient defined by (1.8).

C_b ≡ Cable force coefficient defined by (1.7).

C_d ≡ Profile drag coefficient.

C_D ≡ Drag coefficient.

C_L ≡ Lift coefficient.

C_ℓ, C_m, C_n ≡ Moment stability derivatives defined by (2.45).

C_X, C_Y, C_Z ≡ Force stability derivatives defined by (2.44).

C_{Fi} ≡ General force stability derivative.

C_{Mi} ≡ General moment stability derivative.

$D(\ ), D^2(\ )$ ≡ Nondimensional time derivatives defined by equations (1.22), (2.50), and (2.51).

$\vec{e}_1, \vec{e}_2, \vec{e}_3$ ≡ Space fixed unit vectors defined by Figure 5.

$E_1 \rightarrow E_8$ ≡ Functions of σ defined in equations (3.12) and (3.13).

$\vec{F}$ ≡ Force term.

$\vec{F}_a, \vec{F}_b$ ≡ Cable segment fluid force components defined by (1.2) and (1.3).

F_1, F_2, F_3 ≡ Body forces in the $\vec{n}_1$, $\vec{n}_2$ and $\vec{n}_3$ directions respectively.

F_r, F_j ≡ Functions of λ given by equations (3.26) and (3.27).

g ≡ Gravitational constant.

G_r, G_j ≡ Functions of σ given by equations (3.12) and (3.13).

h_1 ≡ Function of λ defined by (3.24).

h_2 ≡ Function of σ defined by (3.10).

H_1, H_2 ≡ Functions of λ as defined by (3.25).

H_3, H_4 ≡ Functions of σ as defined by (3.11).

i ≡ Nondimensional inertia term defined by (2.49).

I_{xx}, I_{yy}, I_{zz} ≡ Moments of inertia about the x, y and z axes respectively.

I_{xz} ≡ Product of inertia with respect to the x, z axes.

j ≡ $(-1)^{1/2}$

$J, \hat{J}$ ≡ Nondimensional cable terms defined in equation (1.25).

$k_1 \rightarrow k_7$ ≡ Cable coefficients defined by equations (1.26), (1.27), (1.29), (1.30), (1.32), and (1.33).

K ≡ Nondimensional cable equation force coefficient defined by (1.7) and (1.8).

L ≡ Cable length.

L_{cr} ≡ Cable length for which the system is neutrally stable.

m ≡ Body mass.

$\hat{mg}$ ≡ Nondimensional body weight as defined in equation (2.44).

M_1, M_2, M_3 ≡ Body moments about the $\vec{n}_1, \vec{n}_2$ and $\vec{n}_3$ axes respectively.

$\vec{n}_1, \vec{n}_2, \vec{n}_3$ ≡ Body fixed unit vectors defined by Figure 6.

p, q, r ≡ Body angular velocities about the n_1, n_2 and n_3 axes respectively.

$\hat{p}, \hat{q}, \hat{r}$ ≡ Nondimensional body angular velocities defined by equation (2.46).

R ≡ Cable cross-section radius.

R_a ≡ Distance from the body mass center to the cable attachment point.

$\hat{R}_a$ ≡ Nondimensional form of R_a defined by equation (2.46).

R_B ≡ Distance from the body mass center to the center of buoyancy.

$\hat{R}$ ≡ Nondimensional form of R_B defined by equation (2.46).

$\mathcal{R}$ ≡ Reference frame fixed to $\vec{e}_1, \vec{e}_2$ and $\vec{e}_3$, defined in Figure 5.

$\mathcal{R}'$ ≡ Reference frame fixed in the undisturbed fluid stream.

s ≡ Cable length coordinate.

$\tilde{s}$ ≡ Nondimensional cable length coordinate defined by (1.24).

S ≡ Body characteristic area.

$S(\ )$ ≡ Abbreviation for sine ( ).

t ≡ Time.

$\hat{t}$ ≡ Nondimensional time defined by (2.48).

$\vec{T}$ ≡ Cable tension force.

T_o ≡ Mean value of the magnitude of the cable tension force.

$\hat{T}_o$ ≡ Nondimensional value of T_o as defined by equation (2.44).

u, v, w ≡ Body mass center velocity components in $\mathcal{R}$ in the $\vec{n}_1, \vec{n}_2$ and $\vec{n}_3$ directions respectively.

u_r, v_r, w_r ≡ Body mass center velocity components in $\mathcal{R}'$ in the $\vec{n}_1, \vec{n}_2$ and $\vec{n}_3$ directions respectively.

u', v', w' ≡ Perturbation values of u_r, v_r and w_r respectively as defined by (2.33).

$\hat{u}, \hat{v}, \hat{w}$ ≡ Nondimensional values of u', v' and w' respectively, as defined by (2.46).

$\vec{U}$ ≡ Undisturbed fluid velocity with respect to $\mathcal{R}$.

$\vec{v}_c$ ≡ Velocity of the body mass center with respect to $\mathcal{R}$.

$(\vec{v}_c)_r$ ≡ Velocity of the body mass center with respect to $\mathcal{R}'$.

$\vec{v}_r$ ≡ Velocity of a cable element with respect to $\mathcal{R}'$.

$\vec{v}_s$ ≡ Velocity of a cable element with respect to $\mathcal{R}$.

x, y, z ≡ Body coordinates fixed in $\mathcal{R}$ and defined by Figure 5.

$\hat{x}, \hat{y}, \hat{z}$ ≡ Nondimensional forms of x, y and z respectively as defined by equation (2.46).

$\breve{x}, \breve{y}, \breve{z}$ ≡ Cable coordinates fixed in $\mathcal{R}$ and defined by Figure 1.

$\tilde{x}, \tilde{y}, \tilde{z}$ ≡ Nondimensional form of $\breve{x}', \breve{y}', \breve{z}'$ defined by (1.24).

$\breve{x}', \breve{y}', \breve{z}'$ ≡ Perturbed values of $\breve{x}, \breve{y}, \breve{z}$ defined by (1.14) and (2.91).

X, Y, Z ≡ Functions of s defined by equations (3.5) and (3.18).

X_o, Y_o, Z_o ≡ Constants defined by equations (3.5) and (3.18).

Greek Symbols:

α ≡ Wing angle of attack.

$\tilde{\alpha}$ ≡ Angle between the $\breve{x}$ coordinate axis and the ξ coordinate axis as defined in Figure 1.

$\breve{\alpha}$ ≡ Angle of the cable segment as defined in Figure 2.

β ≡ Body sideslip angle, v/U.

Γ ≡ Cable constant as defined by equation (3.17).

Δ ≡ Function of λ as defined by equation (3.17).

$\Delta(\ )$ ≡ A finite difference in the $(\ )$ quantity.

ϵ ≡ An order of magnitude defined by equations (1.17) and (2.22).

ζ ≡ Cable coordinate as defined in Figure 1.

θ ≡ Body Eulerian angle with respect to $\mathcal{R}$ as defined in Figure 6.

$\tilde{\theta}$ ≡ Perturbed value of θ defined by equation (2.19).

θ_o ≡ Equilibrium value of θ defined by equation (2.19).

Θ ≡ Constant defined by equation (3.1).

λ ≡ Stability root for lateral motion.

λ_r ≡ Real part of the stability root, λ.

λ_j ≡ Imaginary part of the stability root, λ.

Λ ≡ Cable constant as defined by equation (3.4).

μ ≡ Nondimensional body mass defined by equation (2.48).

ν ≡ Function of σ defined by equation (3.10).

ξ ≡ Cable coordinate as defined in Figure 1.

$\pi_1 \rightarrow \pi_{60}$ ≡ Constants of the end conditions and auxiliary conditions as defined by equations (2.112), (2.117), (2.127) and (2.132).

ρ ≡ Fluid density.

$\tilde{\rho}$ ≡ Cable density per unit length.

σ ≡ Stability root for longitudinal motion.

σ_r ≡ Real part of the stability root, σ.

σ_j ≡ Imaginary part of the stability root, σ.

τ ≡ Perturbed cable tension defined by equation (1.13).

υ ≡ Function of λ defined by equation (3.24).

ϕ ≡ Body Eulerian angle with respect to $\mathfrak{R}$ as defined in Figure 6.

$\tilde{\phi}$ ≡ Perturbed value of ϕ defined by equation (2.19).

Φ ≡ Constant defined by equation (3.14).

ψ ≡ Body Eulerian angle with respect to $\mathfrak{R}$ as defined in Figure 6.

$\tilde{\psi}$ ≡ Perturbed value of ψ defined by equation (2.19).

Ψ ≡ Constant defined by equation (3.14).

$\vec{\omega}$ ≡ Angular velocity of the body with respect to $\mathfrak{R}$.

$\mathfrak{R} \underset{w}{\rightarrow} \mathfrak{R}'$ ≡ Angular velocity of $\mathfrak{R}'$ with respect to $\mathfrak{R}'$.

Ω ≡ Function of σ as defined by equation (3.4).

Subscripts:

$( )_a$ ≡ With respect to the cable attachment point (except for F_a and C_a).

$( )_\alpha$ ≡ Derivative with respect to α.

$( )_\beta$ ≡ Derivative with respect to β.

$( )_B$ ≡ Buoyancy force term.

$( )_{cr}$ ≡ That value corresponding to L_{cr}.

$( )_{exp}$ ≡ Experimental value.

$( )_f$ ≡ Cable fluid force term.

$( )_g$ ≡ Gravity force term.

$( )_o$ ≡ Reference value.

$( )_p$ ≡ Derivative with respect to $\hat{p}$.

$( )_q$ ≡ Derivative with respect to $\hat{q}$.

$( )_r$ ≡ Derivative with respect to $\hat{r}$.

$( )_u$ ≡ Derivative with respect to $\hat{u}$.

$( )_v$ ≡ Derivative with respect to $\hat{v}$.

$( )_w$ ≡ Derivative with respect to $\hat{w}$.

$( )_{\dot{u}}$ ≡ Derivative with respect to $\hat{a}_1$

$( )_{\dot{v}}$ ≡ Derivative with respect to $\hat{a}_2$.

$( )_{\dot{w}}$ ≡ Derivative with respect to $\hat{a}_3$.

$( )_\theta$ ≡ Derivative with respect to $\tilde{\theta}$.

$( )_\phi$ ≡ Derivative with respect to $\tilde{\phi}$.

$( )_\psi$ ≡ Derivative with respect to $\tilde{\psi}$.

Superscripts:

$(\dot{})$ ≡ Derivative with respect to time.

INTRODUCTION

The objective of this research was to devise a method by which one could predict the dynamic stability of a cable-body system subjected to fluid forces. Examples of such cable-body systems are numerous. Besides the old examples of kites and towed gliders, current examples are towed decelerators for reentering spacecraft (Fig. 15), towed underwater devices (Fig. 16), and towed and tethered "kite balloons" (Fig. 17).

Analysis of cable-body system dynamic stability was initially directed toward kites and towed gliders, and the best examples of this work are given by Glauert (Ref. 6), Söhne (Ref. 1), and Bryant, et. al. (Ref. 1). Current analysis, however, has been directed toward a wider range of cable-body system applications. For instance, besides towed glider research by Maryniak (Ref. 11), towed nonlifting surveillance devices were studied by Etkin and Mackworth (Ref. 5), Mettam (Ref. 12), and Hopkin (Ref. 8). Also, a stability theory for towed underwater devices was developed by Laitinen (Ref. 9); and MacNeal (Ref. 10) derived a stability criterion for towed hypersonic decelerators.

The approaches taken toward the problem by most investigators has been to consider the situation to be solely a body problem, with the cable accounted for by some force condition at the attachment point. This force condition takes the form of cable "stability derivatives", and is derived from the assumption that the cable is in an instantaneous equilibrium configuration with respect to certain of its end conditions. That is, the shape and tension of the cable are assumed to be either functions of the body's position, (Ref. 1), or functions of the body's position and velocity (Ref. 11). This assumption gives a good physical model for a large class of cable-body problems, in particular, those for which the cable is light and the system oscillations are slow. These conditions are met by most towed gliders

and towed and tethered kite balloons. Further, the physical model has the merit of yielding a first order problem composed of a system of second order ordinary differential equations. These, in turn, give a polynomial for the stability roots.

The present approach considers the dynamics of the cable, that is, the system is treated as a cable problem, with the body giving end and auxiliary conditions. Mathematically this means that the body's ordinary differential equations of motion provide end and auxiliary conditions to the cable's partial differential equations of motion. The result of the first order problem —— as shown in Chapter 3 —— is transcendental equations for the stability roots. The author feels that this physical model embodies the essential characterization of the cable-body system because the assumptions —— as shown later —— relate only to details about the cable construction, body construction, and fluid loads, and not about the mechanical nature of the cable-body system. An extension on the present approach is also included in reference 17.

1. THE CABLE EQUATIONS OF MOTION

1.1 The Complete Cable Equations

The physical model of the cable considered is subject to the following assumptions:

a. The cable is uniform along its length, perfectly flexible, inextensible, has a round cross-section, and is totally immersed in a homogeneous fluid.

b. The Reynolds number of the cable's crossflow is subcritical.

The dependent variables of the cable are the coordinates of a point on it, $\xi, \breve{y}$, and ζ, and the tension, T, at that point. The independent variables are the distance along the cable, s, and time, t. The forces acting on an element of the cable, ds, are now found. Considering first the tension force, $\vec{T}$, note that

$$\vec{T} = |T|\vec{n} \text{ and } \vec{T}' = \left|T + \frac{\partial T}{\partial s}ds\right|\left(\vec{n} + \frac{\partial \vec{n}}{\partial s}ds\right),$$

thus,

$$d\vec{T} = \vec{T}' - \vec{T} = \frac{\partial}{\partial s}(T\vec{n})ds.$$

Further,

$$\vec{n} = \frac{\partial \xi}{\partial s}\vec{b}_1 + \frac{\partial \breve{y}}{\partial s}\vec{e}_2 + \frac{\partial \zeta}{\partial s}\vec{b}_3,$$

so, one has

$$d\vec{T} = \frac{\partial}{\partial s}\left(T\frac{\partial \xi}{\partial s}\right)ds\vec{b}_1 + \frac{\partial}{\partial s}\left(T\frac{\partial \breve{y}}{\partial s}\right)ds\vec{e}_2 + \frac{\partial}{\partial s}\left(T\frac{\partial \zeta}{\partial s}\right)ds\vec{b}_3. \tag{1.1}$$

The gravity force, $d\vec{F}_g$, on the element, ds, is given by

$$d\vec{F}_g = -\tilde{\rho}g(C\tilde{\alpha}\vec{b}_1 + S\tilde{\alpha}\vec{b}_3)ds. \tag{1.2}$$

Similarly, the buoyancy force, $d\vec{F}_B$, on the element is given by

$$d\vec{F}_B = \tilde{b}(C\tilde{\alpha}\vec{b}_1 + S\tilde{\alpha}\vec{b}_3)ds. \tag{1.3}$$

Treating now the fluid dynamic force, $d\vec{F}_f$, on the element, ds, note first that

$$\vec{v}_r = \vec{U} - \vec{v}_s,$$

where $\vec{v}_s$ is the cable element's velocity relative to the reference frame $\mathcal{R}$ (see Fig. 1). Note that $\vec{v}_r$ is the relative velocity of the fluid to the cable element. Considering the plane of $\vec{F}_f$ and $\vec{v}_r$, and introducing the cable coefficients, C_a and C_b, one obtains the components of the fluid force, $d\vec{F}_f$, as defined in Fig. 2:

$$d\vec{F}_a = C_a \rho |\vec{v}_r| \vec{v}_r R ds \tag{1.4}$$

and

$$d\vec{F}_b = C_b \rho \vec{v}_r \times (\vec{v}_r \times \vec{n}) R ds. \tag{1.5}$$

Now,

$$\vec{v}_s = \frac{\partial \xi}{\partial t}\vec{b}_1 + \frac{\partial \breve{y}}{\partial t}\vec{e}_2 + \frac{\partial \zeta}{\partial t}\vec{b}_3,$$

so,

$$\vec{v}_r = (UC\tilde{\alpha} - \frac{\partial \xi}{\partial t})\vec{b}_1 - \frac{\partial \breve{y}}{\partial t}\vec{e}_2 - (US\tilde{\alpha} + \frac{\partial \zeta}{\partial t})\vec{b}_3 \tag{1.6}$$

Further, as described in page 3.9 of Hoerner (Ref. 7),

$$C_a = C_{a_o} + K(1 - C^2\breve{\alpha})^{3/2} \tag{1.7}$$

and

$$C_b = K(1 - C^2\breve{\alpha})C\breve{\alpha}, \tag{1.8}$$

where

$$C\breve{\alpha} = \frac{(\vec{v}_r \cdot \vec{n})}{|v_r|} \tag{1.9}$$

Thus, (1.8), (1.9), (1.6), and (1.7) into (1.4) and (1.5) give the fluid-dynamic forces on the element.

Equating all of the forces to the acceleration of the element, one has

$$d\vec{T} + d\vec{F}_g + d\vec{F}_B + d\vec{F}_a + d\vec{F}_b = \tilde{\rho}\frac{\partial}{\partial t}(\frac{\partial \xi}{\partial t}\vec{b}_1 + \frac{\partial \breve{y}}{\partial t}\vec{e}_2 + \frac{\partial \zeta}{\partial t}\vec{b}_3)\, ds \tag{1.10}$$

so, (1.1) → (1.8) into (1.10) give the complete cable equations of motion. Taking components, one has, for the $\vec{b}_1$ direction,

$$\tilde{\rho}\frac{\partial^2\xi}{\partial t^2} = \frac{\partial}{\partial s}(T\frac{\partial\xi}{\partial s}) + \rho R(C_{a_o} + KS^3\breve{\alpha})[(UC\tilde{\alpha} - \frac{\partial\xi}{\partial t})^2 + (\frac{\partial\breve{y}}{\partial t})^2$$

$$+ (US\tilde{\alpha} + \frac{\partial\zeta}{\partial t})^2]^{1/2} (UC\tilde{\alpha} - \frac{\partial\xi}{\partial t}) - KS^2\tilde{\alpha}C\tilde{\alpha}\rho R \times [\{(UC\tilde{\alpha} - \frac{\partial\xi}{\partial t})^2$$

$$+ (\frac{\partial\breve{y}}{\partial t})^2 + (US\tilde{\alpha} + \frac{\partial\zeta}{\partial t})^2\}\frac{\partial\xi}{\partial s} - \{(UC\tilde{\alpha} - \frac{\partial\xi}{\partial t})\frac{\partial\xi}{\partial s} - (\frac{\partial\breve{y}}{\partial t})\frac{\partial\breve{y}}{\partial s}$$

$$- (US\tilde{\alpha} + \frac{\partial\zeta}{\partial t})\frac{\partial\zeta}{\partial s}\} \times (UC\tilde{\alpha} - \frac{\partial\xi}{\partial t})] - (\tilde{\rho}g - \tilde{b})C\tilde{\alpha}. \tag{1.11}$$

Similarly, one has, for the $\vec{e}_2$ direction,

$$\tilde{\rho}\frac{\partial^2\breve{y}}{\partial t^2} = \frac{\partial}{\partial s}(T\frac{\partial\breve{y}}{\partial s}) - \rho R(C_{a_o} + KS^3\breve{\alpha})[(UC\tilde{\alpha} - \frac{\partial\xi}{\partial t})^2 + (\frac{\partial\breve{y}}{\partial t})^2$$

$$+ (US\tilde{\alpha} + \frac{\partial\zeta}{\partial t})^2]^{1/2} \frac{\partial\breve{y}}{\partial t} - KS^2\breve{\alpha}C\breve{\alpha}\rho R \times [\{(UC\tilde{\alpha} - \frac{\partial\xi}{\partial t})^2$$

$$+ (\frac{\partial\breve{y}}{\partial t})^2 + (US\tilde{\alpha} + \frac{\partial\zeta}{\partial t})^2\}\frac{\partial\breve{y}}{\partial s} + \{(UC\tilde{\alpha} - \frac{\partial\xi}{\partial t})\frac{\partial\xi}{\partial s} \tag{1.12}$$

$$- (\frac{\partial\breve{y}}{\partial t})\frac{\partial\breve{y}}{\partial s} - (US\tilde{\alpha} + \frac{\partial\zeta}{\partial t})\frac{\partial\zeta}{\partial s}\}\frac{\partial\breve{y}}{\partial t}].$$

And finally, one has, for the $\vec{b}_3$ direction,

$$\tilde{\rho}\frac{\partial^2\zeta}{\partial t^2} = \frac{\partial}{\partial s}(T\frac{\partial\zeta}{\partial s}) - \rho R(C_{a_o} + KS^3\breve{\alpha})[(UC\tilde{\alpha} - \frac{\partial\xi}{\partial t})^2$$

$$+ (\frac{\partial\breve{y}}{\partial t})^2 + (US\tilde{\alpha} + \frac{\partial\zeta}{\partial t})^2]^{1/2} (US\tilde{\alpha} + \frac{\partial\zeta}{\partial t}) - \rho RKS^2\breve{\alpha}C\breve{\alpha}$$

$$\times [\{(UC\tilde{\alpha} - \frac{\partial\xi}{\partial t})^2 + (\frac{\partial\breve{y}}{\partial t})^2 + (US\tilde{\alpha} + \frac{\partial\zeta}{\partial t})^2\}\frac{\partial\zeta}{\partial s} + \{(UC\tilde{\alpha} - \frac{\partial\xi}{\partial t})\frac{\partial\xi}{\partial s} \tag{1.13}$$

$$- (\frac{\partial\breve{y}}{\partial t})\frac{\partial\breve{y}}{\partial s} - (US\tilde{\alpha} + \frac{\partial\zeta}{\partial t})\frac{\partial\zeta}{\partial s}\}(US\tilde{\alpha} + \frac{\partial\zeta}{\partial t})] - (\tilde{\rho}g - b)S\tilde{\alpha}.$$

1.2 The First Order Cable Equations

In order to simplify equations (1.10) →(1.13), a small perturbation analysis is performed such as to give the first order form of these equations. Consider, now, the ξ axis to be aligned through the end points of the cable's equilibrium configuration (Fig. 3). Further, consider a perturbation from equilibrium such that

$$\xi = \xi_o(s) + \xi'(s,t), \quad \breve{y} = \breve{y}'(s,t) \quad \text{and} \quad \zeta = \zeta_o(s) + \zeta'(s,t), \tag{1.14}$$

where $\xi_o(s)$ and $\zeta_o(s)$ are the equilibrium values and $\xi'(s,t), \breve{y}'(s,t)$, and $\zeta'(s,t)$ are the perturbation values from equilibrium. Also,

$$T = T_o + \tau(s,t), \tag{1.15}$$

where T_o is the mean value of the equilibrium tension and $\tau(s,t)$ is the perturbation value from equilibrium. Note now the important assumption made that the equilibrium tension is constant and equal to T_o over the cable's length. This approximation is closely realized for a large range of cable-body systems, for example, towed reentry decelerators and towed and tethered bodies where

$$(\tilde{\rho}g - \tilde{b})L \leq T_o \quad \text{and} \quad C_a \rho R L \leq T_o. \tag{1.16}$$

Experimental evidence (Refs. 1, 5, 12 and Chapter 4) has indicated that unstable modes of many such systems —— if they are present —— occur within the cable length where conditions (1.16) are still satisfied.

Now, assume small perturbations from the equilibrium position such that

$$\frac{\partial \breve{y}'}{\partial s}, \frac{\partial \zeta'}{\partial s} = 0[\epsilon], \quad \frac{\partial \breve{y}'}{\partial t}, \frac{\partial \zeta'}{\partial t} = 0[\epsilon]U \quad \text{and} \quad \tau(s,t) = 0[\epsilon]T_o \quad \text{where } \epsilon \ll 1. \tag{1.17}$$

Note that it follows that

$$\frac{\partial \xi'}{\partial s} = 0[\epsilon^2] \quad \text{and} \quad \frac{\partial \xi'}{\partial t} = 0[\epsilon^2]U.$$

Proof:

Considering the special case of motion in the $\breve{y}, \xi$ plane, one has

$$d\breve{y} = ds \quad \text{and} \quad d\xi' = \epsilon d\breve{y}, \quad \text{so,} \quad d\xi' = \epsilon^2 ds,$$

which gives

$$\frac{\partial \xi}{\partial s} = \epsilon^2. \quad \text{Also,} \quad \frac{\partial \xi}{\partial t} = \epsilon \frac{\partial \breve{y}}{\partial t}.$$

Allowing for motion in the ζ direction gives the same results. At this point, the assumption is introduced that the cable has a shallow curvature such that

$$\breve{\alpha}_o \approx \tilde{\alpha}, \quad \frac{\partial \zeta_o}{\partial s} \approx 0, \quad \text{and} \quad \frac{\partial \xi_o}{\partial s} \approx 1. \tag{1.18}$$

This assumption is, in fact, consistent with conditions (1.16).

Now, taking (1.17) and (1.6) into (1.9), and taking this, along with (1.17) and (1.18), into the complete cable equations, and further, dropping terms of $0[\epsilon^2]$ and higher, one obtains the first order cable equations of motion. These are

$$\tilde{\rho}\frac{\partial^2 \xi'}{\partial t^2} = T_o \frac{\partial^2 \xi'}{\partial s^2} + \rho R[(C_{a_o} + KS^3\tilde{\alpha})US\tilde{\alpha}C\tilde{\alpha} - 2KUS^3\tilde{\alpha}C\tilde{\alpha}]\frac{\partial \zeta'}{\partial t}$$

$$+ \rho RU^2K[S^2\tilde{\alpha}C^2\tilde{\alpha}(3 - S\tilde{\alpha}) - S^3\tilde{\alpha}(S^2\tilde{\alpha} - 2C^2\tilde{\alpha})]\frac{\partial \zeta'}{\partial s}, \tag{1.19}$$

$$\tilde{\rho}\frac{\partial^2 \breve{y}}{\partial t^2} = T_o \frac{\partial^2 \breve{y}}{\partial s^2} - \rho RU[C_{a_o} + K(S^3\tilde{\alpha} + C^2\tilde{\alpha}S^2\tilde{\alpha})]\frac{\partial \breve{y}'}{\partial t} +$$

$$- \rho RKU^2S^2\tilde{\alpha}C\tilde{\alpha}\frac{\partial \breve{y}'}{\partial s}, \tag{1.20}$$

and

$$\tilde{\rho}\frac{\partial^2 \zeta'}{\partial t^2} = T_o \frac{\partial^2 \zeta'}{\partial s^2} - \rho RU[(C_{a_o} + KS^3\tilde{\alpha})(1 + S^2\tilde{\alpha}) + KS^2\tilde{\alpha}C^2\tilde{\alpha}]\frac{\partial \zeta'}{\partial t}$$

$$- \rho RKU^2[S^2\tilde{\alpha}C\tilde{\alpha}(3S\tilde{\alpha} + 1) - 2S^4\tilde{\alpha}C\tilde{\alpha} + 2C^3\tilde{\alpha}S^2\tilde{\alpha}]\frac{\partial \zeta'}{\partial s}. \tag{1.21}$$

As an aside, the first order equilibrium equations are

$$T_o \frac{\partial^2 \xi_o}{\partial s^2} + \rho R U^2 C\tilde{\alpha}(C_{a_o} + KS^3\tilde{\alpha}) - \rho R K U^2 S^3\tilde{\alpha}C\tilde{\alpha} + C\tilde{\alpha}(\tilde{b} - \tilde{\rho}g) = 0 \tag{1.22}$$

and

$$T_o \frac{\partial^2 \zeta_o}{\partial s^2} - \rho R U^2 S\tilde{\alpha}(C_{a_o} + KS^3\tilde{\alpha}) - \rho R K U^2 S^3\tilde{\alpha}C^2\tilde{\alpha} + S\tilde{\alpha}(\tilde{b} - \tilde{\rho}g) = 0. \tag{1.23}$$

Within the context of assumptions (1.18), equation (1.23) is the defining equation for the first order cable shape.

1.3 The Nondimensional First Order Cable Equations

Define the following factors:

$$\frac{\partial}{\partial t} \equiv (\frac{2U}{b})D, \quad \frac{\partial^2}{\partial t^2} \equiv (\frac{4U^2}{b^2})D^2, \quad \text{and} \quad \tilde{\xi}, \tilde{y}, \tilde{\zeta}, \tilde{s} \equiv \frac{\xi', y', \zeta', s}{L}. \tag{1.24}$$

One can now obtain nondimensional forms of equations (1.19), (1.20), and (1.21). In particular, define the factors:

$$\hat{C}^2 \equiv \frac{T_o b^2}{4\tilde{\rho}U^2L^2}, \quad \hat{J} \equiv \frac{\rho R b}{2\tilde{\rho}}, \quad \text{and} \quad J \equiv \frac{\rho R b^2}{4\tilde{\rho}L}. \tag{1.25}$$

Further, use these to define

$$k_1 \equiv J[(C_{a_o} + KS^3\tilde{\alpha})S\tilde{\alpha}C\tilde{\alpha} - 2KS^3\tilde{\alpha}C\tilde{\alpha}] \tag{1.26}$$

and

$$k_2 \equiv JK[S^2\tilde{\alpha}C^2\tilde{\alpha}(3 - S\tilde{\alpha}) - S^3\tilde{\alpha}(S^2\tilde{\alpha} - 2C^2\tilde{\alpha})]. \tag{1.27}$$

Equation (1.19) now becomes

$$D^2\tilde{\xi} - \hat{C}^2 \frac{\partial^2 \tilde{\xi}}{\partial \tilde{s}^2} - k_1 D\tilde{\zeta} - k_2 \frac{\partial \tilde{\zeta}}{2\partial \tilde{s}} = 0. \tag{1.28}$$

Similarly, define

$$k_6 \equiv \hat{J}(C_{a_o} + KS^3\tilde{\alpha} + KC^2\tilde{\alpha}S^2\tilde{\alpha}) \tag{1.29}$$

and

$$k_7 \equiv JKC\tilde{\alpha}S^2\tilde{\alpha}. \tag{1.30}$$

Equation (1.20) becomes

$$D^2\tilde{y} - \hat{C}^2 \frac{\partial^2\tilde{y}}{\partial\tilde{s}^2} + k_6 D\tilde{y} + k_7 \frac{\partial\tilde{y}}{\partial\tilde{s}} = 0. \tag{1.31}$$

And finally, define

$$k_3 \equiv \hat{J}[(C_{a_o} + KS^3\tilde{\alpha})(1 + S^2\tilde{\alpha}) + KS^2\tilde{\alpha}C^2\tilde{\alpha}] \tag{1.32}$$

and

$$k_4 \equiv JK[S^2\tilde{\alpha}C\tilde{\alpha}(3S\tilde{\alpha} + 1) - 2S^2\tilde{\alpha}C\tilde{\alpha}(S^2\tilde{\alpha} - C^2\tilde{\alpha})]. \tag{1.33}$$

Thus equation (1.21) becomes

$$D^2\tilde{\zeta} - \hat{C}^2 \frac{\partial^2\tilde{\zeta}}{\partial\tilde{s}^2} + k_3 D\tilde{\zeta} + k_4 \frac{\partial\tilde{\zeta}}{\partial\tilde{s}} = 0. \tag{1.34}$$

2. THE BODY EQUATIONS OF MOTION

2.1 The Force and Moment Equations

The physical model of the body is considered to be subject to the following assumptions:

a. The body is rigid, symmetric with respect to the $\vec{n}_1, \vec{n}_3$ plane (see Fig. 5), and completely immersed in a homogeneous fluid.

b. The cable is perfectly free to pivot at the attachment point.

c. The center of buoyancy is on the $\bar{n}_1$ axis.

It is important to note that the body equations will be expressed in terms of x, y, z, and the Eulerian angles ψ, θ and ϕ relative to $\mathcal{R}$. Although this is different from airplane practice, these coordinates are necessary in order to relate the body equations to the cable equations. However, the force and moment equations are derived relative to $\vec{n}_1, \vec{n}_2$ and $\vec{n}_3$ because fluid-dynamic effects on a body are traditionally taken in these directions. But, by transformation equations, these force and moment terms are eventually expressed in terms of x, y, z, ψ, θ and ϕ.

The force-acceleration equations are, as in Etkin (Ref. 4),

$$F_1 = m(\dot{u} + qw - rv), \tag{2.1}$$

$$F_2 = m(\dot{v} + ru - pw), \tag{2.2}$$

and

$$F_3 = m(\dot{w} + pv - qu). \tag{2.3}$$

And similarly, the moment-angular acceleration equations are

$$M_1 = I_{xx}\dot{p} - I_{xz}\dot{r} + q(I_{zz}r - I_{xz}p) - rI_{yy}q, \tag{2.4}$$

$$M_2 = I_{yy}\dot{q} + r(I_{xx}p - I_{xz}r) - p(I_{zz}r - I_{xz}p), \tag{2.5}$$

and

$$M_3 = I_{zz}\dot{r} - I_{xz}\dot{p} + I_{yy}pq - q(I_{xx}p - I_{xz}r). \tag{2.6}$$

Note that u, v, and w are defined by the velocity of the mass center:

$$\vec{v}_c = u\vec{n}_1 + v\vec{n}_2 + w\vec{n}_3. \tag{2.7}$$

Also, p, q, and r are defined by the body's angular velocity with respect to $\mathcal{R}$:

$$\vec{\omega} = p\vec{n}_1 + q\vec{n}_2 + r\vec{n}_3. \tag{2.8}$$

Consider now the relations between $\vec{e}_i$ and $\vec{n}_i$ based on the Eulerian angles as defined in Fig. 6. These are

$$\vec{e}_1 = C\psi C\theta\vec{n}_1 + (C\psi S\theta S\phi - S\psi C\phi)\vec{n}_2 + (C\psi S\theta C\phi + S\psi S\phi)\vec{n}_3, \tag{2.9}$$

$$\vec{e}_2 = S\psi C\theta\vec{n}_1 + (S\psi S\theta S\phi + C\psi C\phi)\vec{n}_2 + (S\psi S\theta S\phi - C\psi S\phi)\vec{n}_3, \tag{2.10}$$

and

$$\vec{e}_3 = -S\theta\vec{n}_1 + C\theta S\phi\vec{n}_2 + C\theta C\phi\vec{n}_3. \tag{2.11}$$

These relations give, by virtue

$$\vec{v}_c = \dot{x}\vec{e}_1 + \dot{y}\vec{e}_2 + \dot{z}\vec{e}_3 \tag{2.12}$$

and equation (2.7), that

$$u = \dot{x}C\psi C\theta + \dot{y}S\psi C\theta - \dot{z}S\theta, \tag{2.13}$$

$$v = \dot{x}(C\psi S\theta S\phi - S\psi C\phi) + \dot{y}(S\psi S\theta S\phi + C\psi C\phi) + \dot{z}C\theta S\phi, \tag{2.14}$$

and

$$w = \dot{x}(C\psi S\theta C\phi + S\psi S\phi) + \dot{y}(S\theta S\psi C\phi - C\psi S\phi) + \dot{z}C\theta C\phi. \tag{2.15}$$

Similarly, resolving (2.8) with (2.9), (2.10), and (2.11), one has

$$p = \dot{\phi} - \dot{\psi}S\theta, \tag{2.16}$$

$$q = \dot{\theta}C\phi + \dot{\psi}C\theta S\phi, \tag{2.17}$$

and

$$r = \dot{\psi}C\theta C\phi - \dot{\theta}S\phi. \tag{2.18}$$

Equations (2.13)→(2.18) into (2.1)→(2.6) give the force and moment equations in terms of $x, y, z, \psi, \theta, \phi$, and their derivatives. These equations are nonlinear, but in the spirit of the stability analysis, a small perturbation is performed, and linear, first order equations are derived.

2.2 The First Order Force and Moment Equations

Consider a perturbation of the Eulerian angles and their derivatives such that

$$\theta = \theta_o + \tilde{\theta}, \quad \phi = \phi_o + \tilde{\phi}, \quad \psi = \psi_o + \tilde{\psi}, \tag{2.19}$$

$$\dot{\theta} = \dot{\theta}_o + \dot{\tilde{\theta}}, \quad \dot{\phi} = \dot{\phi}_o + \dot{\tilde{\phi}}, \quad \text{and} \quad \dot{\psi} = \dot{\psi}_o + \dot{\tilde{\psi}}, \tag{2.20}$$

where the "o" quantities are reference values, and the "$\sim$" quantities are the perturbation values. Further, define the reference configuration of the body to be that of static equilibrium, thus,

$$\phi_o = \psi_o = \dot{\psi}_o = \dot{\theta}_o = \dot{\phi}_o = 0, \tag{2.21}$$

and θ_o is a fixed value according to the condition that the $\bar{n}_1$ axis passes through the attachment point and the mass center (see Fig. 5).

Now, assume small perturbations such that

$$\tilde{\theta}, \tilde{\psi}, \tilde{\phi} = 0[\epsilon], \quad \dot{x}, \dot{y}, \dot{z} = 0[\epsilon]U, \quad \text{and} \quad \dot{\tilde{\theta}}, \dot{\tilde{\psi}}, \dot{\tilde{\phi}} = 0[\epsilon](U/b), \quad \text{where } \epsilon \ll 1. \tag{2.22}$$

Substituting (2.13)→(2.22) into (2.1)→(2.6), and dropping those terms containing an $0[\epsilon^2]$ or higher, one obtains the first order form of the force and moment equations. These are

$$F_1 = m(\ddot{x}C\theta_o - \ddot{z}S\theta_o), \tag{2.23}$$

$$F_2 = m\ddot{y}, \tag{2.24}$$

$$F_3 = m(\ddot{z}C\theta_o + \ddot{x}S\theta_o), \tag{2.25}$$

$$M_1 = I_{xx}\ddot{\tilde{\phi}} - (I_{xx}S\theta_o + I_{xz}C\theta_o)\ddot{\tilde{\psi}}, \tag{2.26}$$

$$M_2 = I_{yy}\ddot{\tilde{\theta}}, \tag{2.27}$$

and

$$M_3 = (I_{zz}C\theta_o + I_{xz}S\theta_o)\ddot{\tilde{\psi}} - I_{xz}\ddot{\tilde{\phi}}. \tag{2.28}$$

Finally, the dynamics of the body deals with its motion with respect to the inertial reference frame, $\mathcal{R}$. However, the fluid dynamics of the body depends on its motion relative to the fluid stream, $\mathcal{R}'$, which is

$$(\vec{v}_c)_r = \vec{v}_c - U\vec{e}_1 \equiv u_r\vec{n}_1 + v_r\vec{n}_2 + w_r\vec{n}_3. \tag{2.29}$$

For motion subject to the small perturbation conditions, (2.19)→(2.22), equations (2.13)→(2.15), and (2.29) give

$$u_r = \dot{x}C\theta_o - \dot{z}S\theta_o - UC\theta_o, \tag{2.30}$$

$$v_r = U\tilde{\psi} + \dot{y} - US\theta_o\tilde{\phi}, \tag{2.31}$$

and

$$w_r = \dot{z}C\theta_o + \dot{x}S\theta_o - US\theta_o - UC\theta_o\tilde{\theta}. \tag{2.32}$$

Now, considering again the equilibrium reference condition, one defines velocity perturbations by

$$u_r = -UC\theta_o + u', \; v_r = v', \text{ and } w_r = -US\theta_o + w'. \tag{2.33}$$

Thus, from (2.30)→(2.32), (2.33) gives

$$u' = \dot{x}C\theta_o - \dot{z}S\theta_o, \tag{2.34}$$

$$v' = U\tilde{\psi} + \dot{y} - US\theta_o\tilde{\phi}, \tag{2.35}$$

and

$$w' = \dot{z}C\theta_o + \dot{x}S\theta_o - UC\theta_o\tilde{\theta}. \tag{2.36}$$

Similarly, the body's acceleration with respect to the fluid stream is given by

$$\vec{a}_{c_r} = \frac{{}^{\mathcal{R}}d\vec{v}_c}{dt} + {}^{\mathcal{R}'\to\mathcal{R}}\vec{a} + {}^{\mathcal{R}\to\mathcal{R}'}\vec{w} \times \vec{v}_c,$$

which gives

$$\vec{a}_{c_r} = \frac{{}^{\mathcal{R}}d\vec{v}_c}{dt} \equiv a_1\vec{n}_1 + a_2\vec{n}_2 + a_3\vec{n}_3. \tag{2.37}$$

And, for the small perturbation case, (2.19)→(2.22), equations (2.13)→(2.15) and (2.37) give

$$a_1 = \ddot{x}C\theta_o - \ddot{z}S\theta_o, \tag{2.38}$$

$$a_2 = \ddot{y}, \tag{2.39}$$

and

$$a_3 = \ddot{z}C\theta_o + \ddot{x}S\theta_o. \tag{2.40}$$

Note that the acceleration of the body with respect to the fluid stream, $\mathcal{R}'$, is identical to that of the body with respect to the inertial reference frame, $\mathcal{R}$.

Finally, one obtains the small perturbation forms of the angular acceleration components by taking (2.19)→(2.22) into (2.16)→(2.18). This gives

$$p = \dot{\phi} - \dot{\psi} S\theta_o, \quad (2.41) \quad q = \dot{\theta}, \quad (2.42) \quad \text{and} \quad r = C\theta_o \dot{\psi}. \tag{2.43}$$

2.3 The Nondimensional Form of the First Order Force and Moment Equations

The factors used to nondimensionalize the terms in the force and moment equations are identical to those used in American airplane analysis, except that no distinction is made between a "longitudinal" and "lateral" characteristic length. Now define

$$C_X, C_Y, C_Z, \hat{B}, \hat{mg}, \hat{T}_o \equiv \frac{F_1, F_2, F_3, B, mg, T_o}{(\rho U^2 S/2)}, \tag{2.44}$$

$$C_\ell C_m, C_n \equiv \frac{M_1, M_2, M_3}{(\rho U^2 Sb/2)}, \tag{2.45}$$

$$\hat{x}, \hat{y}, \hat{z}, 2\hat{R}, 2\hat{R}_a \equiv \frac{x, y, z, R_B, R_a}{(b/2)}, \quad \hat{u}, \hat{v}, \hat{w} \equiv \frac{u', v', w'}{U}, \tag{2.46}$$

$$\hat{a}_1, \hat{a}_2, \hat{a}_3 \equiv \frac{a_1, a_2, a_3}{(2U^2/b)}, \quad \hat{p}, \hat{q}, \hat{r} \equiv \frac{p, q, r}{(2U/b)}, \tag{2.47}$$

$$t \equiv \frac{2U}{b} t, \quad \mu \equiv \frac{4m}{\rho Sb}, \tag{2.48}$$

$$i_{xx}, i_{yy}, i_{zz}, i_{xz} \equiv \frac{I_{xx}, I_{yy}, I_{zz}, I_{xz}}{\rho S(b/2)^3}, \tag{2.49}$$

$$D(\ ) \equiv \frac{b}{2U} \frac{d(\ )}{dt}, \quad (2.50) \quad \text{and} \quad D^2(\ ) \equiv \frac{b^2}{4U^2} \frac{d^2(\ )}{dt^2}. \tag{2.51}$$

Introducing these into the force and moment equations, (2.23)→(2.28), gives

$$C_X = \mu C\theta_o D^2 \hat{x} - \mu S\theta_o D^2 \hat{z}, \tag{2.52}$$

$$C_Y = \mu D^2 \hat{y}, \tag{2.53}$$

$$C_Z = \mu S\theta_o D^2\hat{x} + \mu C\theta_o D^2\hat{z}, \tag{2.54}$$

$$C_\ell = i_{xx} D^2\tilde{\phi} - (i_{xx} S\theta_o + i_{xz} C\theta_o) D^2\tilde{\psi}, \tag{2.55}$$

$$C_m = i_{yy} D^2\tilde{\theta}, \tag{2.56}$$

and

$$C_n = (i_{zz} C\theta_o + i_{xz} S\theta_o) D^2\tilde{\psi} - i_{xz} D^2\tilde{\phi}. \tag{2.57}$$

Further, equations (2.34)→(2.43) become

$$\hat{u} = C\theta_o D\hat{x} - S\theta_o D\hat{z}, \tag{2.58}$$

$$\hat{v} = D\hat{y} + \tilde{\psi} - S\theta_o \tilde{\phi}, \tag{2.59}$$

$$\hat{w} = S\theta_o D\hat{x} + C\theta_o D\hat{z} - C\theta_o \tilde{\theta}, \tag{2.60}$$

$$\hat{a}_1 = C\theta_o D^2\hat{x} - S\theta_o D^2\hat{z}, \tag{2.61}$$

$$\hat{a}_2 = D^2\hat{y}, \tag{2.62}$$

$$\hat{a}_3 = C\theta_o D^2\hat{z} + S\theta_o D^2\hat{x}, \tag{2.63}$$

$$\hat{p} = D\tilde{\phi} - S\theta_o D\tilde{\psi}, \tag{2.64}$$

$$\hat{q} = D\tilde{\theta}, \tag{2.65}$$

and

$$\hat{r} = C\theta_o D\tilde{\psi} \tag{2.66}$$

2.4 The Force and Moment Coefficient Terms

Consider the forces, F_i, and the moments, M_i, $(i = 1,2,3)$ on the body. Rewrite these as

$$F_i = F_{i_o} + \Delta F_i \quad \text{and} \quad M_i = M_{i_o} + \Delta M_i, \quad (i = 1,2,3)$$

where F_{i_o} and M_{i_o} are the reference values, and ΔF_i and ΔM_i are the perturbed quantities. Defining the reference condition to be that of static equilibrium, one obtains

$$F_{i_o} = M_{i_o} = 0. \quad \text{So,} \quad F_i = \Delta F_i \quad \text{and} \quad M_i = \Delta M_i. \tag{2.67}$$

Now, in the spirit of small perturbations, ΔF_i and ΔM_i are assumed to vary linearly in the perturbed velocity, the acceleration, and the angular velocity of the body relative to $\mathfrak{R}'$. Also, accounting for the body weight and buoyancy, one assumes that ΔF_i and ΔM_i vary linearly with the perturbed Eulerian angles. Finally, a cable force and moment contribution is accounted for by ΔF_{Ci} and ΔM_{Ci}. Thus, the general expressions for the force and moment terms are:

$$\Delta F_i = \frac{\partial F_i}{\partial u'}u' + \frac{\partial F_i}{\partial v'}v' + \frac{\partial F_i}{\partial w'}w' + \frac{\partial F_i}{\partial a_1}a_1 + \frac{\partial F_i}{\partial a_2}a_2$$

$$+ \frac{\partial F_i}{\partial a_3}a_3 + \frac{\partial F_i}{\partial p}p + \frac{\partial F_i}{\partial q}q + \frac{\partial F_i}{\partial r}r + \frac{\partial F_i}{\partial \tilde{\phi}}\tilde{\phi} \tag{2.68}$$

$$+ \frac{\partial F_i}{\partial \tilde{\theta}}\tilde{\theta} + \frac{\partial F_i}{\partial \tilde{\psi}}\tilde{\psi} + \Delta F_{Ci} \quad (i = 1,2,3)$$

and

$$\Delta M_i = \frac{\partial M_i}{\partial u'}u' + \frac{\partial M_i}{\partial v'}v' + \frac{\partial M_i}{\partial w'}w' + \frac{\partial M_i}{\partial a_1}a_1 + \frac{\partial M_i}{\partial a_2}a_2$$

$$+ \frac{\partial M_i}{\partial a_3}a_3 + \frac{\partial M_i}{\partial p}p + \frac{\partial M_i}{\partial q}q + \frac{\partial M_i}{\partial r}r + \frac{\partial M_i}{\partial \tilde{\psi}}\tilde{\psi} \tag{2.69}$$

$$+ \frac{\partial M_i}{\partial \tilde{\theta}}\tilde{\theta} + \frac{\partial M_i}{\partial \tilde{\phi}}\tilde{\phi} + \Delta M_{Ci} \quad (i = 1,2,3)$$

Further, when one defines the nondimensional parameters,

$$C_{Fi_u}, C_{Fi_v}, C_{Fi_w} \equiv \left(\frac{2}{\rho US}\right)\frac{\partial F_i}{\partial u'}, \frac{\partial F_i}{\partial v'}, \frac{\partial F_i}{\partial w'}, \tag{2.70}$$

$$C_{Mi_u}, C_{Mi_v}, C_{Mi_w} \equiv \left(\frac{2}{\rho UbS}\right)\frac{\partial M_i}{\partial u'}, \frac{\partial M_i}{\partial v'}, \frac{\partial M_i}{\partial w'}, \tag{2.71}$$

$$C_{Fi_{\dot{u}}}, C_{Fi_{\dot{v}}}, C_{Fi_{\dot{w}}} \equiv \left(\frac{2}{\rho Sb}\right)\frac{\partial F_i}{\partial a_1}, \frac{\partial F_i}{\partial a_2}, \frac{\partial F_i}{\partial a_3}, \tag{2.72}$$

$$C_{Mi_{\dot{u}}}, C_{Mi_{\dot{v}}}, C_{Mi_{\dot{w}}} \equiv \left(\frac{4}{\rho Sb^2}\right)\frac{\partial M_i}{\partial a_1}, \frac{\partial M_i}{\partial a_2}, \frac{\partial M_i}{\partial a_3}, \tag{2.73}$$

$$C_{Fi_p}, C_{Fi_q}, C_{Fi_r} \equiv \left(\frac{4}{\rho USb}\right)\frac{\partial F_i}{\partial p}, \frac{\partial F_i}{\partial q}, \frac{\partial F_i}{\partial r}, \tag{2.74}$$

$$C_{Mi_p}, C_{Mi_q}, C_{Mi_r} \equiv \left(\frac{4}{\rho USb^2}\right)\frac{\partial M_i}{\partial p}, \frac{\partial M_i}{\partial q}, \frac{\partial M_i}{\partial r}, \tag{2.75}$$

$$C_{Fi_{\tilde{\psi}}}, C_{Fi_{\tilde{\theta}}}, C_{Fi_{\tilde{\phi}}} \equiv \left(\frac{2}{\rho U^2 S}\right)\frac{\partial F_i}{\partial \tilde{\psi}}, \frac{\partial F_i}{\partial \tilde{\theta}}, \frac{\partial F_i}{\partial \tilde{\phi}}, \tag{2.76}$$

$$C_{Mi_{\tilde{\psi}}}, C_{Mi_{\tilde{\theta}}}, C_{Mi_{\tilde{\phi}}} \equiv \left(\frac{2}{\rho USb^2}\right)\frac{\partial M_i}{\partial \tilde{\psi}}, \frac{\partial M_i}{\partial \tilde{\theta}}, \frac{\partial M_i}{\partial \tilde{\phi}} \tag{2.77}$$

$$C_{Fi_C} \equiv \frac{2\Delta F_{i_C}}{\rho U^2 S} = \frac{2\Delta F_{i_C}}{\rho U^2 LR}\left(\frac{LR}{S}\right), \tag{2.78}$$

and

$$C_{Mi_C} \equiv \frac{2\Delta M_{i_C}}{\rho U^2 Sb} = \frac{2\Delta M_{i_C}}{\rho U^2 LRb}\left(\frac{LR}{S}\right), \tag{2.79}$$

equations (2.68) and (2.69) become

$$\begin{aligned} C_{Fi} = {} & C_{Fi_u}\hat{u} + C_{Fi_v}\hat{v} + C_{Fi_w}\hat{w} + C_{Fi_u}\hat{a}_1 + C_{Fi_v}\hat{a}_2 + C_{Fi_w}\hat{a}_3 \\ & + C_{Fi_p}\hat{p} + C_{Fi_q}\hat{q} + C_{Fi_r}\hat{r} + C_{Fi_{\tilde{\psi}}}\tilde{\psi} + C_{Fi_{\tilde{\theta}}}\tilde{\theta} + C_{Fi_{\tilde{\phi}}}\tilde{\phi} + C_{Fi_C} \\ & (i = 1, 2, 3) \end{aligned} \tag{2.80}$$

and

$$C_{Mi} = C_{Mi_u}\hat{u} + C_{Mi_v}\hat{v} + C_{Mi_w}\hat{w} + C_{Mi_{\dot{u}}}\hat{a}_1 + C_{Mi_{\dot{v}}}\hat{a}_2 + C_{Mi_{\dot{w}}}\hat{a}_3$$

$$+ C_{Mi_p}\hat{p} + C_{Mi_q}\hat{q} + C_{Mi_r}\hat{r} + C_{Mi_{\tilde{\psi}}}\tilde{\psi} + C_{Mi_{\tilde{\theta}}}\tilde{\theta} + C_{Mi_{\tilde{\phi}}}\tilde{\phi} + C_{Mi_C} \qquad (2.81)$$

$(i = 1, 2, 3)$

Now, as in airplane stability analysis, cross derivative terms are dropped; that is, fluid dynamic stability derivatives of symmetrical quantities with respect to unsymmetrical variables are dropped. Thus,

$$C_{m_v}, C_{m_{\dot{v}}}, C_{m_p}, C_{m_r}, C_{X_v}, C_{X_{\dot{v}}}, C_{X_p}, \text{ and } C_{X_r} = 0. \qquad (2.82)$$

Similarly, fluid dynamic derivatives of unsymmetrical quantities with respect to symmetrical variables are dropped. So,

$$C_{Y_u}, C_{Y_w}, C_{Y_{\dot{u}}}, C_{Y_{\dot{w}}}, C_{Y_q}, C_{Z_v}, C_{Z_{\dot{v}}}, C_{Z_p}, C_{Z_r}, C_{\ell_u}, C_{\ell_w},$$
$$C_{\ell_{\dot{u}}}, C_{\ell_{\dot{w}}}, C_{\ell_q}, C_{n_u}, C_{n_w}, C_{n_{\dot{u}}}, C_{n_{\dot{w}}}, \text{ and } C_{n_q} = 0. \qquad (2.83)$$

Further, considering the gravity and buoyancy effects, one has

$$\vec{F}_g + \vec{B} = (B - mg)\vec{e}_3 \qquad \text{(see Fig. 7),}$$

which, by (2.11), gives

$$\vec{F}_g + \vec{B} = (B - mg)(-S\theta\vec{n}_1 + C\theta S\phi\vec{n}_2 + C\theta C\phi\vec{n}_3).$$

Further, the perturbation value from equilibrium is found by using (2.19)→(2.22), and dropping terms of order ϵ^2 and higher. This gives

$$\Delta(\vec{F}_g + \vec{B}) = (B - mg)(-C\theta_o\tilde{\theta}\vec{n}_1 + C\theta_o\tilde{\phi}\vec{n}_2 - S\theta_o\tilde{\theta}\vec{n}_3). \qquad (2.84)$$

Thus, (2.84) and (2.76) give

$$C_{X_\psi}, C_{X_\phi}, C_{Y_\psi}, C_{Y_\theta}, C_{Z_\psi}, \text{ and } C_{Z_\phi} = 0 \qquad (2.85)$$

and

$$C_{X_\theta} = -(\hat{B} - m\hat{g})C\theta_o, \; C_{Y_\phi} = (\hat{B} - m\hat{g})C\theta_o, \text{ and } C_{Z_\theta} = -(\hat{B} - m\hat{g})S\theta_o \qquad (2.86)$$

Similarly, the moment about the mass center due to buoyancy effects is given by

$$\vec{M}_B = \vec{R}_B \times \vec{B} = R_B B(\vec{n}_1 \times \vec{e}_3) \qquad \text{(see Fig. 7).}$$

Using (2.11), one obtains

$$\vec{M}_B = R_B B(-C\theta C\phi \vec{n}_2 + C\theta S\phi \vec{n}_3),$$

for which, again, the perturbation value from equilibrium is found by using (2.19)→(2.22), and dropping terms of order ϵ^2 and higher. This gives

$$\Delta\vec{M}_B = R_B B(S\theta_o \breve{\theta}\vec{n}_2 + C\theta_o \breve{\phi}\vec{n}_3). \tag{2.87}$$

Thus, (2.77) and (2.87) give

$$C_{m_\phi}, C_{m_\psi}, C_{n_\theta}, C_{n_\psi}, C_{\ell_\phi}, C_{\ell_\theta}, \text{ and } C_{\ell_\psi} = 0, \tag{2.88}$$

$$C_{m_\theta} = \hat{\hat{R}}\hat{B}S\theta_o \quad \text{and} \quad C_{n_\phi} = \hat{\hat{R}}\hat{B}C\theta_o . \tag{2.89}$$

Now, the cable effects on the body are considered. The cable terms in the force and moment equations provide the mathematical link between the body's motion and the cable's motion. The cable force is

$$\vec{T}_a = -T_o[(\frac{\partial \breve{x}}{\partial s})_a \vec{e}_1 + (\frac{\partial \breve{y}}{\partial s})_a \vec{e}_2 + (\frac{\partial \breve{z}}{\partial s})_a \vec{e}_3]. \tag{2.90}$$

Using equations (2.9)→(2.11), one may resolve this into the $\vec{n}_1, \vec{n}_2$, and $\vec{n}_3$ coordinate directions. Further, consider a perturbation of the cable from equilibrium such that

$$(\frac{\partial \breve{x}}{\partial s})_a = (\frac{\overline{\partial \breve{x}}}{\partial s})_a + (\frac{\partial \breve{x}'}{\partial s})_a , \quad (\frac{\partial \breve{y}}{\partial s})_a = (\frac{\partial \breve{y}'}{\partial s})_a \quad \text{and} \quad (\frac{\partial \breve{z}}{\partial s})_a = (\frac{\overline{\partial \breve{z}}}{\partial s})_a + (\frac{\partial \breve{z}'}{\partial s})_a , \tag{2.91}$$

where the "$\overline{\ \ }$" quantities are the equilibrium values, and the primed quantities are the perturbation variables. Consistent with the previous small perturbation analysis, (1.17), the primed terms are said to be of order ϵ. Thus, substituting (2.91) into equation (2.90), and dropping terms of order ϵ^2 and higher, one obtains the first order cable force. Now, the equilibrium cable force is

$$\vec{T}_o = -T_o[\{(\overline{\frac{\partial \check{x}}{\partial s}})_a C\theta_o - (\overline{\frac{\partial \check{z}}{\partial s}})_a S\theta_o\}\vec{n}_1 + \{(\overline{\frac{\partial \check{x}}{\partial s}})_a S\theta_o + (\overline{\frac{\partial \check{z}}{\partial s}})_a C\theta_o\}\vec{n}_3, \tag{2.92}$$

and, subtracting this from the first order cable force gives one the expression for the perturbation value of the cable force from equilibrium. Nondimensionalizing by (2.78), one obtains the components of this expression:

$$C_{X_C} = \hat{T}_o[(\frac{\partial \check{z}'}{\partial s})_a S\theta_o - (\frac{\partial \check{x}'}{\partial s})_a C\theta_o + \{(\overline{\frac{\partial \check{x}}{\partial s}})_a S\theta_o + (\overline{\frac{\partial \check{z}}{\partial s}})_a C\theta_o\}\tilde{\theta}], \tag{2.93}$$

$$C_{Y_C} = -\hat{T}_o[(\frac{\partial \check{y}'}{\partial s})_a + \{(\overline{\frac{\partial \check{x}}{\partial s}})_a S\theta_o + (\overline{\frac{\partial \check{z}}{\partial s}})_a C\theta_o\}\tilde{\phi} - (\overline{\frac{\partial \check{x}}{\partial s}})_a \tilde{\psi}], \tag{2.94}$$

and

$$C_{Z_C} = -\hat{T}_o[(\frac{\partial \check{z}'}{\partial s})_a C\theta_o + (\frac{\partial \check{x}'}{\partial s})_a S\theta_o + \{(\overline{\frac{\partial \check{x}}{\partial s}})_a C\theta_o - (\overline{\frac{\partial \check{z}}{\partial s}})_a S\theta_o\}\tilde{\theta}]. \tag{2.95}$$

In a similar fashion, the cable moment terms are derived. The moment on the body due to the cable force is

$$M_C = \vec{T}_a \times R_o\vec{n}_1, \tag{2.96}$$

where $\vec{T}_a$ is given by (2.90). Again, when one uses equations (2.9)→(2.11), equation (2.96) may be resolved into $\vec{n}_1, \vec{n}_2$, and $\vec{n}_3$ components. And further, as by (2.91), a small perturbation from equilibrium is taken, and terms of order ϵ^2 and higher are dropped. This gives the first order form of the cable moment. Now, the equilibrium cable moment is

$$M_{C_o} = -R_a T_o[(\overline{\frac{\partial \check{x}}{\partial s}})_a S\theta_o + (\overline{\frac{\partial \check{z}}{\partial s}})_a C\theta_o]\vec{n}_2, \tag{2.97}$$

and subtracting this from the first order cable moment gives one an expression for the perturbation value of the cable moment from equilibrium. Nondimensionalizing by (2.79), one finds that the components of this expression are

$$C_{\ell_C} = 0, \tag{2.98}$$

$$C_{m_C} = -\hat{R}_a \hat{T}_o [(\frac{\partial \check{x}'}{\partial s})_o S\theta_o + (\frac{\partial \check{z}'}{\partial s})_a C\theta_o + \{(\overline{\frac{\partial \check{x}}{\partial s}})_a C\theta_o - (\overline{\frac{\partial \check{z}}{\partial s}})_a S\theta_o\}\tilde{\theta}], \tag{2.99}$$

and

$$C_{n_C} = \hat{R}_a \hat{T}_o [(\frac{\partial \check{y}'}{\partial s})_a + \{(\overline{\frac{\partial \check{x}}{\partial s}})_a S\theta_o + (\overline{\frac{\partial \check{z}}{\partial s}})_a C\theta_o\}\tilde{\phi} - (\overline{\frac{\partial \check{x}}{\partial s}})_a \tilde{\psi}]. \tag{2.100}$$

Finally, substituting (2.82), (2.83), (2.85), (2.86), (2.88), (2.89), and (2.58)→(2.66) into (2.80) and (2.81) gives one the force and moment expressions in terms of the $\hat{x}, \hat{y}, \hat{z}, \tilde{\psi}, \tilde{\theta}, \tilde{\phi}$ coordinates, namely,

$$\begin{aligned} C_X = {} & [(C_{X_{\dot{u}}} C\theta_o + C_{X_{\dot{w}}} S\theta_o)D^2 + (C_{X_u} C\theta_o + C_{X_w} S\theta_o)D]\hat{x} + [(C_{X_{\dot{w}}} C\theta_o \\ & - C_{X_{\dot{u}}} S\theta_o)D^2 + (C_{X_w} C\theta_o - C_{X_u} S\theta_o)D]\hat{z} + [C_{X_q} D - C\theta_o\{C_{X_w} \\ & + (\hat{B} - m\hat{g})\}]\tilde{\theta} + C_{X_C}, \end{aligned} \tag{2.101}$$

$$\begin{aligned} C_Y = {} & (C_{Y_{\dot{v}}} D^2 + C_{Y_v} D)\hat{y} + [(C\theta_o C_{Y_r} - S\theta_o C_{Y_p})D + C_{Y_v}]\tilde{\psi} \\ & + [C_{Y_p} D - \{S\theta_o C_{Y_v} - (\hat{B} - m\hat{g})C\theta_o\}]\tilde{\phi} + C_{Y_C}, \end{aligned} \tag{2.102}$$

$$\begin{aligned} C_Z = {} & [(C_{Z_{\dot{w}}} C\theta_o - C_{Z_{\dot{u}}} S\theta_o)D^2 + (C_{Z_w} C\theta_o - C_{Z_u} S\theta_o)D]\hat{z} \\ & + [(C_{Z_{\dot{u}}} C\theta_o + C_{Z_{\dot{w}}} S\theta_o)D^2 + (C_{Z_u} C\theta_o + C_{Z_w} S\theta_o)D]\hat{x} \\ & + [C_{Z_q} D - \{C_{Z_w} C\theta_o + S\theta_o(\hat{B} - m\hat{g})\}]\tilde{\theta} + C_{Z_C}, \end{aligned} \tag{2.103}$$

$$\begin{aligned} C_{\ell} = {} & (C_{\ell_{\dot{v}}} D^2 + C_{\ell_v} D)\hat{y} + (C_{\ell_p} D - C_{\ell_v} S\theta_o)\tilde{\phi} \\ & + [(C_{\ell_r} C\theta_o - C_{\ell_p} S\theta_o)D + C_{\ell_v}]\tilde{\psi}, \end{aligned} \tag{2.104}$$

$$C_m = [(C_{m_{\dot{w}}} C\theta_o - C_{m_{\dot{u}}} S\theta_o)D^2 + (C_{m_w} C\theta_o - C_{m_u} S\theta_o)D]\hat{z}$$

$$+ [(C_{m_{\dot{u}}} C\theta_o + C_{m_{\dot{w}}} S\theta_o)D^2 + (C_{m_u} C\theta_o + C_{m_w} S\theta_o)D]\hat{x} \qquad (2.105)$$

$$+ [C_{m_q} D - \{C_{m_w} C\theta_o - \hat{R}\hat{B}\, S\theta_o \}]\tilde{\theta} + C_{m_C},$$

and

$$C_n = (C_{n_{\dot{v}}} D^2 + C_{n_v} D)\hat{y} + [(C_{n_r} C\theta_o - C_{n_p} S\theta_o)D + C_{n_v}]\tilde{\psi}$$

$$+ [C_{n_p} D + \{\hat{R}\hat{B}\, C\theta_o - C_{n_v} S\theta_o\}]\tilde{\phi} + C_{n_C}. \qquad (2.106)$$

Thus, equations (2.93)→(2.95) and (2.98)→(2.100) into equations (2.101)→(2.106) and these, in turn, into equations (2.52)→(2.57) constitute the complete force and moment equations for the body. Note that the fluid dynamic force coefficient terms, (2.70)→(2.75), may be directly related to the "stability derivatives" of standard airplane notation. The transformation equations to relate one to the other are given in the Appendix.

2.5 The End and Auxiliary Conditions as Given by the Force and Moment Equations

As mentioned in the introduction, the key to the solution of the cable-body problem is to solve the cable equations, where the body equations of motion provide end and auxiliary conditions. To this purpose, the body equations of motion must be rearranged and combined so as to isolate the cable terms. First, note that (2.94) and (2.100) combine to give an auxiliary condition:

$$C_{n_C} + \hat{R}_a C_{Y_C} = 0 \qquad (2.107)$$

A second auxiliary condition is given by (2.95) and (2.99):

$$C_{m_C} - \hat{R}_a C_{Z_C} = 0. \qquad (2.108)$$

Also, a third auxiliary condition is given by (2.98):

$$C_{\ell_C} = 0. \qquad (2.98)$$

Further, (2.94) gives an end condition:

$$\left(\frac{\partial \breve{y}'}{\partial s}\right)_a = -\frac{C_{Y_C}}{\hat{T}_o} - \left(\frac{\overline{\partial \breve{x}}}{\partial s}\right)_a (S\theta_o \breve{\phi} - \breve{\psi}) - \left(\frac{\overline{\partial \breve{z}}}{\partial s}\right)_a C\theta_o \breve{\phi}. \tag{2.109}$$

Similarly, (2.93) $\times S\theta_o$ - (2.95) $\times C\theta_o$ gives a second end condition:

$$\left(\frac{\partial \breve{z}'}{\partial s}\right)_a = \frac{1}{\hat{T}_o}(C_{X_C} S\theta_o - C_{Z_C} C\theta_o) - \left(\frac{\overline{\partial \breve{x}}}{\partial s}\right)_a \breve{\theta}. \tag{2.110}$$

And finally, a third end condition is given by (2.93) $\times C\theta_o$ + (2.95) $\times S\theta_o$:

$$\left(\frac{\partial \breve{x}'}{\partial s}\right)_a = \frac{1}{\hat{T}_o}(C_{X_C} C\theta_o + C_{Z_C} S\theta_o) + \left(\frac{\overline{\partial \breve{z}}}{\partial s}\right)_a \breve{\theta}. \tag{2.111}$$

Now, these conditions may be expanded into full form by using equations (2.101)→(2.106), (2.93)→(2.95), (2.98)→(2.100) and the force and moment equations (2.58)→(2.66). Doing such, one finds that the auxiliary condition, (2.107), becomes

$$(\pi_{21} D^2 + \pi_{22} D)\hat{y} + (-i_{xz} D^2 + \pi_{23} D + \pi_{24})\breve{\phi} + (\pi_{25} D^2 + \pi_{26} D + \pi_{27})\breve{\psi} = 0, \tag{2.112}$$

where

$$\pi_{21} \equiv \hat{R}_a(\mu - C_{Y_{\dot{v}}}) - C_{n_{\dot{v}}},$$

$$\pi_{22} \equiv -(C_{n_v} + \hat{R}_a C_{Y_v}),$$

$$\pi_{23} \equiv -(C_{n_p} + \hat{R}_a C_{Y_p}),$$

$$\pi_{24} \equiv S\theta_o(C_{n_v} + \hat{R}_a C_{Y_v}) - C\theta_o[\hat{R}\hat{B} + \hat{R}_a(\hat{B} - m\hat{g})],$$

$$\pi_{25} \equiv i_{zz} C\theta_o + i_{xz} S\theta_o,$$

$$\pi_{26} \equiv C_{n_p} S\theta_o - C_{n_r} C\theta_o - \hat{R}_a(C\theta_o C_{Y_r} - S\theta_o C_{Y_p}),$$

and

$$\pi_{27} \equiv -(C_{n_{\dot{v}}} + \hat{R}_a C_{Y_{\dot{v}}}).$$

Similarly, (2.108) becomes

$$(\pi_{28}D^2 + \pi_{29}D)\hat{x} + (\pi_{30}D^2 + \pi_{31}D)\hat{z} + (i_{yy}D^2 + \pi_{32}D + \pi_{33})\tilde{\theta} = 0, \tag{2.113}$$

where

$$\pi_{28} \equiv \hat{R}_a[S\theta_o(C_{Z_{\dot{w}}} - \mu) + C\theta_o C_{Z_{\dot{u}}}] - (C\theta_o C_{m_{\dot{u}}} + S\theta_o C_{m_{\dot{w}}}),$$

$$\pi_{30} \equiv \hat{R}_a[C\theta_o(C_{Z_{\dot{w}}} - \mu) - S\theta_o C_{Z_{\dot{u}}}] + S\theta_o C_{m_{\dot{u}}} - C\theta_o C_{m_{\dot{w}}},$$

$$\pi_{29} \equiv \hat{R}_a(C\theta_o C_{Z_u} + S\theta_o C_{Z_w}) - C\theta_o C_{m_u} - S\theta_o C_{m_w},$$

$$\pi_{31} \equiv \hat{R}_a(C\theta_o C_{Z_w} - S\theta_o C_{Z_u}) + S\theta_o C_{m_u} - C\theta_o C_{m_w},$$

$$\pi_{32} \equiv \hat{R}_a C_{Z_q} - C_{m_q},$$

and

$$\pi_{33} \equiv C\theta_o(C_{m_w} - \hat{R}_a C_{Z_w}) - S\theta_o[\hat{R}\hat{B} + \hat{R}_a(\hat{B} - m\hat{g})].$$

Also, in the same fashion, (2.98) becomes

$$(C_{\ell_{\dot{v}}}D^2 + C_{\ell_v}D)\hat{y} - (i_{xx}D^2 - C_{\ell_p}D + S\theta_o C_{\ell_v})\tilde{\phi} + (\pi_{19}D^2 + \pi_{20}D + C_{\ell_v})\tilde{\psi} = 0, \tag{2.114}$$

where

$$\pi_{19} \equiv i_{xx}S\theta_o + i_{xz}C\theta_o \quad \text{and} \quad \pi_{20} \equiv C_{\ell_r}C\theta_o - C_{\ell_p}S\theta_o.$$

Further, the end condition, (2.109), becomes

$$\left(\frac{\partial \check{y}'}{\partial s}\right)_a = (\pi_7 D^2 + \pi_8 D)\hat{y} + (\pi_9 D + \pi_{10})\tilde{\phi} + (\pi_{11}D + \pi_{12})\tilde{\psi}, \tag{2.115}$$

where

$$\pi_7 \equiv \frac{(C_{Y_{\dot{v}}} - \mu)}{\hat{T}_o}, \quad \pi_8 \equiv \frac{C_{Y_v}}{\hat{T}_o}, \quad \pi_9 \equiv \frac{C_{Y_p}}{\hat{T}_o},$$

$$\pi_{10} \equiv \frac{1}{\hat{T}_o}[(\hat{B} - \hat{mg})C\theta_o - S\theta_o C_{Y_v}] - S\theta_o(\overline{\overline{\frac{\partial \check{x}}{\partial s}}})_a - C\theta_o(\overline{\overline{\frac{\partial \check{z}}{\partial s}}})_a ,$$

$$\pi_{11} \equiv \frac{1}{\hat{T}_o}(C\theta_o C_{Y_r} - S\theta_o C_{Y_p}),$$

and

$$\pi_{12} \equiv \frac{C_{Y_v}}{\hat{T}_o} + (\overline{\overline{\frac{\partial \check{x}}{\partial s}}})_a .$$

Also, the end condition, (2.110), becomes

$$(\frac{\partial \check{z}'}{\partial s})_a = (\pi_{13}D^2 + \pi_{14}D)\hat{x} + (\pi_{15}D^2 + \pi_{16}D)\hat{z} + (\pi_{17}D + \pi_{18})\tilde{\theta}, \qquad (2.116)$$

where

$$\pi_{13} \equiv \frac{1}{\hat{T}_o}[C\theta_o(C\theta_o C_{Z_{\dot{u}}} + S\theta_o C_{Z_{\dot{w}}}) - S\theta_o(C\theta_o C_{X_{\dot{u}}} + S\theta_o C_{X_{\dot{w}}})],$$

$$\pi_{14} \equiv \frac{-1}{\hat{T}_o}[S\theta_o(C\theta_o C_{X_u} + S\theta_o C_{X_w}) - C\theta_o(C\theta_o C_{Z_u} + S\theta_o C_{Z_w})],$$

$$\pi_{15} \equiv \frac{1}{\hat{T}_o}[S\theta_o(S\theta_o C_{X_{\dot{u}}} - C\theta_o C_{X_{\dot{w}}}) + C\theta_o(C\theta_o C_{Z_{\dot{w}}} - S\theta_o C_{Z_{\dot{u}}}) - \mu],$$

$$\pi_{16} \equiv \frac{1}{\hat{T}_o}[S\theta_o(S\theta_o C_{X_u} - C\theta_o C_{X_w}) + C\theta_o(C\theta_o C_{Z_w} - S\theta_o C_{Z_u})],$$

$$\pi_{17} \equiv \frac{1}{\hat{T}_o}(C\theta_o C_{Z_q} - S\theta_o C_{X_q}),$$

and

$$\pi_{18} \equiv \frac{1}{\hat{T}_o}C\theta_o(S\theta_o C_{X_w} - C\theta_o C_{Z_w}) - (\overline{\overline{\frac{\partial \check{x}}{\partial s}}})_a .$$

And finally, the end condition, (2.111), becomes

$$\left(\frac{\partial \check{\mathbf{x}}'}{\partial s}\right)_a \equiv (\pi_1 D^2 + \pi_2 D)\hat{x} + (\pi_3 D^2 + \pi_4 D)\hat{z} + (\pi_5 D + \pi_6)\tilde{\theta}, \tag{2.117}$$

where

$$\pi_1 \equiv \frac{1}{\hat{T}_o}[C\theta_o(C_{X_{\dot{u}}} C\theta_o + C_{X_{\dot{w}}} S\theta_o) + S\theta_o(C\theta_o C_{Z_{\dot{u}}} + S\theta_o C_{Z_{\dot{w}}}) - \mu],$$

$$\pi_2 \equiv \frac{1}{\hat{T}_o}[C\theta_o(C_{X_u} C\theta_o + C_{X_w} S\theta_o) + S\theta_o(C\theta_o C_{Z_u} + S\theta_o C_{Z_w})],$$

$$\pi_3 \equiv \frac{1}{\hat{T}_o}[C\theta_o(C\theta_o C_{X_{\dot{w}}} - S\theta_o C_{X_{\dot{u}}}) + S\theta_o(C\theta_o C_{Z_{\dot{w}}} - S\theta_o C_{Z_{\dot{u}}})],$$

$$\pi_4 \equiv \frac{1}{\hat{T}_o}[C\theta_o(C\theta_o C_{X_w} - S\theta_o C_{X_u}) + S\theta_o(C\theta_o C_{Z_w} - S\theta_o C_{Z_u})],$$

$$\pi_5 \equiv \frac{1}{\hat{T}_o}(C\theta_o C_{X_q} + S\theta_o C_{Z_q}),$$

and

$$\pi_6 \equiv \frac{1}{\hat{T}_o}[C\theta_o(C\theta_o C_{X_w} + S\theta_o C_{Z_w}) + \hat{B} - m\hat{g}] + \left(\frac{\overline{\partial \check{z}}}{\partial s}\right)_a .$$

2.6 The Transformation of the End and Auxiliary Conditions to the Cable Coordinates

Note that the end and auxiliary conditions, (2.112)→(2.117), are expressed in terms of the $\check{x}', \check{y}'$ and $\check{z}'$ coordinates of the cable, and the $\hat{x}, \hat{y}$, and $\hat{z}$ coordinates of the body's mass center. Thus, in order to apply these conditions directly to the cable equations, (1.28), (1.31), and (1.34), one must transform them to the cable coordinates $\tilde{\xi}, \tilde{y}$ and $\tilde{\zeta}$. Consider now the following transformation equations (see Fig. 8):

$$x = C\tilde{\alpha}\xi(1,t) - S\tilde{\alpha}\zeta(1,t) + R_a C\psi C\theta, \tag{2.118}$$

$$y = \check{y} + R_a S\psi C\theta, \tag{2.119}$$

and

$$z = C\tilde{\alpha}\zeta(1,t) + S\tilde{\alpha}\xi(1,t) - R_a S\theta. \tag{2.120}$$

Using the small perturbation assumptions for the cable (1.14)→(1.17), and the small perturbation assumptions for the body, (2.19)→(2.22), one obtains the transformation equations for the first order problem. Further, nondimensionalizing by equations (1.24), (2.46), (2.50) and (2.51), one has

$$D\hat{x} = -(\frac{2L}{b})S\tilde{\alpha}D\tilde{\zeta}(1,\hat{t}) - 2\hat{R}_a S\theta_o D\tilde{\theta},$$

$$D^2\hat{x} = -(\frac{2L}{b})S\tilde{\alpha}D^2\tilde{\zeta}(1,\hat{t}) - 2\hat{R}_a S\theta_o D^2\tilde{\theta}, \tag{2.121}$$

$$D\hat{y} = (\frac{2L}{b})D\tilde{y}(1,\hat{t}) + 2\hat{R}_a C\theta_o D\tilde{\psi},$$

$$D^2\hat{y} = (\frac{2L}{b})D^2\tilde{y}(1,\hat{t}) + 2\hat{R}_a C\theta_o D^2\tilde{\psi}, \tag{2.122}$$

$$D\hat{z} = (\frac{2L}{b})C\tilde{\alpha}D\tilde{\zeta}(1,\hat{t}) - 2\hat{R}_a C\theta_o D\tilde{\theta},$$

and

$$D^2\hat{z} = (\frac{2L}{b})C\tilde{\alpha}D^2\tilde{\zeta}(1,\hat{t}) - 2\hat{R}_a C\theta_o D^2\tilde{\theta}. \tag{2.123}$$

Note now that, at the attachment point, one has the following relationships:

$$(\overline{\overline{\frac{\partial\tilde{x}}{\partial s}})}_a = (\overline{\overline{\frac{\partial\tilde{x}}{\partial s}})}_a \frac{\partial\xi}{\partial s}(1,\hat{t}) - (\overline{\overline{\frac{\partial\tilde{z}}{\partial s}})}_a \frac{\partial\zeta}{\partial s}(1,\hat{t}), \tag{2.124}$$

and

$$(\overline{\overline{\frac{\partial\tilde{z}}{\partial s}})}_a = (\overline{\overline{\frac{\partial\tilde{x}}{\partial s}})}_a \frac{\partial\zeta}{\partial s}(1,\hat{t}) + (\overline{\overline{\frac{\partial\tilde{z}}{\partial s}})}_a \frac{\partial\xi}{\partial s}(1,\hat{t}). \tag{2.125}$$

Multiplying (2.124) by $(\overline{\overline{\partial\tilde{z}/\partial s}})_a$ and (2.125) by $(\overline{\overline{\partial\tilde{x}/\partial s}})_a$ and adding the two, one obtains a relationship for the cable slope in the two coordinate systems. Using the small perturbation relations, (1.14)→(1.17) and (2.91), and nondimensionalizing by (1.24), one obtains the relationship in the following form:

$$\frac{\partial\tilde{\zeta}}{\partial\tilde{s}}(1,\hat{t}) = \left(\frac{\partial\check{x}}{\partial s}\right)_a \left(\frac{\partial\check{z}'}{\partial s}\right)_a - \left(\frac{\partial\check{z}}{\partial s}\right)_a \left(\frac{\partial\check{x}'}{\partial s}\right)_a . \tag{2.126}$$

Now, when one uses equations (2.121)→(2.123) and (2.126), the end and auxiliary conditions (2.112)→(2.117) may be expressed in the cable coordinates. First, (2.121) and (2.123) into (2.113) give the auxiliary condition:

$$(\pi_{45}D^2 + \pi_{46}D)\tilde{\zeta}(1,\hat{t}) + (\pi_{47}D^2 + \pi_{48}D + \pi_{33})\tilde{\theta} = 0, \tag{2.127}$$

where

$$\pi_{45} \equiv \left(\frac{2L}{b}\right)(\pi_{30}C\tilde{\alpha} - \pi_{28}S\tilde{\alpha}),$$

$$\pi_{46} \equiv \left(\frac{2L}{b}\right)(\pi_{31}C\tilde{\alpha} - \pi_{29}S\tilde{\alpha}),$$

$$\pi_{47} \equiv i_{yy} - 2\hat{R}_a(\pi_{28}S\theta_o + \pi_{30}C\theta_o),$$

and

$$\pi_{48} \equiv \pi_{32} - 2\hat{R}_a(\pi_{29}S\theta_o + \pi_{31}C\theta_o).$$

Similarly, (2.122) into (2.112) gives an auxiliary condition:

$$(\pi_{49}D^2 + \pi_{50}D)\tilde{y}(1,\hat{t}) + (-i_{xz}D^2 + \pi_{23}D + \pi_{24})\tilde{\phi} + (\pi_{51}D^2 + \pi_{52}D + \pi_{27})\tilde{\psi} = 0, \tag{2.128}$$

where

$$\pi_{49} \equiv \left(\frac{2L}{b}\right)\pi_{21}, \quad \pi_{50} \equiv \left(\frac{2L}{b}\right)\pi_{22},$$

$$\pi_{51} \equiv 2\hat{R}_a C\theta_o \pi_{21} + \pi_{25} \quad \text{and} \quad \pi_{52} \equiv \pi_{26} + 2\hat{R}_a \pi_{22} C\theta_o.$$

Further, equations (2.122) into (2.114) give another auxiliary condition:

$$(\pi_{53}D^2 + \pi_{54}D)\tilde{y}(1,\hat{t}) + (-i_{xx}D^2 + C_{\ell_p}D - S\theta_o C_{\ell_v})\tilde{\phi} + (\pi_{55}D^2 + \pi_{56}D + C_{\ell_v})\tilde{\psi} = 0 \tag{2.129}$$

where

$$\pi_{53} \equiv (\frac{2L}{b})C_{\ell_v}, \quad \pi_{54} \equiv (\frac{2L}{b})C_{\ell_v},$$

$$\pi_{55} \equiv \pi_{19} + 2\hat{R}_a C\theta_o, \quad \text{and} \quad \pi_{56} \equiv \pi_{20} + 2\hat{R}_a C\theta_o.$$

Now, an end condition is given by (2.121), (2.123), (2.116), and (2.117) into (2.126). This becomes

$$\frac{\partial\tilde{\zeta}}{\partial\tilde{s}}(1,\hat{t}) = (\pi_{40}D^2 + \pi_{41}D)\tilde{\zeta}(1,\hat{t}) + (\pi_{42}D^2 + \pi_{43}D + \pi_{44})\tilde{\theta}, \tag{2.130}$$

where

$$\pi_{40} \equiv (\frac{2L}{b})[(\overline{\frac{\partial\tilde{x}}{\partial s}})_a (\pi_{15}C\tilde{\alpha} - \pi_{13}S\tilde{\alpha}) - (\overline{\frac{\partial\tilde{z}}{\partial s}})_a (\pi_3 C\tilde{\alpha} - \pi_1 S\tilde{\alpha})],$$

$$\pi_{41} \equiv (\frac{2L}{b})[(\overline{\frac{\partial\tilde{x}}{\partial s}})_a (\pi_{16}C\tilde{\alpha} - \pi_{14}S\tilde{\alpha}) - (\overline{\frac{\partial\tilde{z}}{\partial s}})_a (\pi_4 C\tilde{\alpha} - \pi_2 S\tilde{\alpha})],$$

$$\pi_{42} \equiv \hat{R}_a[(\overline{\frac{\partial\tilde{z}}{\partial s}})_a (\pi_1 S\theta_o + \pi_3 C\theta_o) - (\overline{\frac{\partial\tilde{x}}{\partial s}})_a (\pi_{13}S\theta_o + \pi_{15}C\theta_o)],$$

$$\pi_{43} \equiv [(\overline{\frac{\partial\tilde{x}}{\partial s}})_a \{\pi_{17} - 2\hat{R}_a(\pi_{14}S\theta_o + \pi_{16}C\theta_o)\} - (\overline{\frac{\partial\tilde{z}}{\partial s}})_a \{\pi_5 - 2\hat{R}_a(\pi_2 S\theta_o + \pi_4 C\theta_o)\}],$$

and

$$\pi_{44} \equiv (\overline{\frac{\partial\tilde{x}}{\partial s}})_a \pi_{18} - (\overline{\frac{\partial\tilde{z}}{\partial s}})_a \pi_6.$$

Also, an end condition is given by (2.122) into (2.115):

$$\frac{\partial\tilde{y}}{\partial\tilde{s}}(1,\hat{t}) = (\pi_{57}D^2 + \pi_{58}D)\tilde{y} + (\pi_9 D + \pi_{10})\tilde{\phi} + (\pi_{59}D^2 + \pi_{60}D + \pi_{12})\tilde{\psi}, \tag{2.131}$$

where

$$\pi_{57} \equiv (\frac{2L}{b})\pi_7, \quad \pi_{58} \equiv (\frac{2L}{b})\pi_8,$$

$$\pi_{59} \equiv 2\hat{R}_a C\theta_o \pi_7, \quad \text{and} \quad \pi_{60} \equiv \pi_{11} + 2\hat{R}_a C\theta_o \pi_8.$$

Finally, to complete the set of end conditions, assume that the cable is fixed at the origin of the $\check{x},\check{y},\check{z}$ coordinate system. This gives

$$\tilde{\xi}(0,\hat{t}) = 0, \quad (2.132), \quad y(0,\hat{t}) = 0, \quad (2.133), \quad \text{and} \quad \tilde{\zeta}(0,\hat{t}) = 0. \qquad (2.134)$$

Thus, (2.127)→(2.134) give the end and auxiliary conditions for the cable equations (1.28), (1.31), and (1.34). The nature of the solution is such that initial conditions need not be specified, that is, the general solution is sought. Therefore, the problem statement is now complete.

3. THE SOLUTION OF THE CABLE-BODY EQUATIONS

3.1 A Discussion of the Equations

Note the very important fact that the equations uncouple into two separate problems. The cable equation, (1.34), along with the end conditions, (2.130) and (2.134), and auxiliary condition, (2.127), constitutes a complete problem for the general solution of $\tilde{\zeta}(\tilde{s},t)$ and $\tilde{\theta}(\hat{t})$. Similarly, the cable equation, (1.31), with the end conditions, (2.131) and (2.133), along with the auxiliary conditions, (2.128) and (2.129), gives a complete problem for the general solution of $\tilde{y}(\tilde{s},\hat{t})$, $\tilde{\phi}(\hat{t})$ and $\tilde{\vartheta}(\hat{t})$. Physically, this means that the first order problem uncouples into two distinct modes: lateral and longitudinal motions. Such uncoupling is, in fact, observed by experiment (Chapter 4 and Ref. (1)). Further, these motions have certain analogies to uncoupled airplane motion, although the comparison must not be carried too far, since the two mechanical systems are fundamentally different. Each of these problems is now treated separately.

Note finally that, consistent with condition (1.15), the $\tilde{\xi}(\tilde{s},\hat{t})$ coordinate is of no significance in the first order problem.

3.2 The Longitudinal Solution

The longitudinal problem is described by the following equations:

Cable Equation:

$$D^2\tilde{\zeta} - \hat{C}^2\frac{\partial^2\tilde{\zeta}}{\partial\tilde{s}^2} + k_3 D\tilde{\zeta} + k_4\frac{\partial\tilde{\zeta}}{\partial\tilde{s}} = 0. \tag{1.34}$$

End Conditions:

$$\frac{\partial\tilde{\zeta}}{\partial\tilde{s}}(1,\hat{t}) = (\pi_{40}D^2 + \pi_{41}D)\tilde{\zeta}(1,\hat{t}) + (\pi_{42}D^2 + \pi_{43}D + \pi_{44})\tilde{\theta}, \tag{2.130}$$

and

$$\tilde{\zeta}(0,\hat{t}) = 0. \tag{2.134}$$

Auxiliary Condition:

$$(\pi_{45}D^2 + \pi_{46}D)\tilde{\zeta}(1,\hat{t}) + (\pi_{47}D^2 + \pi_{48}D + \pi_{33})\tilde{\theta} = 0. \tag{2.127}$$

These equations are linear, and have constant coefficients. Therefore, in the spirit of linear differential equation theory, the solution is assumed to be of the following form:

$$\tilde{\zeta}(\tilde{s},\hat{t}) = Z(\tilde{s})e^{\sigma\hat{t}} \quad \text{and} \quad \tilde{\theta} = \Theta e^{\sigma\hat{t}}, \tag{3.1}$$

where Θ is a constant. Now, substituting this into the partial differential equation, (1.34), one obtains an ordinary differential equation for $Z(\tilde{s})$:

$$(\sigma^2 + k_3\sigma)Z + k_4 \frac{dZ}{d\tilde{s}} - \hat{C}^2 \frac{d^2Z}{d\tilde{s}^2} = 0. \tag{3.2}$$

Also, by ordinary differential equation theory, the general solution of this is

$$Z(\tilde{s}) = Z_{o_1} e^{(\Lambda + \Omega)\tilde{s}} + Z_{o_2} e^{(\Lambda - \Omega)\tilde{s}}, \tag{3.3}$$

where

$$\Lambda \equiv \frac{k_4}{2\hat{C}^2} \quad \text{and} \quad \Omega \equiv \left[\frac{k_4}{4\hat{C}^4} + \frac{(\sigma^2 + k_3\sigma)}{\hat{C}^2} \right]^{1/2}. \tag{3.4}$$

Now, by the end condition, (2.134):

$$Z(0) = 0 = Z_{o_1} + Z_{o_2}.$$

Thus, (3.3) becomes

$$Z(\tilde{s}) = Z_o e^{\Lambda\tilde{s}}(e^{\Omega\tilde{s}} - e^{-\Omega\tilde{s}}). \tag{3.5}$$

Using this, and substituting (3.1) into the end condition (2.130), one obtains

$$e^{\Lambda}(e^{\Omega} - e^{-\Omega}) \left[\pi_{40}\sigma^2 + \pi_{41}\sigma - \Lambda - \Omega \frac{(e^{\Omega} + e^{-\Omega})}{(e^{\Omega} - e^{-\Omega})} \right] Z_o + (\pi_{42}\sigma^2 + \pi_{43}\sigma + \pi_{44})\Theta = 0. \tag{3.6}$$

Further, (3.5) and (3.1) into the auxiliary condition, (2.127), give

$$e^{\Lambda}(e^{\Omega} - e^{-\Omega})(\pi_{45}\sigma^2 + \pi_{46}\sigma)Z_o + (\pi_{47}\sigma^2 + \pi_{48}\sigma + \pi_{33})\Theta = 0. \tag{3.7}$$

Equations (3.6) and (3.7) are two linear homogeneous equations in Z_o and Θ. Thus, it follows that an equation for σ (characteristic equation) may be obtained

by putting these two equations into a determinant, and setting it equal to zero. Doing this, one obtains

$$\begin{vmatrix} (\pi_{40}\sigma^2 + \pi_{41}\sigma - \Lambda - \Omega \coth \Omega), & (\pi_{42}\sigma^2 + \pi_{43}\sigma + \pi_{44}) \\ (\pi_{45}\sigma^2 + \pi_{46}\sigma), & (\pi_{47}\sigma^2 + \pi_{48}\sigma + \pi_{33}) \end{vmatrix} = 0, \qquad (3.8)$$

where

$$\coth \Omega \equiv \frac{(e^{\Omega} + e^{-\Omega})}{(e^{\Omega} - e^{-\Omega})}.$$

Note that σ is, in general, complex; that is,

$$\sigma = \sigma_r + j\sigma_j, \quad \text{where} \quad j = (-1)^{1/2}. \qquad (3.9)$$

Thus, the characteristic equation, (3.8), is a complex transcendental function in a complex variable. To facilitate finding the roots of this, one expands it into two real characteristic equations in two real variables, σ_r and σ_j. To this end, note first the expansion of $\Omega \coth \Omega$:

$$\Omega = \Omega_r + j\Omega_j, \qquad (3.10)$$

where

$$\Omega_r \equiv \frac{h_2}{\hat{C}} C\nu, \quad \Omega_j \equiv \frac{h_2}{\hat{C}} S\nu,$$

$$h_2 \equiv \left[\left(\frac{k_4^2}{4\hat{C}^2} + \sigma_r^2 - \sigma_j^2 + k_3\sigma_r\right)^2 + (2\sigma_r\sigma_j + k_3\sigma_j)^2\right]^{1/4},$$

and

$$\nu \equiv \frac{\tan^{-1}}{2}\left[(2\sigma_r\sigma_j + k_3\sigma_j)/\left(\frac{k_4^2}{4\hat{C}^2} + \sigma_r^2 - \sigma_j^2 + k_3\sigma_r\right)\right].$$

Thus,

$$\Omega \coth \Omega = H_3 + jH_4, \qquad (3.11)$$

where

$$H_3 \equiv \frac{\Omega_r \coth \Omega_r(1+\cot^2\Omega_j) - \Omega_j \cot \Omega_j(1+\coth^2\Omega_r)}{\coth^2\Omega_r + \cot^2\Omega_j},$$

and

$$H_4 \equiv \frac{\Omega_j \coth \Omega_r(1+\cot^2\Omega_j) + \Omega_r \cot \Omega_j(1-\coth^2\Omega_r)}{\coth^2\Omega_r + \cot^2\Omega_j}.$$

Now, this and (3.9) are substituted into the characteristic equation (3.8). Expanding this, and separating into the real and imaginary parts, one obtains two simultaneous real characteristic equations in two real variables, σ_r and σ_j. These are

$$G_r(\sigma_r, \sigma_j) = E_1E_7 - E_2E_8 - E_5E_3 + E_6E_4 = 0 \tag{3.12}$$

and

$$G_j(\sigma_r, \sigma_j) = E_1E_8 + E_2E_7 - E_5E_4 - E_6E_3 = 0, \tag{3.13}$$

where

$$E_1 \equiv \pi_{40}(\sigma_r^2 - \sigma_j^2) + \pi_{41}\sigma_r - (\Lambda + H_3),$$

$$E_2 \equiv 2\pi_{40}\sigma_r\sigma_j + \pi_{41}\sigma_j - H_4,$$

$$E_3 \equiv \pi_{42}(\sigma_r^2 - \sigma_j^2) + \pi_{43}\sigma_r + \pi_{44},$$

$$E_4 \equiv 2\pi_{42}\sigma_r\sigma_j + \pi_{43}\sigma_j,$$

$$E_5 \equiv \pi_{45}(\sigma_r^2 - \sigma_j^2) + \pi_{46}\sigma_r,$$

$$E_6 \equiv 2\pi_{45}\sigma_r\sigma_j + \pi_{46}\sigma_j,$$

$$E_7 \equiv \pi_{47}(\sigma_r^2 - \sigma_j^2) + \pi_{48}\sigma_r + \pi_{33},$$

and

$$E_8 \equiv 2\pi_{47}\sigma_r\sigma_j + \pi_{48}\sigma_j.$$

An electronic computer is used to solve equations (3.12) and (3.13). This is explained in detail in Section 3.4.

3.3 The Lateral Solution

The lateral problem is described by the following equations:

Cable Equation:

$$D^2\tilde{y} - \hat{C}^2 \frac{\partial^2 \tilde{y}}{\partial \tilde{s}^2} + k_6 D\tilde{y} + k_7 \frac{\partial \tilde{y}}{\partial \tilde{s}} = 0. \tag{1.31}$$

End Conditions:

$$\frac{\partial \tilde{y}}{\partial \tilde{s}}(1, \hat{t}) = (\pi_{57}D^2 + \pi_{58}D)\tilde{y} + (\pi_9 D + \pi_{10})\tilde{\phi} + (\pi_{59}D^2 + \pi_{60}D + \pi_{12})\tilde{\psi} \tag{2.131}$$

and

$$\tilde{y}(0, \hat{t}) = 0. \tag{2.133}$$

Auxiliary Conditions:

$$(\pi_{49}D^2 + \pi_{50}D)\tilde{y}(1, \hat{t}) + (-i_{xz}D^2 + \pi_{23}D + \pi_{24})\tilde{\phi} + (\pi_{51}D^2 + \pi_{52}D + \pi_{27})\tilde{\psi} = 0 \tag{2.128}$$

and

$$(\pi_{53}D^2 + \pi_{54}D)\tilde{y}(1, \hat{t}) + (-i_{xx}D^2 + C_{\ell_p}D - S\theta_o C_{\ell_v})\tilde{\phi} + (\pi_{55}D^2 + \pi_{56}D + C_{\ell_v})\tilde{\psi} = 0. \tag{2.129}$$

As in the longitudinal case, these equations are linear, and have constant coefficients. Therefore, the solution is assumed to be of the form:

$$\tilde{y}(\tilde{s}, \hat{t}) = Y(\tilde{s})e^{\lambda \hat{t}}, \quad \tilde{\psi} = \Psi e^{\lambda \hat{t}}, \quad \text{and} \quad \tilde{\phi} = \Phi e^{\lambda \hat{t}}, \tag{3.14}$$

where Ψ and Φ are constants. Now, substituting this into the partial differential equation, (1.31), one obtains an ordinary differential equation for $Y(\tilde{s})$:

$$(\lambda^2 + k_6\lambda)Y + k_7 \frac{dY}{d\tilde{s}} - \hat{C}^2 \frac{d^2Y}{d\tilde{s}^2} = 0. \tag{3.15}$$

Further, the general solution of this equation is

$$Y(\tilde{s}) = Y_{o_1} e^{(r + \Delta)\tilde{s}} + Y_{o_2} e^{(r - \Delta)\tilde{s}}, \tag{3.16}$$

where

$$\Gamma \equiv \frac{k_7}{2\hat{C}^2} \quad \text{and} \quad \Delta \equiv \left[\frac{k_7^2}{4\hat{C}^2} + \frac{(\lambda^2 + k_6\lambda)}{\hat{C}^2}\right]^{1/2}. \tag{3.17}$$

The end condition, (2.133), gives

$$Y(0) = 0 = Y_{o_1} + Y_{o_2}.$$

Thus (3.16) becomes

$$Y(\tilde{s}) = Y_o e^{\Gamma\tilde{s}}(e^{\Delta\tilde{s}} - e^{-\Delta\tilde{s}}). \tag{3.18}$$

Using this, and substituting (3.14) into the end condition, (2.131), one obtains

$$e^{\Gamma}(e^{\Delta} - e^{-\Delta})[\pi_{57}\lambda^2 + \pi_{58}\lambda - \Gamma - \Delta\frac{(e^{\Delta} + e^{-\Delta})}{(e^{\Delta} - e^{-\Delta})}]Y_o$$
$$+ (\pi_9\lambda + \pi_{10})\Phi + (\pi_{59}\lambda^2 + \pi_{60}\lambda + \pi_{12})\Psi = 0. \tag{3.19}$$

Further, (3.18) and (3.14) into the auxiliary conditions, (2.128) and (2.129), give

$$e^{\Gamma}(e^{\Delta} - e^{-\Delta})(\pi_{49}\lambda^2 + \pi_{50}\lambda)Y_o + (-i_{xz}\lambda^2 + \pi_{23}\lambda + \pi_{24})\Phi$$
$$+ (\pi_{51}\lambda^2 + \pi_{52}\lambda + \pi_{27})\Psi = 0 \tag{3.20}$$

and

$$e^{\Gamma}(e^{\Delta} - e^{-\Delta})(\pi_{53}\lambda^2 + \pi_{54}\lambda)Y_o + (-i_{xx}\lambda^2 + C_{\ell_p}\lambda - S\theta_o C_{\ell_v})\Phi$$
$$+ (\pi_{55}\lambda^2 + \pi_{56}\lambda + C_{\ell_v})\Psi = 0. \tag{3.21}$$

Equations (3.19), (3.20), and (3.21) constitute a set of three linear homogeneous equations in Y_o, Ψ, and Φ. Thus, as in the longitudinal case, a characteristic equation for λ is obtained by putting these into a determinant, and setting it equal to zero. One then obtains

$$\begin{vmatrix} (\pi_{57}\lambda^2 + \pi_{58}\lambda - \Gamma - \Delta \coth \Delta), & (\pi_9\lambda + \pi_{10}), & (\pi_{59}\lambda^2 + \pi_{60}\lambda + \pi_{12}) \\ (\pi_{49}\lambda^2 + \pi_{50}\lambda), & (-i_{xz}\lambda^2 + \pi_{23}\lambda + \pi_{24}), & (\pi_{51}\lambda^2 + \pi_{52}\lambda + \pi_{27}) \\ (\pi_{53}\lambda^2 + \pi_{54}\lambda), & (-i_{xx}\lambda^2 + C_{\ell_p}\lambda - S\theta_o C_{\ell_v}), & (\pi_{55}\lambda^2 + \pi_{56}\lambda + C_{\ell_v}) \end{vmatrix} = 0 \quad (3.22)$$

where

$$\coth \Delta \equiv \frac{(e^{\Delta} + e^{-\Delta})}{(e^{\Delta} - e^{-\Delta})}.$$

Note that λ is, in general, complex; that is

$$\lambda = \lambda_r + j\lambda_j, \quad \text{where} \quad j = (-1)^{1/2}. \tag{3.23}$$

Thus, the characteristic equation, (3.22), is a complex transcendental function in a complex variable, λ. As in Section 3.2, the equation is expanded into two real characteristic equations in two real variables, λ_r and λ_j. Note now the expansion of $\Delta \coth \Delta$:

$$\Delta = \Delta_r + j\Delta_j, \tag{3.24}$$

where

$$\Delta_r \equiv \frac{h_1}{\hat{C}} C\upsilon, \quad \Delta_j \equiv \frac{h_1}{\hat{C}} S\upsilon,$$

$$h_1 \equiv \left[\left(\frac{k_7}{4\hat{C}^2} + \lambda_r^2 - \lambda_j^2 + k_6\lambda_r\right)^2 + (2\lambda_r\lambda_j + k_6\lambda_j)^2\right]^{1/4},$$

and

$$\upsilon \equiv \frac{\tan^{-1}}{2}\left[(2\lambda_r\lambda_j + k_6\lambda_j)/\left(\frac{k_7^2}{4\hat{C}^2} + \lambda_r^2 - \lambda_j^2 + k_6\lambda_j\right)\right].$$

Thus,

$$\Delta \coth \Delta = H_1 + jH_2, \tag{3.25}$$

where

$$H_1 \equiv \frac{\Delta_r \coth \Delta_r(1+\cot^2\Delta_j) - \Delta_j \cot \Delta_j(1-\coth^2\Delta_r)}{\coth^2\Delta_r + \cot^2\Delta_j},$$

and

$$H_2 \equiv \frac{\Delta_j \coth \Delta_r(1+\cot^2\Delta_j) + \Delta_r \cot \Delta_j(1-\coth^2\Delta_r)}{\coth^2\Delta_r + \cot^2\Delta_j}.$$

This and (3.23) are substituted into the characteristic equation (3.22). Expanding this, and separating into the real and imaginary parts, one obtains two simultaneous real characteristic equations in two real variables, λ_r and λ_j. These are

$$F_r(\lambda_r, \lambda_j) = A_1A_{19} - A_2A_{20} - A_{11}A_{21} + A_{12}A_{22} + A_{17}A_{23} - A_{18}A_{24} = 0 \quad (3.26)$$

and

$$F_j(\lambda_r, \lambda_j) = A_2A_{19} + A_1A_{20} - A_{12}A_{21} - A_{11}A_{22} + A_{18}A_{23} + A_{17}A_{24} = 0, \quad (3.27)$$

where

$$A_1 \equiv \pi_{57}(\lambda_r^2 - \lambda_j^2) + \pi_{58}\lambda_r - \Gamma - H_1,$$

$$A_2 \equiv 2\pi_{57}\lambda_r\lambda_j + \pi_{58}\lambda_j - H_2,$$

$$A_3 \equiv -i_{xz}(\lambda_r^2 - \lambda_j^2) + \pi_{23}\lambda_r + \pi_{24},$$

$$A_4 \equiv -2i_{xz}\lambda_r\lambda_j + \pi_{23}\lambda_j,$$

$$A_5 \equiv \pi_{51}(\lambda_r^2 - \lambda_j^2) + \pi_{52}\lambda_r + \pi_{27},$$

$$A_6 \equiv 2\pi_{51}\lambda_r\lambda_j + \pi_{52}\lambda_j,$$

$$A_7 \equiv -i_{xx}(\lambda_r^2 - \lambda_j^2) + C_{\ell_p}\lambda_r - S\theta_o C_{\ell_v},$$

$$A_8 \equiv -2i_{xx}\lambda_r\lambda_j + C_{\ell_p}\lambda_j,$$

$$A_9 \equiv \pi_{55}(\lambda_r^2 - \lambda_j^2) + \pi_{56}\lambda_r + C_{\ell_v},$$

$$A_{10} \equiv 2\pi_{55}\lambda_r\lambda_j + \pi_{56}\lambda_j,$$

$$A_{11} \equiv \pi_{49}(\lambda_r^2 - \lambda_j^2) + \pi_{50}\lambda_r,$$

$$A_{12} \equiv 2\pi_{49}\lambda_r\lambda_j + \pi_{50}\lambda_j,$$

$$A_{13} \equiv \pi_9\lambda_r + \pi_{10},$$

$$A_{14} \equiv \pi_9\lambda_j,$$

$$A_{15} \equiv \pi_{59}(\lambda_r^2 - \lambda_j^2) + \pi_{60}\lambda_j + \pi_{12},$$

$$A_{16} \equiv 2\pi_{59}\lambda_r\lambda_j + \pi_{60}\lambda_j,$$

$$A_{17} \equiv \pi_{53}(\lambda_r^2 - \lambda_j^2) + \pi_{54}\lambda_r,$$

$$A_{18} \equiv 2\pi_{53}\lambda_r\lambda_j + \pi_{54}\lambda_j,$$

$$A_{19} \equiv A_3A_9 + A_6A_8 - A_4A_{10} - A_5A_7,$$

$$A_{20} \equiv A_3A_{10} + A_4A_9 - A_5A_8 - A_6A_7,$$

$$A_{21} \equiv A_{13}A_9 + A_{16}A_8 - A_{14}A_{10} - A_{15}A_7,$$

$$A_{22} \equiv A_{13}A_{10} + A_{14}A_9 - A_{15}A_8 - A_{16}A_7,$$

$$A_{23} \equiv A_{13}A_5 + A_4A_{16} - A_{14}A_6 - A_3A_{15},$$

and

$$A_{24} \equiv A_{13}A_6 + A_5A_{14} - A_{15}A_4 - A_{16}A_3.$$

An electronic computer is used to solve equations (3.26) and (3.27). This is explained in Section 3.4.

3.4 The Computer Solution of the Characteristic Equations

Since equation set (3.12) and (3.13) and equation set (3.26) and (3.27) are mathematically similar, that is, both sets are two simultaneous nonlinear transcendental equations in two unknowns, the method of root extraction applies to both cases. This method is a roots locus plot, such as used by Dugundji and Gareeb (Ref. 3). For example, consider solving for the λ roots. λ_r and λ_j are systematically sequenced through a range of values. For each of these values, F_r and F_j are calculated. Now, for each λ_r, λ_j pair for which either

F_r or F_j equals zero, this λ_r, λ_j location is marked on a λ_r, λ_j coordinate system (Fig. 9). Thus, after sequencing λ_r and λ_j through their full range of values, one obtains a series of these zero points —— through which one may draw $F_r = 0$ and $F_j = 0$ curves (Fig. 9). The intersection of a $F_r = 0$ curve and a $F_j = 0$ curve defines a λ root on the coordinate system.

Now, an electronic computer was used to find F_r and F_j for sequenced values of λ_r and λ_j (similarly G_r and G_j for σ_r and σ_j); but the plotting and root extraction was done by hand. This was done in order to keep the computer run time to less than one minute. However, the hand plotting was by no means difficult and gave roots in less than five minutes. Also, the plots had the virtue of showing trends, when compared with other plots in a series of runs. Examples of roots locus plots are shown in Figures 18 and 19.

4. A COMPARISON OF THEORY WITH EXPERIMENT

4.1 The Test System

For the test system, a kite, as shown in Fig. 21, was chosen. This choice was based on the fact that a kite contains all of the essential features of the theory's physical model and is much more general than a nonlifting design, such as tested by Etkin and Mackworth (Ref. 5). Further, the kite was inexpensive to construct, easy to test, and perfectly suitable for the Stanford low speed open throat wind tunnel, which has a test section diameter of 7 ft. By virtue of the tunnel design and low wind velocities, it was possible to study the system's unstable motion without great risk of damaging it.

The system, however, has certain limitations. Aside from being representative of only one cable-body application, wind tunnel test section size limited the cable length such that cable dynamic terms were very small compared with body terms. To offset this, a certain amount of outdoor testing at long cable lengths was attempted. Although outdoor experimentation is difficult because of atmospheric vagaries, as discovered by Bryant and coauthors (Ref. 1) and NASA researcher Tracy Redd (Ref.15) with his towed balloon experiments(fig.17), reasonable information was obtained, and the sum total gave a good spectrum of the system's stability characteristics.

As for the body itself, note from Fig. 20 that its design was kept purposely simple to facilitate calculation and measurement of its properties. By virtue of this, the moments of inertia were evaluated by a combination of theory and compound pendulum tests. Their values with respect to the reference axes (Fig. 20) are

$$(I_{xx})_o = 2.57 \times 10^{-2} \text{ slug-ft.}^2, \quad (I_{yy})_o = 2.99 \times 10^{-2} \text{ slug-ft.}^2,$$

$$(I_{xz})_o = -.177 \times 10^{-2} \text{ slug-ft.}^2, \text{ and } (I_{zz})_o = 5.50 \times 10^{-2} \text{ slug-ft.}^2.$$

Further, the stability derivatives were calculated according to Campbell and McKinney (Ref. 2), Etkin (Ref. 4), and Purser and Campbell (Ref. 14). A

certain amount of difficulty was encountered in calculating the contribution of the "V" tail to the stability derivatives. The theory of Ref. 14 is primarily for tails with dihedral angles of 30 degrees or less. Moreover, no information on a "V" tail's contribution to C_{Y_p} and C_{ℓ_p} was available. However, for lack of a better method, $(C_{Y_\beta})_T$, $(C_{\ell_\beta})_T$ and $(C_{Z_\alpha})_T$ were found from References 2 and 14; and $(C_{Y_p})_T$ and $(C_{\ell_p})_T$ were calculated based on assuming the section lift curve slope to vary elliptically over the tail's span. An estimation of the error in $(C_{Y_\beta})_T$, $(C_{\ell_\beta})_T$, and $(C_{Y_p})_T$ is given in Section 4.4. The primary motivation for using a "V" tail, as opposed to a more conventional design (for which there is much more information), is that a "V" tail is much less susceptible to damage in the case of the body's tumbling. Further, a tethered lifting body often flies fully stalled in certain conditions, for instance, during launching, and experience shows that a "V" tail gives superior directional stability for this situation.

In order to facilitate studying the tail's contribution to the lateral stability derivatives, in particular, the effects of $(C_{Y_\beta})_T$, $(C_{\ell_\beta})_T$, and $(C_{Y_p})_T$, the author wrote the lateral stability derivatives as functions of these terms. Note also that these stability derivatives are with respect to the wind reference axes of standard aircraft practice (see the Appendix).

The values calculated for the stability derivatives are

$$(C_{X_u})_o = 0,\ (C_{Z_u})_o = 0,\ (C_{m_u})_o = 0,\ (C_{X_{\dot{u}}})_o = 0,$$

$$(C_{Z_{\dot{u}}})_o = 0,\ (C_{m_{\dot{u}}})_o = 0,\ (C_{X_\alpha})_o = .223C_{L_o},$$

$$(C_{Z_\alpha})_o = -4.12 - C_{D_o},\ (C_{m_\alpha})_o = 2.61,\ (C_{X_{\dot{\alpha}}})_o = 0,$$

$$(C_{Z_{\dot{\alpha}}})_o = -1.58,\ (C_{m_{\dot{\alpha}}})_o = -3.41,\ (C_{X_q}) = 0$$

$$(C_{Z_q})_o = 5.42,\ (C_{m_q})_o = -17.10,\ (C_{Y_\beta})_T = -.75,$$

$$(C_{Y_\beta})_w = -.05,\ C_{Y_\beta} = (C_{Y_\beta})_T + (C_{Y_\beta})_w,$$

$$(C_{n_\beta})_o = -.45(C_{Y_\beta})_T + .225(C_{Y_\beta})_w + .02C_{L_w}^2,$$

$$(C_{\ell_\beta})_T = -.154 + .336\alpha_b,\ (C_{\ell_\beta})_w = -.127 - .07C_{L_w},$$

$$(C_{\ell_\beta})_o = (C_{\ell_\beta})_T + (C_{\ell_\beta})_w,\ (C_{Y_r})_o = 2(C_{n_\beta})_o,$$

$$(C_{n_r})_o = -.90(C_{n_\beta})_T + .45(C_{n_\beta})_w - .023C_{L_w}^2 - .30(C_{d_w}),$$

$$(C_{\ell_r})_o = -.90(C_{\ell_\beta})_T + .45(C_{\ell_\beta})_w + .26C_{L_w} + .127,$$

$$(C_{Y_p})_T = -.207 + .907\alpha_b,\ (C_{Y_p})_w = -.225,$$

$$(C_{Y_p})_o = (C_{Y_p})_T + (C_{Y_p})_w,$$

$$(C_{n_p})_o = -.45(C_{Y_p})_T + .23(C_{Y_p})_w - .06C_{L_w} + 9.0(C_{d_w})_\alpha,$$

$$(C_{\ell_p})_o = -.379 - .13C_{D_w} - .0012(3.78 - 16.6\alpha_b)^2,$$

$$(C_{Y_\cdot})_{\beta_o} = 0,\ (C_{\ell_\cdot})_{\beta_o} = 0,\ \text{and}\ (C_{n_\cdot})_{\beta_o} = 0,$$

where $\alpha_b \equiv$ the body's fuselage angle in radians (see Fig. 10). For these equations, the subscript $(\ )_w$ refers to the wing. Also, the cable used was stranded nylon with the following properties:

$$\tilde{\rho} = 1.78 \times 10^{-5}\ \text{slug/ft.},\quad R = .0023\ \text{ft.},$$

and according to Hoerner (Ref. 7),

$$C_{a_o} = .035 \quad \text{and} \quad K = 1.15.$$

Now, the equilibrium configuration of the system for given wind speeds, U, and cable attachment point, R_a, is specified by the quantities $\tilde{\alpha}$, $\hat{T}_o$, and θ_o. Values for these were obtained directly from the experimental investigation of a large number of equilibrium situations. A beam balance was used to

measure the vertical component of the cable tension, $T_o \sin \tilde{\alpha}$, and a 3 degree inclined manometer measured the velocity, U. Also, the angles $\tilde{\alpha}$ and θ_o were found directly from photographs of each test (Fig. 21). From these data, values for $\hat{T}_o$ were calculated from

$$\hat{T}_o = \frac{2(T_o \sin \tilde{\alpha})}{\rho U^2 S \sin \tilde{\alpha}} \tag{4.1}$$

Graphs of $\hat{T}_o, \tilde{\alpha}$, and θ_o vs. U are given in Figures 22, 23, and 24, and the estimated error in these values is given in Section 4.4 and shown in the graphs.

Also required, for the stability derivative equations, are the equilibrium values: $C_{L_o}, C_{D_o}, C_{L_w}, C_{D_w}, C_{d_w}, (C_{d_w})_\alpha$, and α_b. These are found by a combination of theory and the experimental equilibrium quantities. C_{L_o} is given by

$$C_{L_o} = \hat{T}_o S \tilde{\alpha} - \hat{mg}, \tag{4.2}$$

and C_{D_o} is calculated from

$$C_{D_o} = \hat{T}_o C \tilde{\alpha}. \tag{4.3}$$

α_b was measured directly from the photographs; and, from the geometry of the body, one has that

$$\alpha_w = \alpha_b + 4.5^o. \tag{4.4}$$

Now, in order to obtain the wing properties, the author used the experimental curves by Pinkerton and Greenberg (Ref. 13) for a rectangular wing with the same airfoil, but of aspect ratio 6. The angle of attack of a wing of aspect ratio 6 such as to give the same C_L as a wing of aspect ratio 4.83 is given by

$$\alpha_6 = \frac{(1 + (C_{L_\alpha})_\infty / 6\pi)}{(1 + (C_{L_\alpha})_\infty / 4.83\pi)} \alpha_{4.83} = .947 \alpha_w. \tag{4.5}$$

So, this equation and the experimental curve of C_L versus α gives C_{L_w} for each α_w value. Similarly, the angle of attack for a wing of aspect ratio infinity

is related to α_w by

$$\alpha_\infty = .727\alpha_w. \tag{4.6}$$

This equation, with the experimental curve of C_{d_w} versus α_∞, gives C_{d_w} for each α_w (and thereby C_{L_w}) value. Further, the slope of the curve at that point gives $(C_{d_w})_\alpha$. Finally, C_{D_w} is calculated from

$$C_{D_w} = C_{d_w} + .066C_{L_w}^2. \tag{4.7}$$

It is important to note that for all equilibrium quantities except $\tilde{\alpha}$, the effects of the cable weight and drag are ignored. This is by virtue of the fact that a cable length of 4 feet or less was used during the equilibrium measurements, and cable weight and drag were very much less than cable tension and body drag —— for the wind velocities, U, considered. This gave an essentially straight cable which directly yielded

$$\overline{\left(\frac{\partial x}{\partial s}\right)}_a = C\tilde{\alpha} \quad \text{and} \quad \overline{\left(\frac{\partial z}{\partial s}\right)}_a = S\tilde{\alpha} \tag{4.8}$$

Also, since most stability measurements were made at a cable length of 4 feet or less, the assumption of constant equilibrium parameters for a given U and R_a, and varying L, is very good. However, for the case where L = 100 ft., note again that the cable weight is still much less than T_o for the range of U and R_a values considered, that is,

$$\tilde{\rho}gL = 0[10^{-2}]\text{lb.} \quad \text{and} \quad T_o = 0[1]\text{lb.} \tag{4.9}$$

But, the cable drag is of the same order as the body drag:

$$\rho KRU^2L = 0[10^{-2}] \quad \text{and} \quad D = 0[10^{-2}]. \tag{4.10}$$

Its only contribution, though, is to give the cable a bow, and to lower the cable mean angle, $\tilde{\alpha}$. The cable slope at the attachment point remains unchanged. Thus, the equilibrium quantities for the L = 100 ft. case are the same as for L = 4 ft. or less, with the exception that $\tilde{\alpha}$ is different.

In order to find the change in $\tilde{\alpha}$, note first that (4.9) and (4.10) satisfy

conditions (1.16). So, the cable bow is shallow. Also, for this particular model, the $\tilde{\alpha}$ value is very high (70^{o} or more), so that one has for the angle decrease, $\Delta\tilde{\alpha}$,

$$\Delta\tilde{\alpha} = \frac{\rho K R U^2 L}{2T_o}.$$

This now completes the set of parameters and equations necessary to describe the equilibrium configuration of the system. These parameters, along with the inertial properties, stability derivatives, and characteristic dimensions give all the information needed by the theory to define the stability roots.

4.2 The Stability Tests

For a given free stream velocity, U, and attachment point position, R_a, the stability quantities measured were the cable's critical length and the system's lateral and longitudinal oscillations. The cable's critical length is that value of L at which the system went unstable. This appears to be an important phenomenon of cable-body systems, and has been observed by Bryant, et al. (Ref. 1) and Etkin and Mackworth (Ref. 5). As for the oscillations, the properties recorded were the frequency and qualitative damping of the lateral and longitudinal motions. Finally, a very qualitative measure of the system's stability at long cable lengths was made.

The methods of testing were very straightforward and direct, which was one of the virtues of using a low speed kite system. Critical cable length was measured in the wind tunnel by slowly unreeling the cable until unstable oscillations occurred. The cable was then marked, and the critical length, L_{cr}, was directly measured. To produce the lateral oscillations, $\lambda_{j_{exp}}$, and the longitudinal oscillations, $\sigma_{j_{exp}}$, at $L < L_{cr}$, the cable was perturbed a given amount by hand and then suddenly released (Fig. 12). For this system, it was very easy to produce almost pure lateral or longitudinal motions by this method. Frequency was then measured by using a stopwatch and counting integral numbers of periods. Damping measurement was somewhat more qualitative, and involved counting the number of periods until equilibrium was essentially reached.

Stability studies for the long cable case involved outdoor flying, which thereby restricted quantitative measurements. However, it could be determined whether the system were indeed stable or not, and if so, it was. Moreover, the system was stable during rapid unreeling of the cable. So it was possible to test unstable motions for values of L much larger than L_{cr}.

Now, for those properties for which quantitative measurement was possible, L_{cr}, $\lambda_{j_{exp}}$, and $\sigma_{j_{exp}}$, the repeatability was very good, and the values given (Figs. 25 and 26) are based on the average of several runs. The largest estimated error in L_{cr} is $\pm$ .2 ft.; and for $\lambda_{j_{exp}}$ and $\sigma_{j_{exp}}$, the largest estimated error is $\pm$ .01. Further, the maximum estimated error in U, for the velocity range considered, was 6%. Somewhat large tunnel turbulence precluded an accurate damping measurement. This was the reason why a movie camera was not used. It was actually more meaningful to measure the damping as described, and to make a qualitative judgment. Insofar as comparisons of damping from one test to the other were concerned, this was quite adequate.

4.3 The Computer Examples

For the experimental cases, the wing lift coefficient, C_{L_w}, is no less than .70. Moreover, for a wing operating at a high C_{L_w}, the stability derivatives may be strongly modified by partial flow separation. Thus, since the calculation of the wing's contribution to the stability derivatives is based largely on the assumption of attached flow (Ref. 2), the lowest value of U that was selected for the computer examples is 25.0 ft./sec. Nevertheless, C_{L_w} was still higher than desired, and it is felt that this introduced a certain amount of error in relating the theoretical results to the experimental results. This is discussed further in the next section.

For the lateral stability study, the particular examples chosen are

$$U = 25.0, 28.0, 30.0 \text{ ft./sec.} \begin{cases} R_a = .948 \text{ ft.} & \begin{cases} L = 1.00 \text{ ft.} \\ L = 2.00 \text{ ft.} \\ L = 3.00 \text{ ft.} \end{cases} \\ R_a = 1.09 \text{ ft.} & \begin{cases} L = 1.00 \text{ ft.} \\ L = 2.00 \text{ ft.} \\ L = 3.00 \text{ ft.} \end{cases} \\ R_a = 1.24 \text{ ft.} & \begin{cases} L = 1.00 \text{ ft.} \\ L = 2.00 \text{ ft.} \\ L = 3.00 \text{ ft.} \end{cases} \end{cases}$$

and

$$U = 30.0 \text{ ft./sec.}, \quad R_a = 1.09 \text{ ft.}, \quad L = 100.00 \text{ ft.}$$

For the longitudinal stability study, the particular examples chosen are

$$U = 25.0, 28.0 \text{ ft./sec.} \begin{cases} R_a = 1.09 \text{ ft.}, & L = 2.35 \text{ ft.} \\ R_a = 1.24 \text{ ft.}, & L = 1.76 \text{ ft.} \end{cases}$$

The equilibrium data for these examples is obtained from Figures 22, 23, 24, and 27, and equations (4.2)→(4.7). The values obtained are tabulated below:

U (ft./sec.)	25.0			28.0			30.0		
R_a(ft.)	.948	1.09	1.24	.948	1.09	1.24	.948	1.09	1.24
$\hat{T}_o$	.972	.650	.460	.938	.592	.407	.903	.564	.390
θ_o(rad)	-.541	-.532	-.497	-.576	-.562	-.523	-.592	-.579	-.541
α_b(rad)	.134	.040	0	.100	.020	-.028	.078	-.010	-.052
C_{L_o}	1.21	.898	.700	1.13	.790	.600	1.07	.730	.560
C_{D_o}	.176	.111	.091	.151	.099	.086	.138	.093	.085
C_{L_w}	1.42	1.03	.94	1.31	.97	.82	1.27	.92	.74
C_{D_w}	.159	.088	.075	.137	.079	.059	.110	.072	.049
C_{d_w}	.026	.018	.016	.024	.017	.014	.023	.016	.013
$(C_{d_w})_\alpha$	.0022	.0019	.0017	.0021	.0018	.0015	.0021	.0017	.0013

For L less than 5 ft.,

U (ft./sec.)	25.0			28.0			30.0		
R_a(ft.)	.948	1.09	1.24	.948	1.09	1.24	.948	1.09	1.24
$\tilde{\alpha}$(rad)	1.380	1.405	1.364	1.412	1.408	1.358	1.422	1.406	1.351

and for L = 100.00 ft., the previous $\tilde{\alpha}$ values and equation (4.11) give

U (ft./sec.)	30.0
R_a(ft.)	1.09
$\tilde{\alpha}$(rad)	.958

4.4 Computer Results and Comparison of Theory with Experiment

Using the method described in Section 3.4, one directly obtains values of λ_r, λ_j and σ_r, σ_j for the computer examples listed in Section 4.3. Further, for the lateral case, the range of L values went through a critical length, L_{cr}, at which the system had theoretical neutral stability. In order to obtain L_{cr} and $\lambda_{j_{cr}}$, the following technique was used. On a λ_r, λ_j versus L coordinate system (Fig. 13), points of λ_r and λ_j are plotted and curves are drawn through them, thus giving a $\lambda_r(L)$ curve and a $\lambda_j(L)$ curve. Further, the intersection point of the $\lambda_r(L)$ curve with the L axis gives L_{cr}. Finally, the λ_j value corresponding to $L_{cr}(\lambda_j)$ is $\lambda_{j_{cr}}$.

Now, for the lateral case, the theoretical and experimental results are listed on the next page.

U (ft./sec.)	R_a (ft.)	L_{cr} (ft.)	$L_{cr_{exp}}$ (ft.)	$\lambda_{j_{cr}}$	$(\lambda_{j_{cr}})_{exp}$
25.0	1.24	1.30	1.83	.397	.306
	1.09	1.82	2.38	.400	.284
	.948	2.28	4.00	.426	.284
28.0	1.24	1.40	1.92	.380	.278
	1.09	2.00	2.44	.378	.270
	.948	2.50	4.40	.407	.270
30.0	1.24	1.85	1.94	.345	.268
	1.09	2.17	2.45	.362	.268
	.948	2.58	4.50	.390	.268

U (ft./sec.)	R_a (ft.)	L (ft.)	λ_r	λ_j
30.0	1.09	100.00	.046	.057

And, for the longitudinal case,

U (ft./sec.)	R_a (ft.)	L (ft.)	σ_j	$\sigma_{j_{exp}}$	σ_r	qualitative experimental damping
25.0	1.24	1.76	.472	.437	-.072	lightly
	1.09	2.35	.465	.458	-.110	moderately
28.0	1.24	1.76	.450	.435	-.058	lightly
	1.09	2.35	.447	.442	-.095	moderately

Notice that the theoretical results are somewhat different from the experimental values. L_{cr} is uniformly less than $L_{cr_{exp}}$ and $\lambda_{j_{cr}}$ is consistently greater than $(\lambda_{j_{cr}})_{exp}$. In order to investigate the reasons for this, the author studied the effect of the input data on λ_r and λ_j. Considering first the equilibrium values, the author found the significant parameters to be $\hat{T}_o$, θ_o, U, and $\tilde{\alpha}$. So, starting from the U = 30.0, L = 2.0, R_a = 1.09 case (as a representative example), a finite difference study using the computer gave

$$\frac{\partial \lambda_r}{\partial \hat{T}_o} = -.15, \quad \frac{\partial \lambda_r}{\partial \theta_o} = .25, \quad \frac{\partial \lambda_r}{\partial U} = .01, \quad \frac{\partial \lambda_r}{\partial \tilde{\alpha}} = .06,$$

$$\frac{\partial \lambda_j}{\partial \hat{T}_o} = .10, \quad \frac{\partial \lambda_j}{\partial \theta_o} = .19, \quad \frac{\partial \lambda_j}{\partial U} = .01, \quad \text{and} \quad \frac{\partial \lambda_j}{\partial \tilde{\alpha}} = .03,$$

Also, the estimated error in the equilibrium values gives

$$\Delta \hat{T}_o = .08, \quad \Delta \theta_o = .06, \quad \Delta U = 1.8, \quad \text{and} \quad \Delta \tilde{\alpha} = .06.$$

So, from

$$\Delta \lambda_r = \left| \frac{\partial \lambda_r}{\partial \hat{T}_o} \Delta \hat{T}_o \right| + \left| \frac{\partial \lambda_r}{\partial \theta_o} \Delta \theta_o \right| + \left| \frac{\partial \lambda_r}{\partial U} \Delta U \right| + \left| \frac{\partial \lambda_r}{\partial \tilde{\alpha}} \Delta \tilde{\alpha} \right|$$

and

$$\Delta \lambda_j = \left| \frac{\partial \lambda_j}{\partial \hat{T}_o} \Delta \hat{T}_o \right| + \left| \frac{\partial \lambda_j}{\partial \theta_o} \Delta \theta_o \right| + \left| \frac{\partial \lambda_j}{\partial U} \Delta U \right| + \left| \frac{\partial \lambda_j}{\partial \tilde{\alpha}} \Delta \tilde{\alpha} \right|,$$

one obtains

$$\Delta \lambda_r = .034 \quad \text{and} \quad \Delta \lambda_j = .021.$$

Thus, whereas errors in the equilibrium values have a small effect on λ_j, they have a significant effect on λ_r, and thereby, L_{cr}.

A second source for error was the stability derivatives. One problem, as mentioned before, was that the wing was operating near stall for the test cases considered. This was unanticipated as it was originally planned to test at a much larger U, and, consequently, at a much smaller C_{L_w}. But the body's structure was dangerously strained at U greater than 31.7 ft./sec., so the test speeds were lower. Further, the airfoil chosen has very gentle stall characteristics; thus the body could fly well, even though a significant part of the wing's flow was separated. Under such conditions it is not only difficult to assess the wing's contribution to the stability derivatives, but one also encounters the question of nonlinear effects. Nevertheless, for lack of other methods, the wing's stability derivatives were calculated using Ref. 2. Note, however, that one of the wing's stability

derivatives that is most affected by partial stall is $(C_{n_p})_w$. For the $U = 30.0$, $R_a = 1.09$, $L = 2.0$ case,

$$\frac{\partial \lambda_r}{\partial (C_{n_p})_w} = -.3, \quad \text{and} \quad \frac{\partial \lambda_j}{\partial (C_{n_p})_w} = -2.0.$$

Thus, even though it is difficult to give a value to the error in $(C_{n_p})_w$, it is seen that relatively small changes in its nominal estimated value of .03 can make large changes in λ_j.

Another source of error in the stability derivatives was the "V" tail. Its area is large $(S_T/S = .48)$, and thus it gives a major contribution to the stability derivatives. Unfortunately, the study of wings of very large dihedral has never been a very popular research topic, and the only report available for estimating some "V" tail properties is Ref. 14. However, it was desired to use a "V" tail for this body, for the reasons mentioned earlier; thus the tail's stability derivatives were calculated as best as was possible. The significant tail stability derivatives are $(C_{Y_\beta})_T$, $(C_{\ell_\beta})_T$, and $(C_{Y_p})_T$. For the long tail moment arm of the body, the other tail stability derivatives, such as $(C_{n_\beta})_T$, come directly from the previous ones. Now, the estimated error in these values is

$$\Delta(C_{Y_\beta})_T = .3, \quad \Delta(C_{\ell_\beta})_T = .04, \quad \text{and} \quad \Delta(C_{Y_p})_T = .02.$$

Further, the partial derivatives for the $U = 30.0$, $R_a = 1.09$, $L = 2.0$ case are

$$\frac{\partial \lambda_r}{\partial (C_{Y_\beta})_T} = .10, \quad \frac{\partial \lambda_r}{\partial (C_{\ell_\beta})_T} = -.20, \quad \frac{\partial \lambda_r}{\partial (C_{Y_p})_T} = 0,$$

$$\frac{\partial \lambda_j}{\partial (C_{Y_\beta})_T} = -.16, \quad \frac{\partial \lambda_j}{\partial (C_{\ell_\beta})_T} = .30, \quad \text{and} \quad \frac{\partial \lambda}{\partial (C_{Y_p})_T} = .12.$$

So, from

$$\Delta\lambda_r = \left| \frac{\partial \lambda_r}{\partial (C_{Y_\beta})_T} \Delta (C_{Y_\beta})_T \right| + \left| \frac{\partial \lambda_r}{\partial (C_{\ell_\beta})_T} \Delta (C_{\ell_\beta})_T \right| + \left| \frac{\partial \lambda_r}{\partial (C_{Y_p})_T} \Delta (C_{Y_p})_T \right|,$$

and

$$\Delta\lambda_j = \left| \frac{\partial \lambda_j}{\partial (C_{Y_\beta})_T} \Delta (C_{Y_\beta})_T \right| + \left| \frac{\partial \lambda_j}{\partial (C_{\ell_\beta})_T} \Delta (C_{\ell_\beta})_T \right| + \left| \frac{\partial \lambda_j}{\partial (C_{Y_p})_T} \Delta (C_{Y_p})_T \right| .$$

one obtains

$$\Delta\lambda_r = .042 \quad \text{and} \quad \Delta\lambda_j = .062.$$

Thus, errors in the estimation of the tail stability derivatives are seen to have a significant effect on λ_j and L_{cr} (through λ_r).

Note, though, that even with all of the sources of error combined in the worse possible way, the theoretical results should still be at least within the same order of magnitude as the experimental data. Indeed, this is not only so, but even better, for the error in $\lambda_{j_{cr}}$ from experiment is no greater than 40%, and for L_{cr}, the error is no greater than 80%. More important, the theory predicts the essential features shown by the experiments. For instance, not only does it predict an L_{cr} for lateral motion, but it shows the correct variation of L_{cr} with U and R_a. Moreover, for the U range considered, both theory and experiment show a decrease in $\lambda_{j_{cr}}$ with U. Note, however, that the variation of $(\lambda_{j_{cr}})_{exp}$ with R_a is difficult to assess within the error limits of the experimental data; but the theoretical results likewise show no conclusive trend. Similarly, for the longitudinal motion, both theory and experiment show no definite variation of σ_j with U and R_a, for the cases considered. But otherwise, the σ_j values compare very well, with an error no greater than 1%. This is most likely due to the fact that the model —— being very "long-coupled" —— experienced negligible pitching; and further, the high cable angle allowed little motion in the $\check{z}$ direction compared with motion in the $\check{x}$ direction. So, the aerodynamic forcing effects, which were derived from theory, were small compared with the cable tension, which was directly measured. Thus the frequency, σ_j, was largely

determined by T_o and m, which gave, consequently, less error. Note also that for the motion described, aerodynamic damping is largely due to the body's drag; so it would therefore be expected that for a given U, damping would increase with a decrease in R_a. This is, in fact, borne out by the comparison of the quantitative experimental damping with σ_r. This type of motion therefore has an analogy in airplane long mode "phugoid" oscillations.

Finally, the theory qualitatively bears out the fact that the system is laterally unstable at L = 100 ft. and that it was observed to have a low lateral frequency.

4.5 Conclusion

Within the limits of the assumptions listed at the beginnings of Chapters 1 and 2, the present theory provides a method for predicting the first order motion of a large variety of cable-body systems. The key assumptions are that the cable's curve must be shallow and that its tension must be essentially constant along its length. Otherwise, there are no restrictions on the cable's motion, i.e., no "instantaneous equilibrium" physical model. Thus the theory may be as readily applied to a high frequency system, such as a towed cone in hypersonic flow, as to low frequency systems such as towed balloons or the present experimental model.

The essential feature of the theory is that the cable-body system is treated as a cable problem, with the body providing end and auxiliary conditions. This physical model can lend itself readily to a variety of further applications. For instance, the problem of two bodies connected by a cable may be treated by replacing the fixed end condition at $\hat{s} = 0$ with a set of end conditions similar to those at $\hat{s} = 1$, only that these conditions would pertain to the body at that end.

Another variation could allow for varying cable shape and tension by assuming the cable to be composed of finite cable segments —— each with a given $\hat{T}_o$ and $\tilde{\alpha}$. The equations for each segment are then matched, one to the other, through the end conditions of displacement and slope; whereas the end condition of the final segment is given by the body equations —— as before. Similarly,

a further application would be to consider a finite body midway along the cable. In this case, the end conditions on the two adjacent cable segments are found from the equations of motion of the midcable body.

REFERENCES

1. Bryant, L. W., Brown, W. S., and Sweeting, N. E.: "Collected Researches on the Stability of Kites and Towed Gliders," Aero. Research Council R. and M. 2303, February 1942.
2. Campbell, John P. and McKinney, Marion O.: "Summary of Methods for Calculating Dynamic Lateral Stability and Response and for Estimating Lateral Stability Derivatives," NACA Report 1098, 1952.
3. Dugundji, J. and Ghareeb, N.: "Pure Bending Flutter of a Swept Wing in a High-Density, Low-Speed Flow," AIAA Journal, June 1965.
4. Etkin, Bernard: Dynamics of Flight, John Wiley and Sons, 1959.
5. Etkin, B. and Mackworth, J.: "Aerodynamic Instability of Non-Lifting Bodies Towed Beneath an Aircraft," University of Toronto, TN65, 1963.
6. Glauert, H.: "The Stability of a Body Towed by a Light Wire," Aero. Research Council R. and M. 1312, February 1932.
7. Hoerner, S. F.: "Fluid Dynamic Drag," Hoerner, Midland Park, 1958.
8. Hopkin, H. R.: "An Approximate Treatment of the Stability of a Towed Unbanked Object in a Condition of Zero Lift," RAE TR 69076, 1969.
9. Laitinen, P. O.: "Cable Towed Underwater Body Design," U. S. Navy Electronics Laboratory NEL/Report 1452, April 1967.
10. MacNeal, Richard H.: "Flutter of Towed Rigid Decelerators," NASA CR-766, 1967.
11. Maryniak, Jerzy: "Dynamic Longitudinal Stability of a Towed Sailplane," Mechanika Teoretyczna I Stosowana, March, 1967.
12. Mettam, A. R.: "Wind Tunnel Investigations of Instability in a Cable-Towed Body System," RAE TR 69022, 1969.
13. Pinkerton, R. M. and Greenberg, H.: "Aerodynamic Characteristics of a Large Number of Airfoils Tested in the Variable-Density Wind Tunnel," NACA Report 628.

14. Purser, Paul E. and Campbell, John P.: "Experimental Verification of a Simplified Vee-Tail Theory, and Analysis of Available Data on Complete Models with Vee-Tails," NACA Report 823, 1945.

15. Redd, L. Tracy: "A Towing Technique For Determining The Aerodynamic Forces on Tethered Balloons", presented at the Sixth AFCRL Scientific Balloon Symposium, Portsmouth, New Hampshire, June 8-10, 1970.

16. Sohne, W.: "Directional Stability of Towed Airplanes", NACA TM 1401, 1956

17. DeLaurier, James D.: "A First Order Theory for Predicting the Stability of Cable Towed and Tethered Bodies where the Cable Has a General Curvature and Tension Variation", Von Karman Institute Technical Note 68, March 1971.

APPENDIX I

The Relation of the Stability Derivatives to the Stability Derivatives of Standard Aircraft Convention

Due to the fact that most information available on stability derivatives is based on the x_o, y, z_o "wind axis" coordinate system, (Fig. 14) it is profitable to give the relations between these and the stability derivatives defined in Chapter 2, which are based on the $\vec{n}_1, \vec{n}_2, \vec{n}_3$ coordinate system. These are

$$C_{X_u} = (C_{X_u})_o C^2\theta_o + (C_{Z_\alpha})_o S^2\theta_o - [(C_{X_\alpha})_o + (C_{Z_u})_o] S\theta_o C\theta_o,$$

$$C_{X_{\dot{u}}} = (c/b)[(C_{X_{\dot{u}}})_o C^2\theta_o + (C_{Z_{\dot{\alpha}}})_o S^2\theta_o - [(C_{X_{\dot{\alpha}}})_o + (C_{Z_{\dot{u}}})_o] S\theta_o C\theta_o],$$

$$C_{X_w} = (C_{X_\alpha})_o C^2\theta_o - (C_{Z_u})_o S^2\theta_o + [(C_{X_u})_o - (C_{Z_\alpha})_o] S\theta_o C\theta_o,$$

$$C_{X_{\dot{w}}} = (c/b)[(C_{X_{\dot{\alpha}}})_o C^2\theta_o - (C_{Z_{\dot{u}}})_o S^2\theta_o + [(C_{X_{\dot{u}}})_o - (C_{Z_{\dot{\alpha}}})_o] S\theta_o C\theta_o],$$

$$C_{X_q} = -(c/b)[(C_{Z_q})_o C\theta_o + (C_{X_q})_o S\theta_o],$$

$$C_{Y_v} = (C_{Y_\beta})_o,$$

$$C_{Y_{\dot{v}}} = (C_{Y_{\dot{\beta}}})_o,$$

$$C_{Y_p} = -(C_{Y_p})_o C\theta_o + (C_{Y_r})_o S\theta_o,$$

$$C_{Y_r} = -(C_{Y_r})_o C\theta_o - (C_{Y_p})_o S\theta_o,$$

$$C_{Z_u} = (C_{Z_u})_o C^2\theta_o - (C_{X_\alpha})_o S^2\theta_o - [(C_{Z_\alpha})_o - (C_{X_u})_o] S\theta_o C\theta_o,$$

$$C_{Z_{\dot{u}}} = (c/b)[(C_{Z_{\dot{u}}})_o C^2\theta_o - (C_{X_{\dot{\alpha}}})_o S^2\theta_o + [(C_{X_u})_o - (C_{Z_{\dot{\alpha}}})_o]S\theta_o C\theta_o],$$

$$C_{Z_w} = (C_{Z_\alpha})_o C^2\theta_o + (C_{X_u})_o S^2\theta_o + [(C_{Z_u})_o + (C_{X_\alpha})_o]S\theta_o C\theta_o,$$

$$C_{Z_{\dot{w}}} = (c/b)[(C_{Z_{\dot{\alpha}}})_o C^2\theta_o + (C_{X_{\dot{u}}})_o S^2\theta_o + [(C_{Z_{\dot{u}}})_o + (C_{X_{\dot{\alpha}}})_o]S\theta_o C\theta_o],$$

$$C_{\ell_v} = -(C_{\ell_\beta})_o C\theta_o + (C_{n_\beta})_o S\theta_o,$$

$$C_{\ell_{\dot{v}}} = -(C_{\ell_{\dot{\beta}}})_o C\theta_o + (C_{n_{\dot{\beta}}})_o S\theta_o,$$

$$C_{\ell_p} = (C_{\ell_p})_o C^2\theta_o + (C_{n_r})_o S^2\theta_o - [(C_{n_p})_o + (C_{\ell_r})_o]S\theta_o C\theta_o,$$

$$C_{\ell_r} = (C_{\ell_r})_o C^2\theta_o - (C_{n_p})_o S^2\theta_o + [(C_{\ell_p})_o - (C_{n_r})_o]S\theta_o C\theta_o,$$

$$C_{m_u} = -(c/b)[(C_{m_u})_o C\theta_o + (C_{m_\alpha})_o S\theta_o],$$

$$C_{m_{\dot{u}}} = -(c/b)^2[(C_{m_{\dot{u}}})_o C\theta_o + (C_{m_{\dot{\alpha}}})_o S\theta_o],$$

$$C_{m_w} = -(c/b)[(C_{m_\alpha})_o C\theta_o + (C_{m_u})_o S\theta_o],$$

$$C_{m_{\dot{w}}} = -(c/b)^2[(C_{m_{\dot{\alpha}}})_o C\theta_o + (C_{m_{\dot{u}}})_o S\theta_o],$$

$$C_{m_q} = (c/b)^2(C_{m_q})_o,$$

$$C_{n_v} = -(C_{n_\beta})_o C\theta_o - (C_{\ell_\beta})_o S\theta_o,$$

$$C_{n_{\dot{v}}} = -(C_{n_{\dot{\beta}}})_o C\theta_o - (C_{\ell_{\dot{\beta}}})_o S\theta_o,$$

$$C_{n_p} = (C_{n_p})_o C^2\theta_o - (C_{\ell_r})_o S^2\theta_o + [(C_{\ell_p})_o - (C_{n_r})_o] S\theta_o C\theta_o,$$

and

$$C_{n_r} = (C_{n_r})_o C^2\theta_o + (C_{\ell_p})_o S^2\theta_o + [(C_{n_p})_o + (C_{\ell_r})_o] S\theta_o C\theta_o.$$

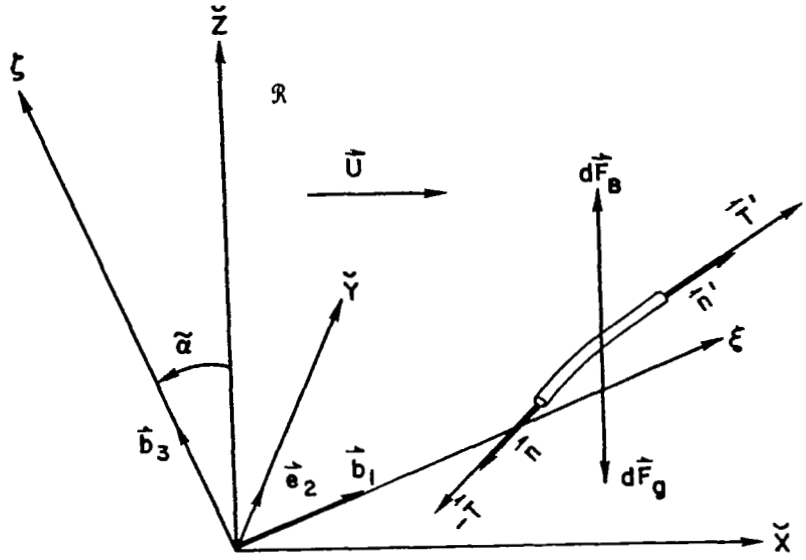

Fig. 1 Cable coordinate system and non-fluid-dynamic forces acting on a cable element.

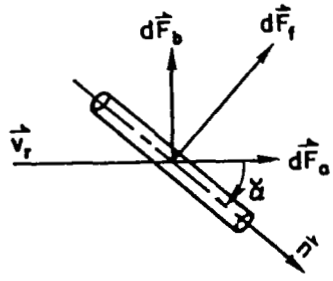

Fig. 2 The fluid-dynamic forces acting on the cable element.

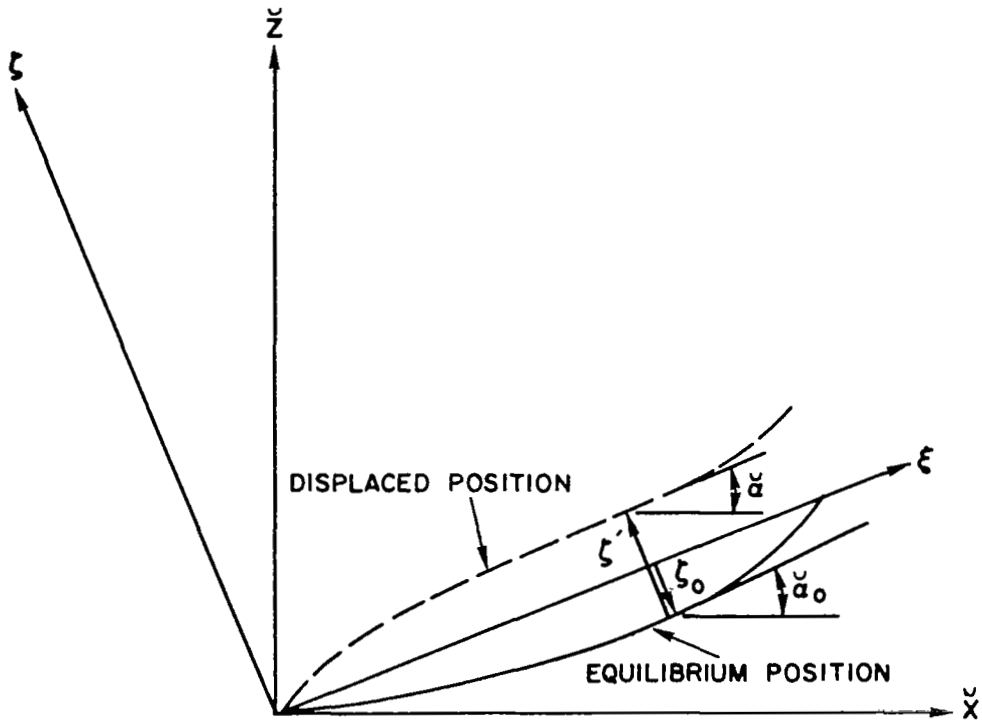

Fig. 3 Coordinates for the displaced cable.

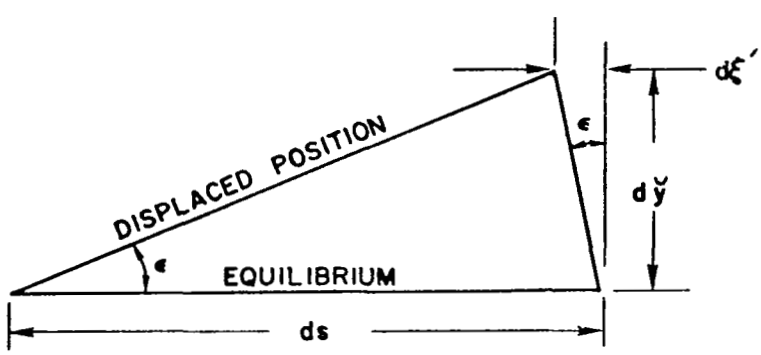

Fig. 4 A perturbation of the cable element in the $\check{y}, \xi$ plane.

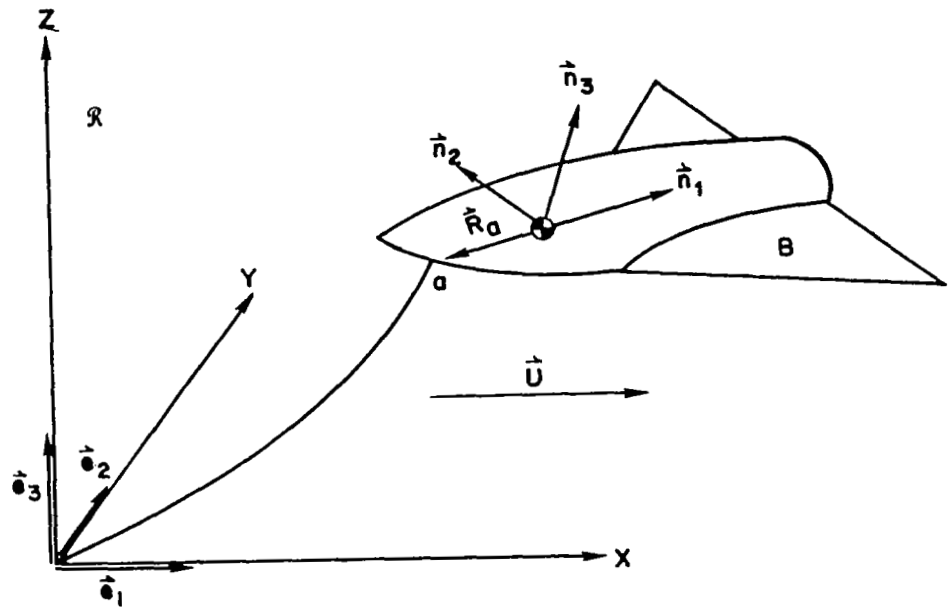

Fig. 5 The body's coordinate systems.

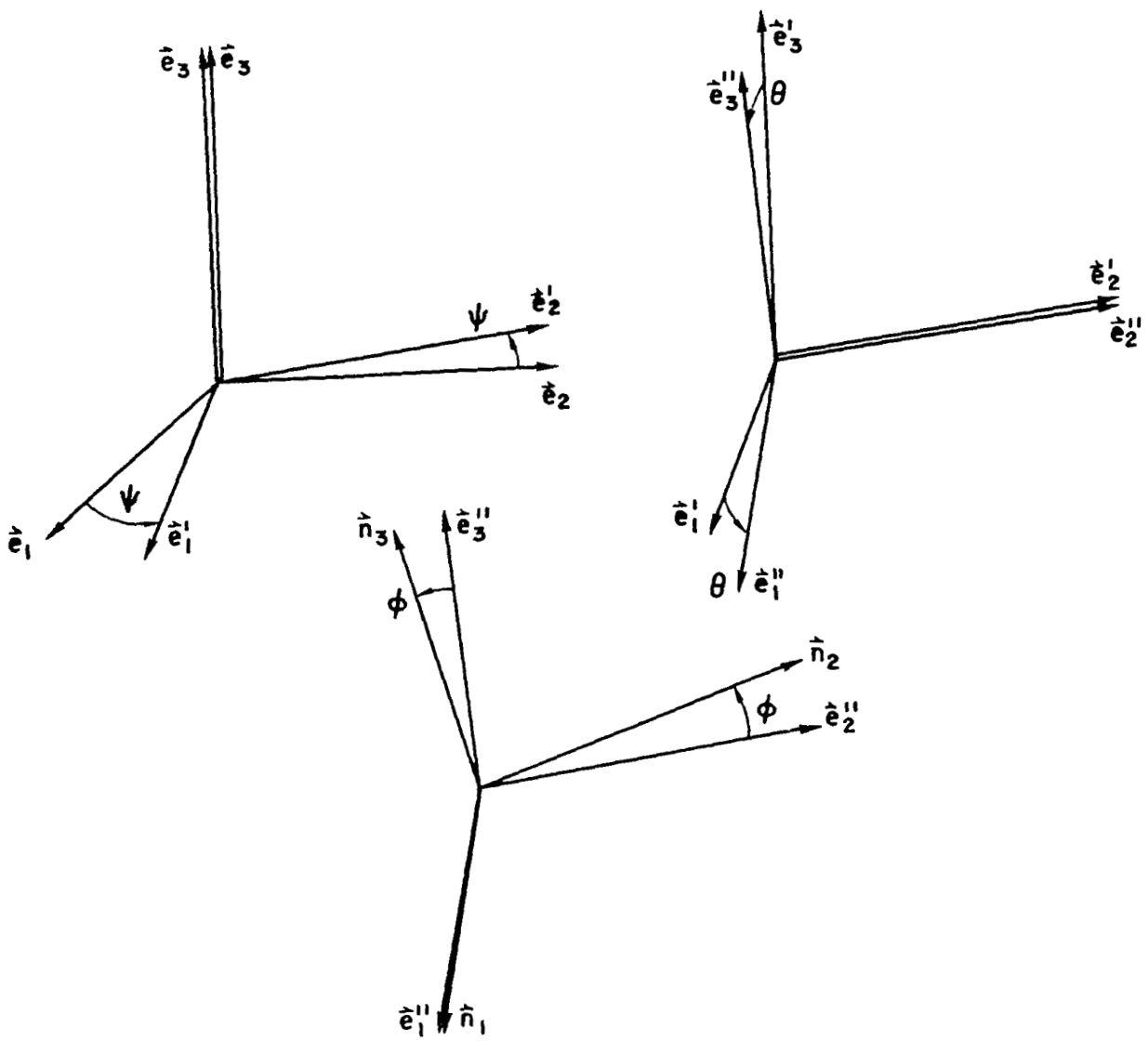

Fig. 6 The Eulerian angles.

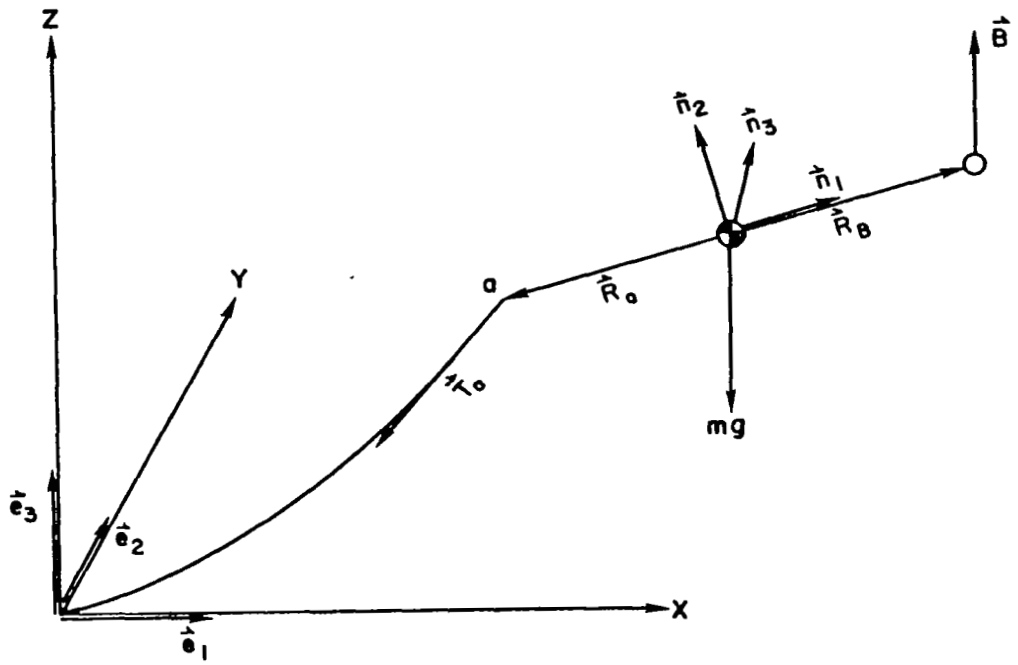

Fig. 7 Cable, buoyancy, and gravity forces on the body.

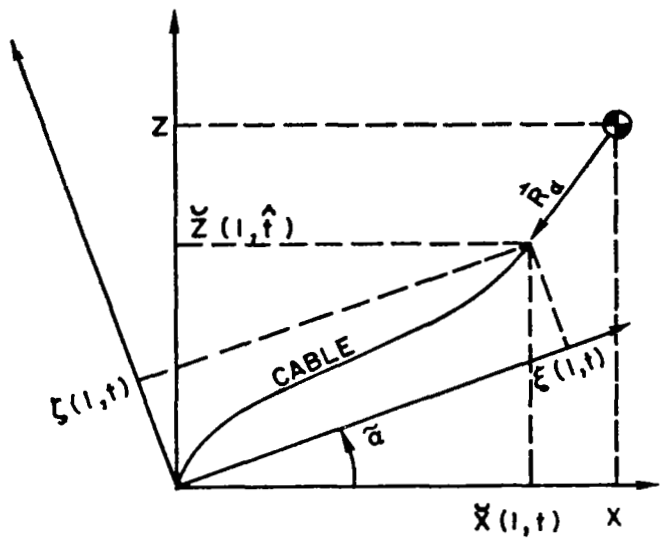

Fig. 8 Coordinate transformation.

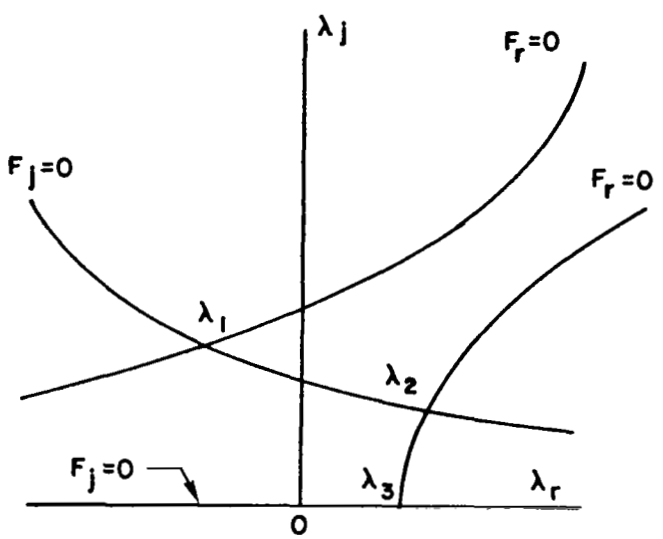

Fig. 9 Sample lateral roots locus plot.

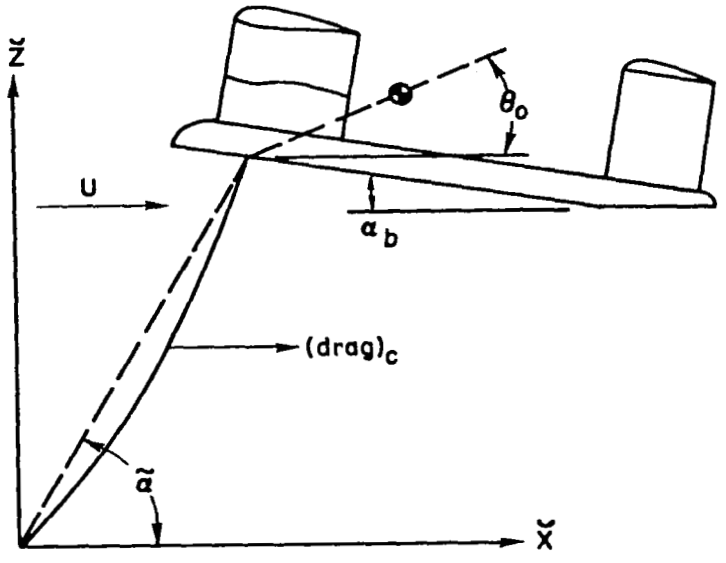

Fig. 10 System equilibrium coordinates.

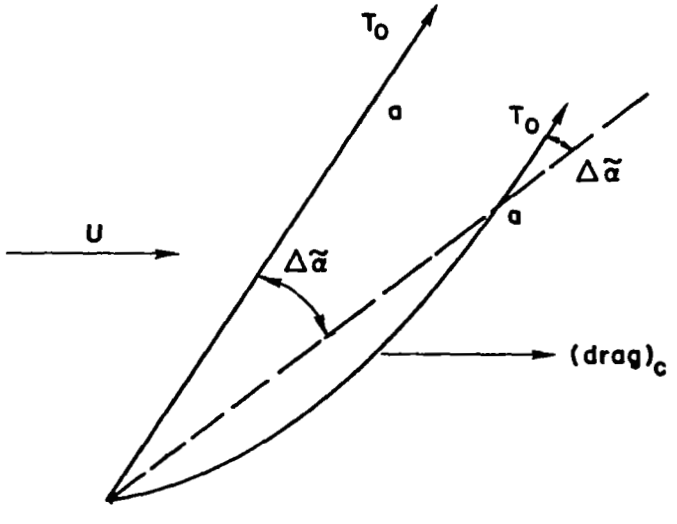

Fig. 11 Cable displacement due to cable drag.

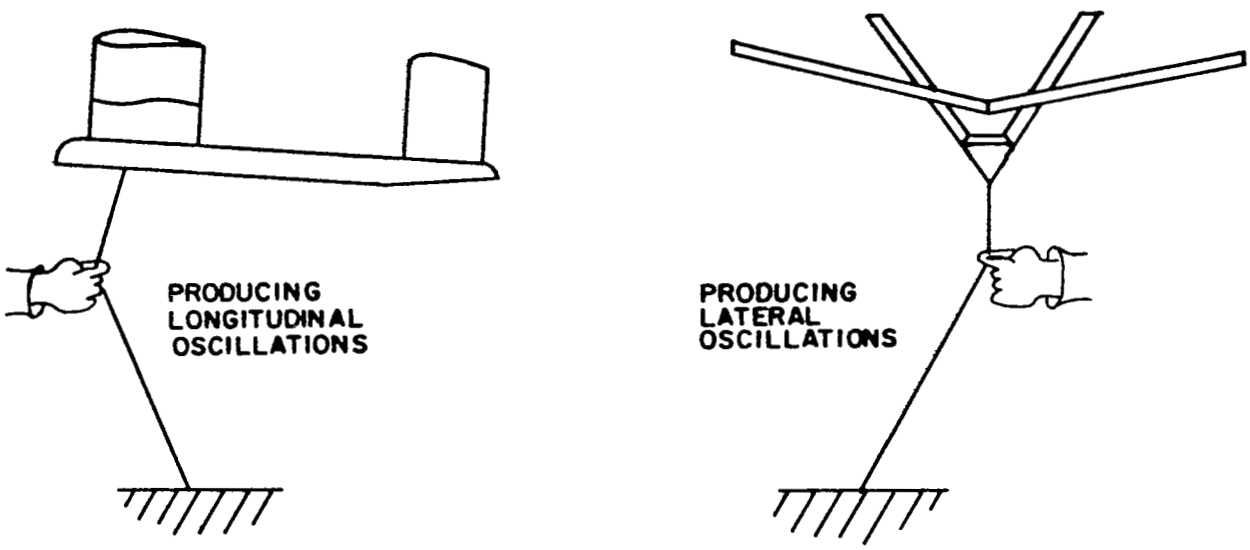

Fig. 12 Producing longitudinal and lateral oscillations.

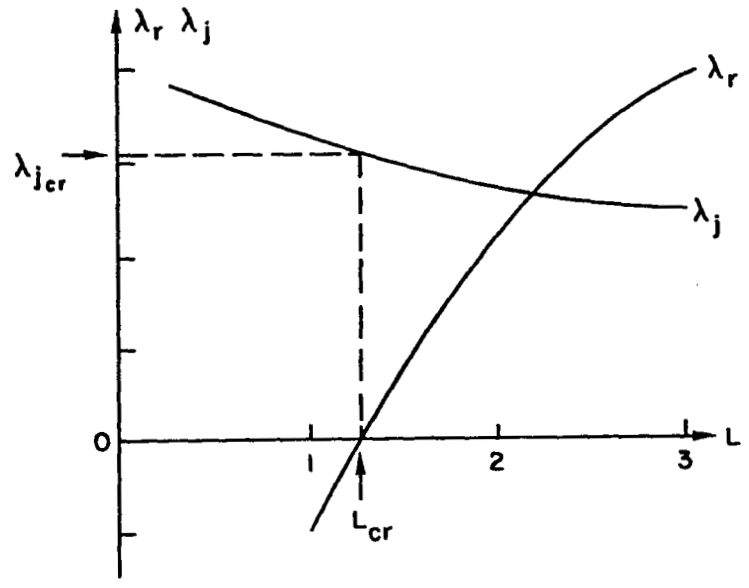

Fig. 13 Plot for finding L_{cr} and λ_{cr}.

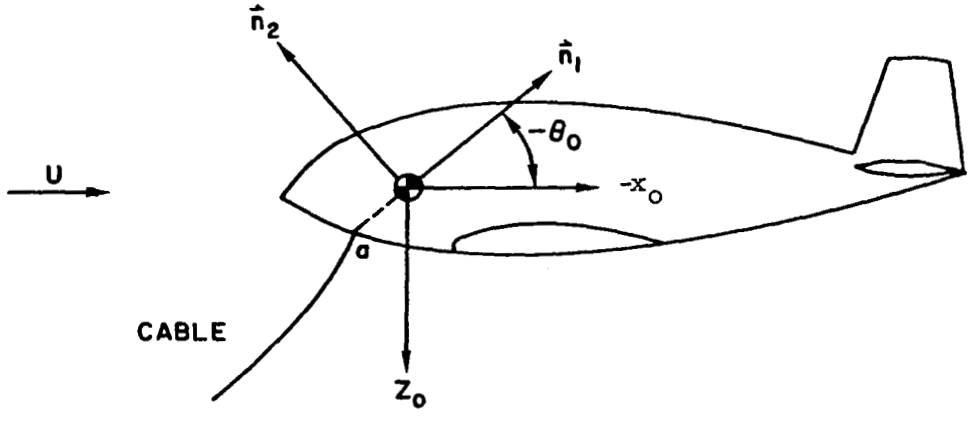

Fig. 14 Thesis coordinates and the standard aircraft coordinates.

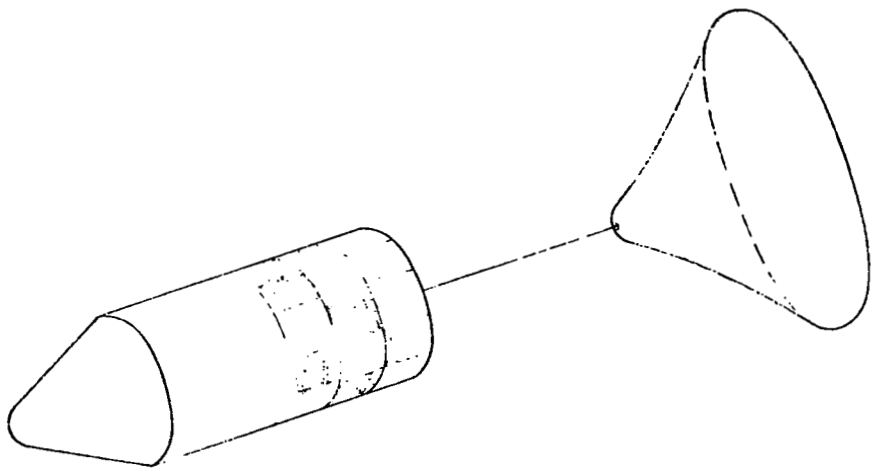

Fig. 15 Towed decelerator.

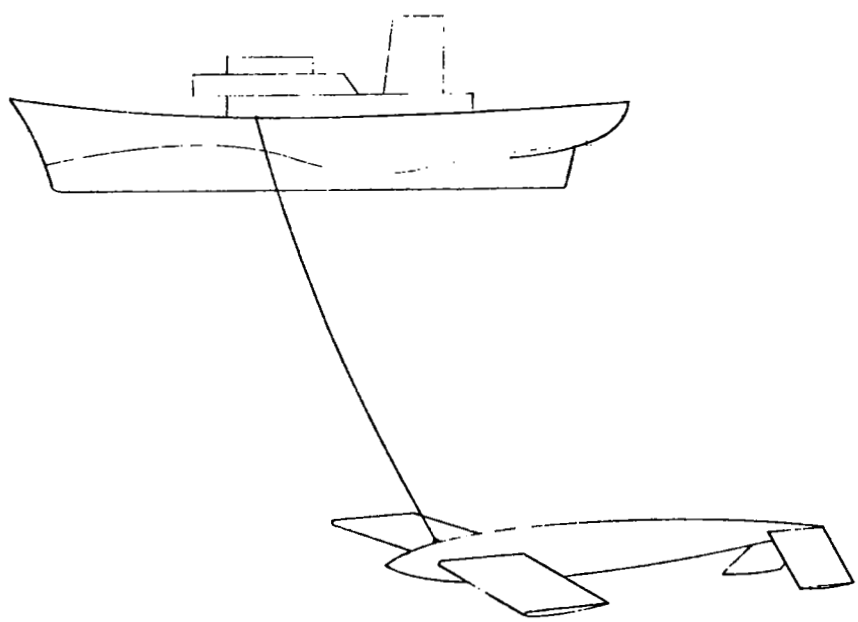

Fig. 16 Towed underwater device.

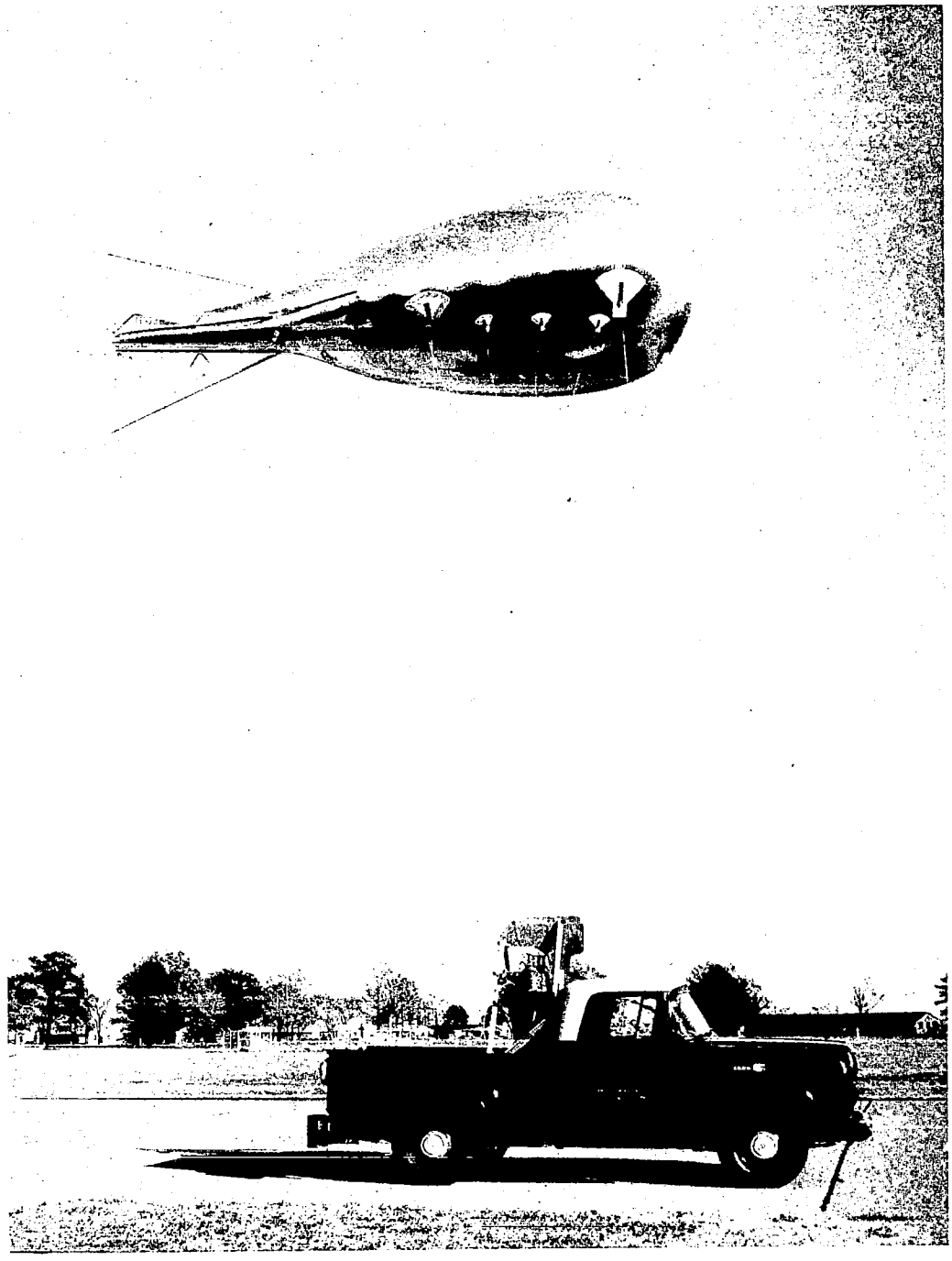

Fig. 17 Towed balloon tested at NASA Langley.

Roots Locus Plot for the Lateral
Case; U = 28.0, R_a = 1.09, L = 2.00

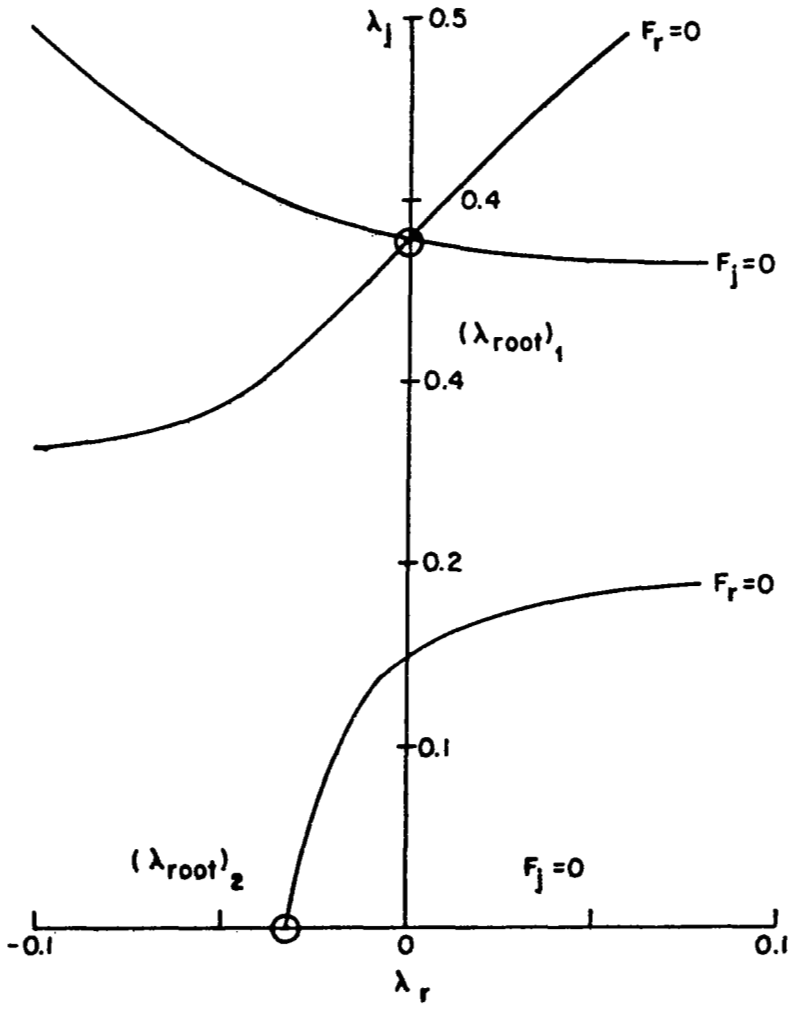

Fig. 18 A lateral roots locus plot.

Roots Locus Plot for the Longitudinal Case; $U = 25.0$, $R_a = 1.24$, $L = 1.76$

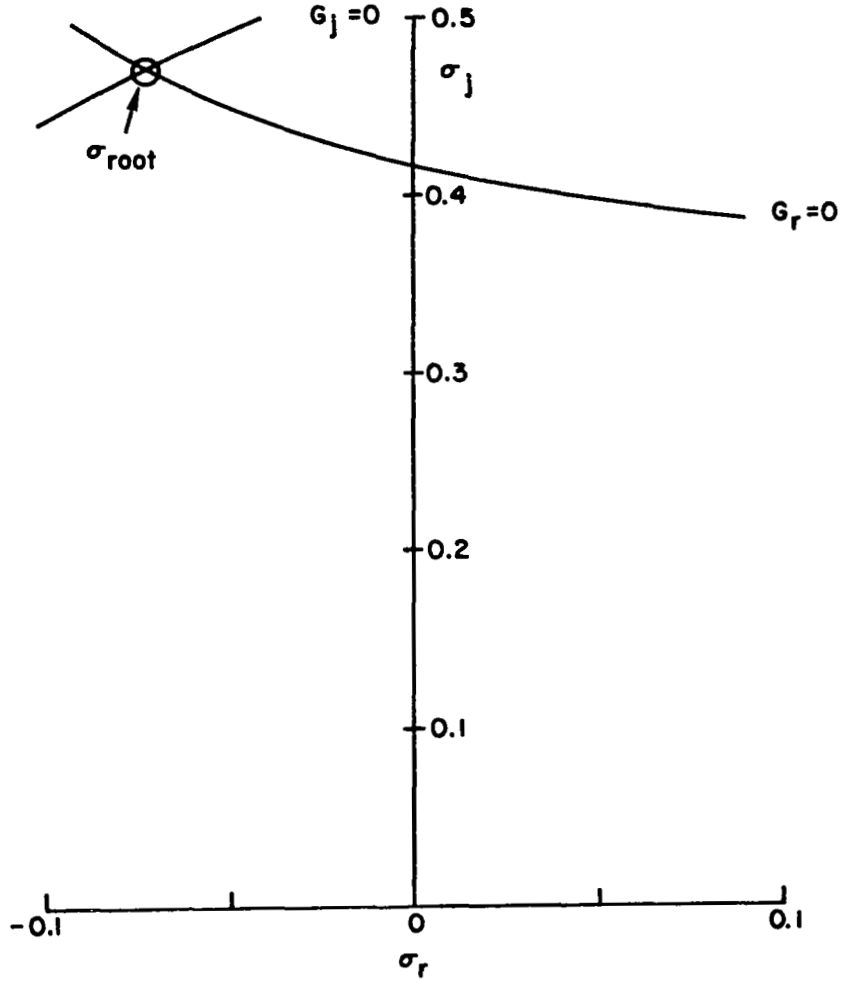

Fig. 19 A longitudinal roots locus plot.

Tethered Lifting Body Model

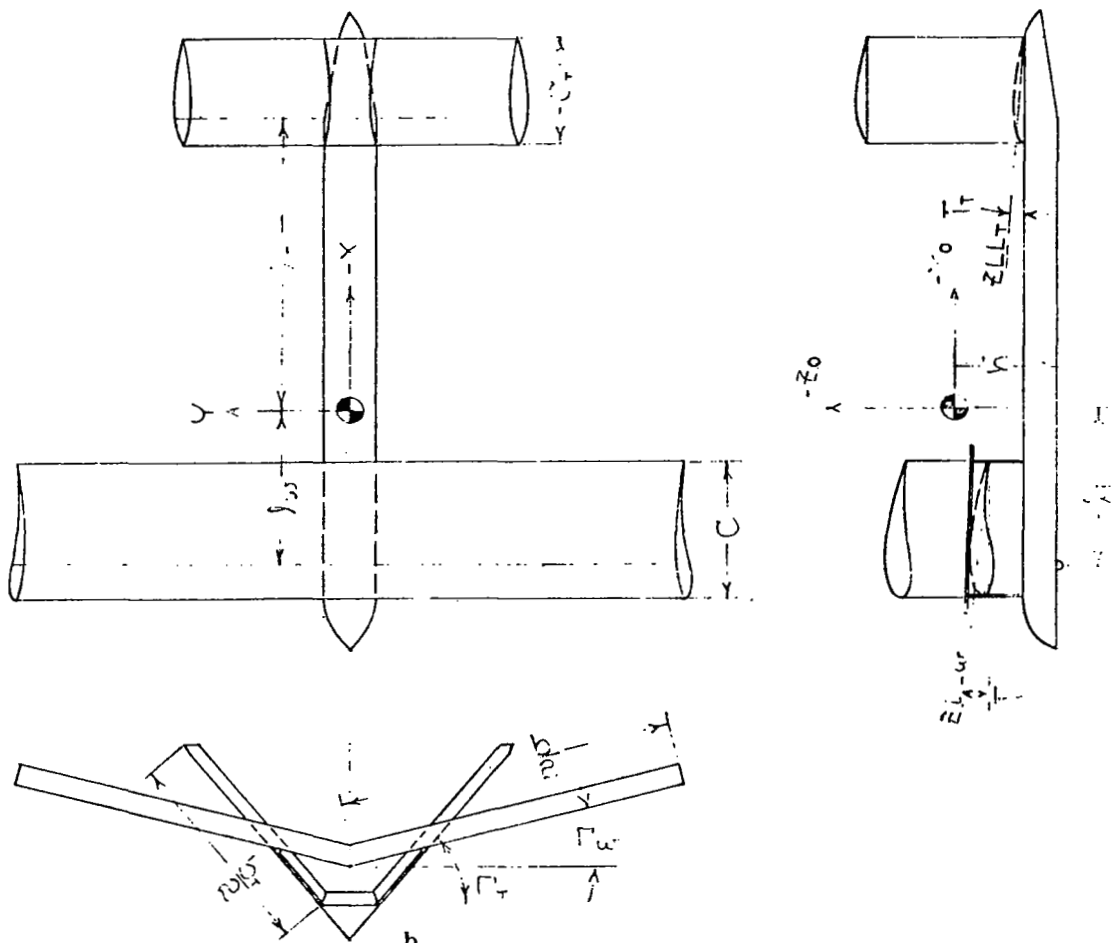

$\frac{b}{2}$ = 24.5 in., $\frac{b_T}{2}$ = 15.0 in., C = 10.15 in.
C_T = 8.0 in., ℓ_T = 22 in., ℓ_w = 11 in.
$\bar{h}$ = 7.12 in., Γ_ω = 7.4°, Γ_T = 49°,
$\bar{i}_w$ = 14.8°, $\bar{i}_T$ = 4.6°,
wing airfoil: Sikorsky GS-M
tail airfoil: Clark-Y
ℓ_1 = 13 1/8 in., ℓ_2 = 11 in., ℓ_3 = 8 7/8 in.

Fig. 20 Geometry of the test body.

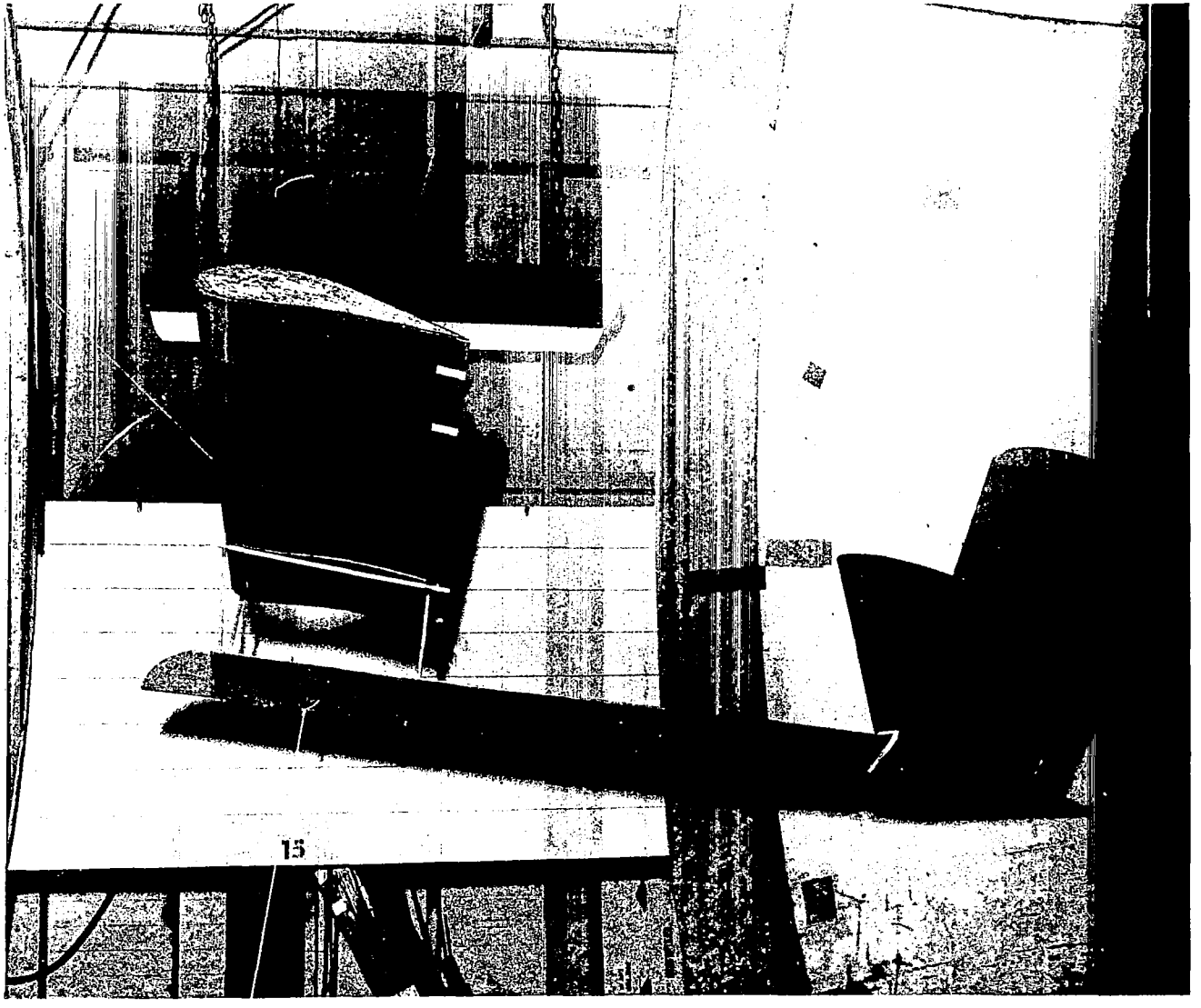

Fig. 21 The test system in the Stanford wind tunnel.

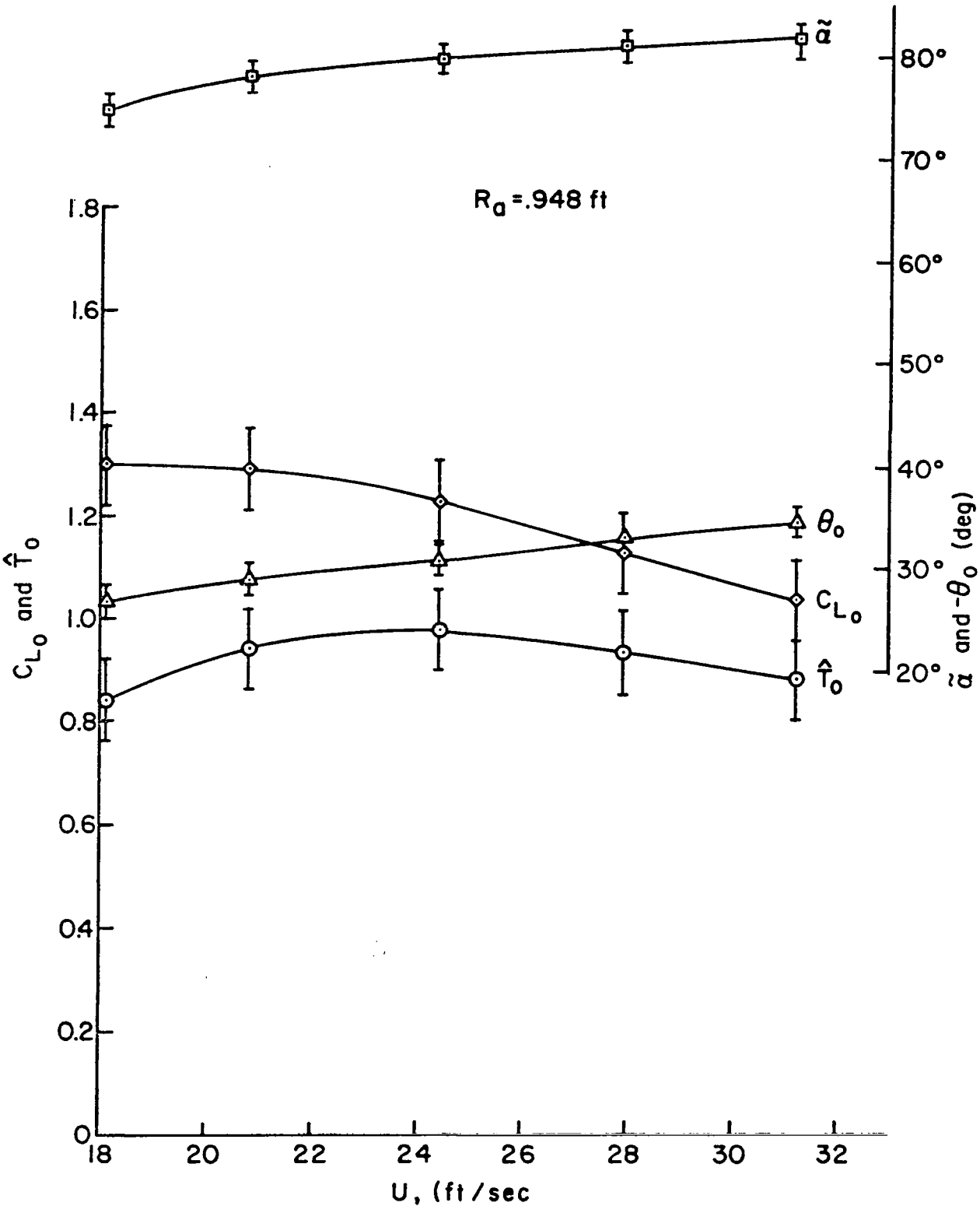

Fig. 22 The equilibrium values of the test model for R_a = .948 ft.

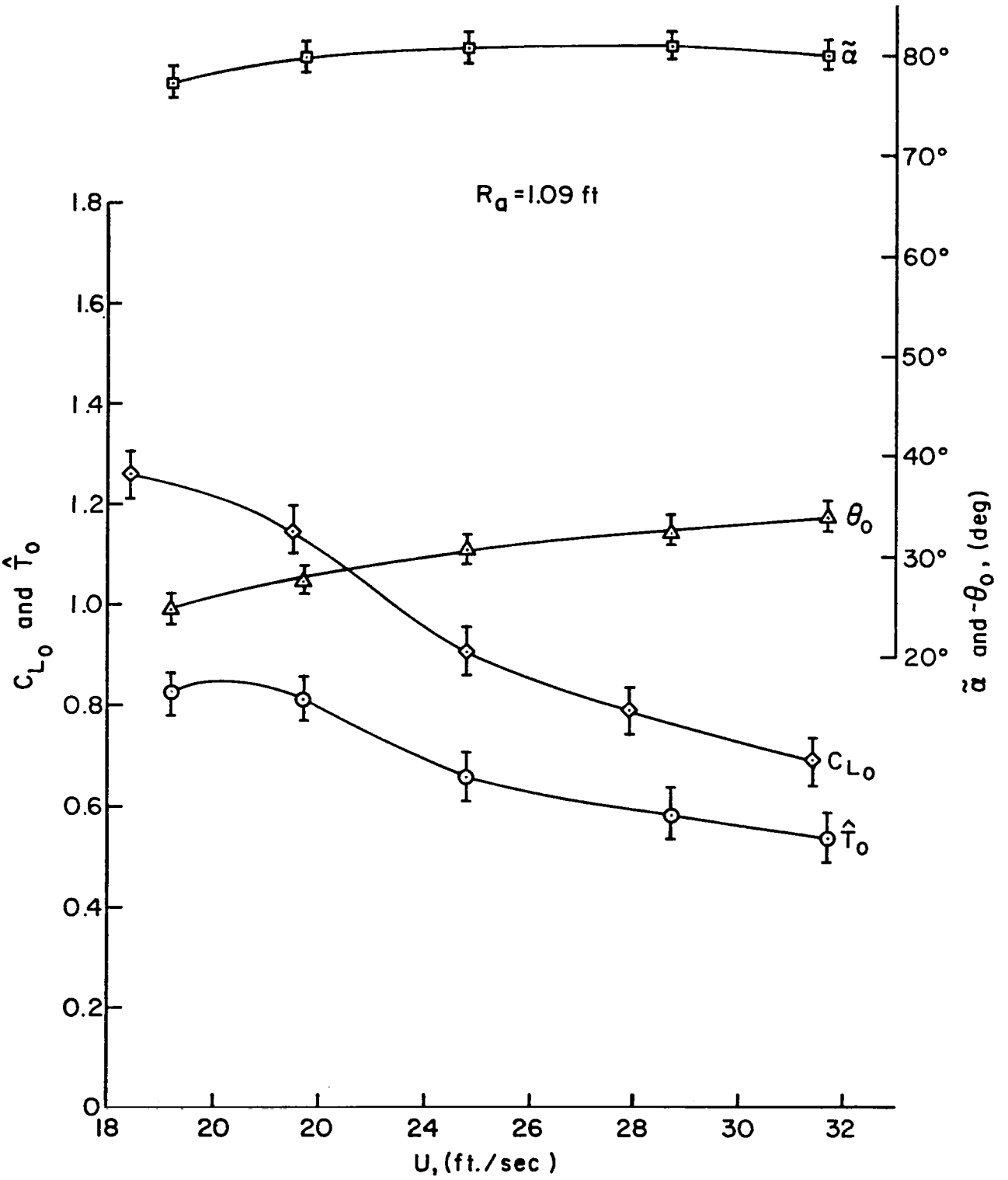

Fig. 23 The equilibrium values of the test model for R_a = 1.09 ft.

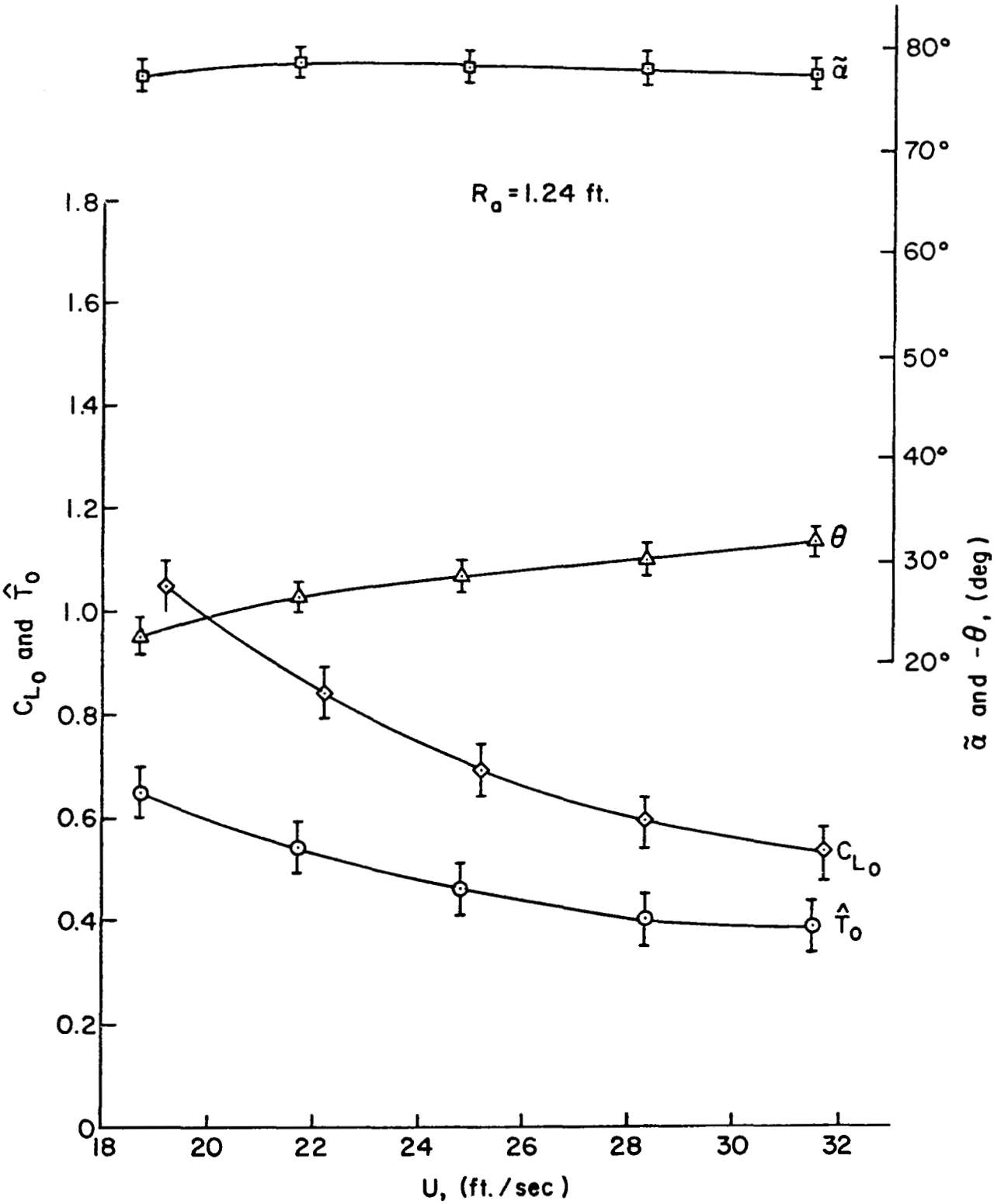

Fig. 24 The equilibrium values of the test model for R_a = 1.24 ft.

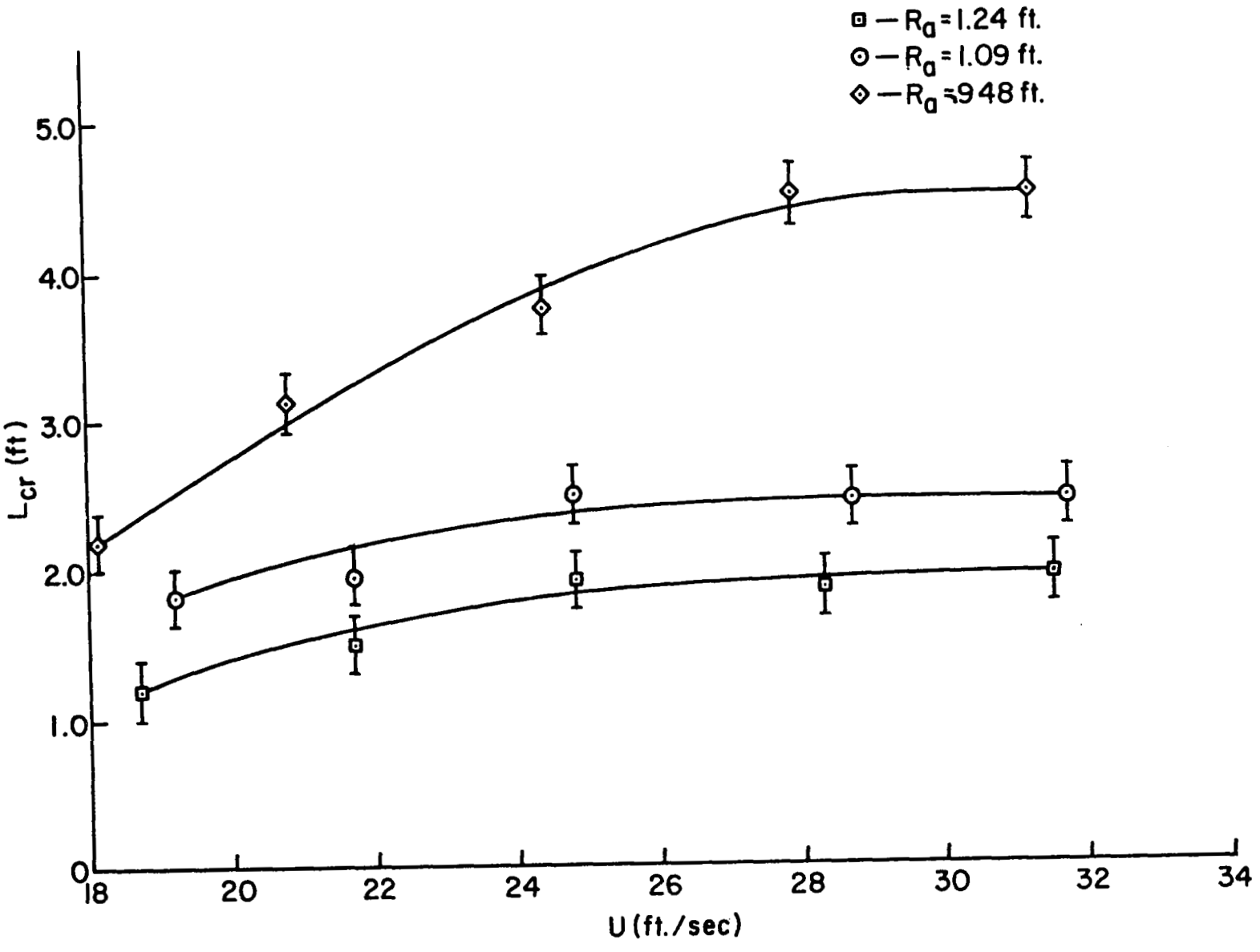

Fig. 25 Experimental values of cable critical length, L_{cr}, vs. wind speed, U.

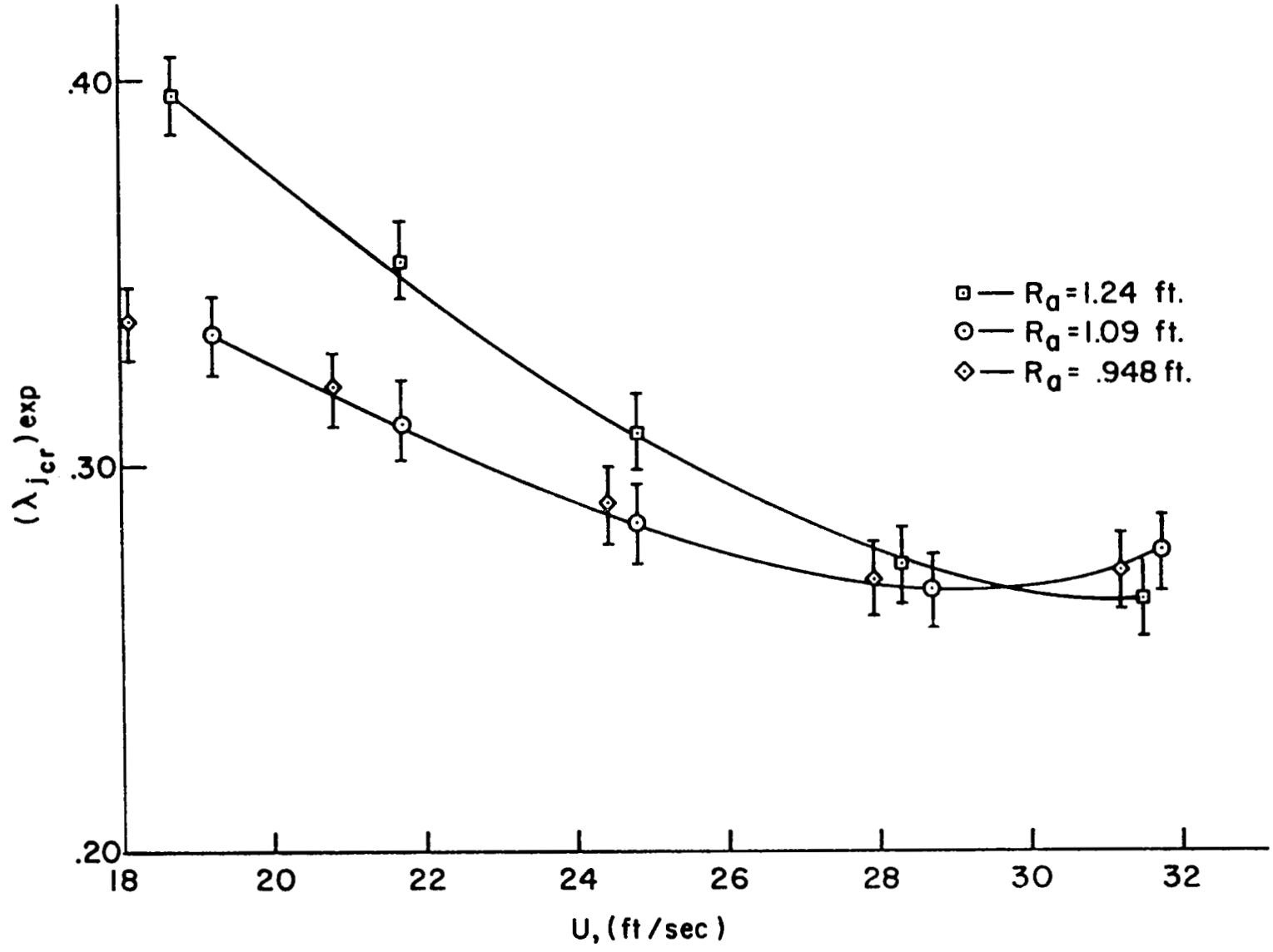

Fig. 26 Experimental lateral frequency of oscillation, $(\lambda_j)_{exp}$, for $L = L_{cr}$, vs. wind speed, U.

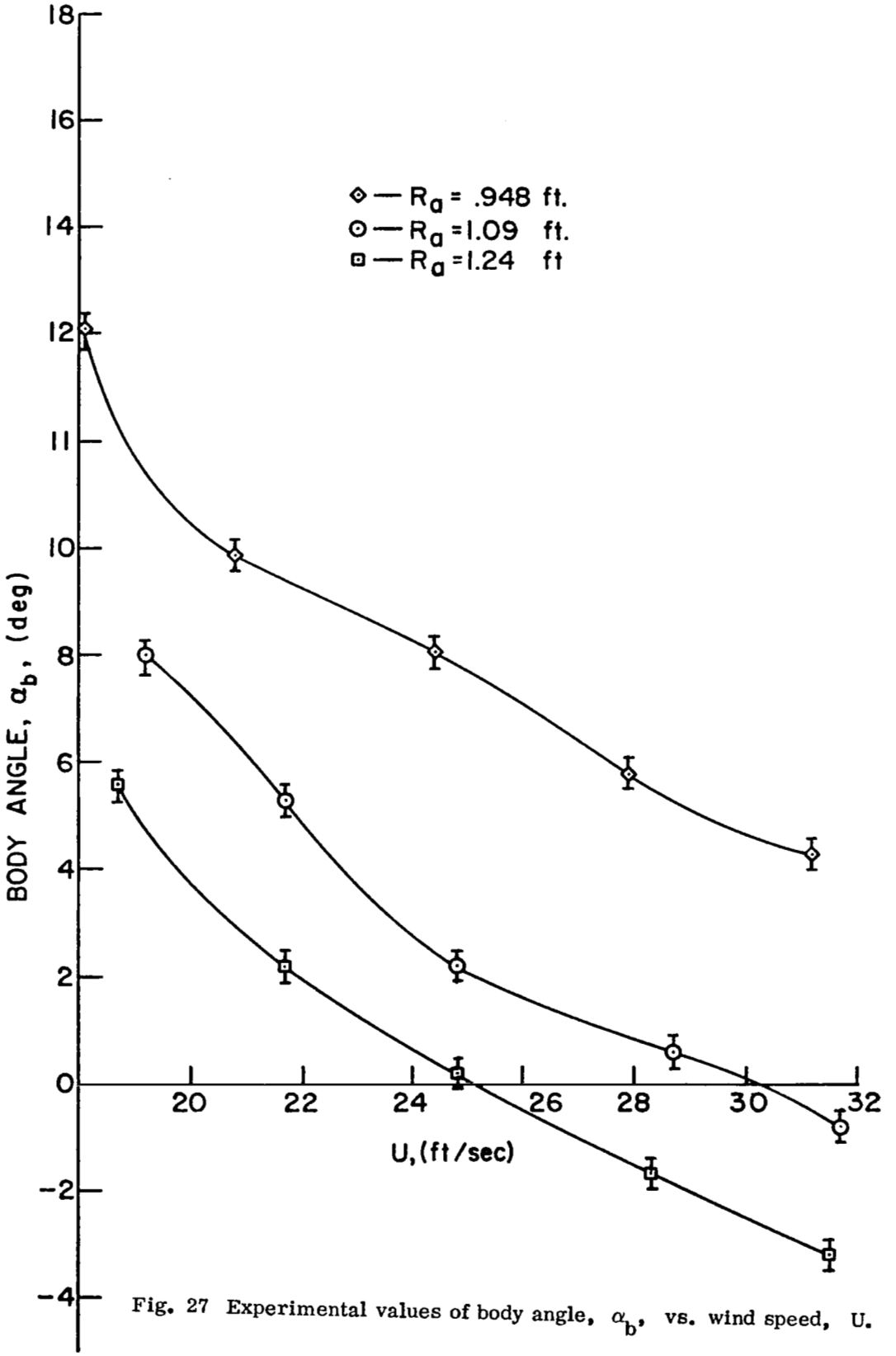

Fig. 27 Experimental values of body angle, α_b, vs. wind speed, U.

Fig. 27 Experimental values of body angle, α_b, vs. wind speed, U.

NASA-Langley, 1972 —— 1 CR-2021